PB98-107014

Information is our business.

EXPLORATORY CRASH TESTS OF AN FRP END-TERMINAL: FOIL TEST NUMBERS 96-007, 96F016, 96F024, AND 96F027

JUL 97

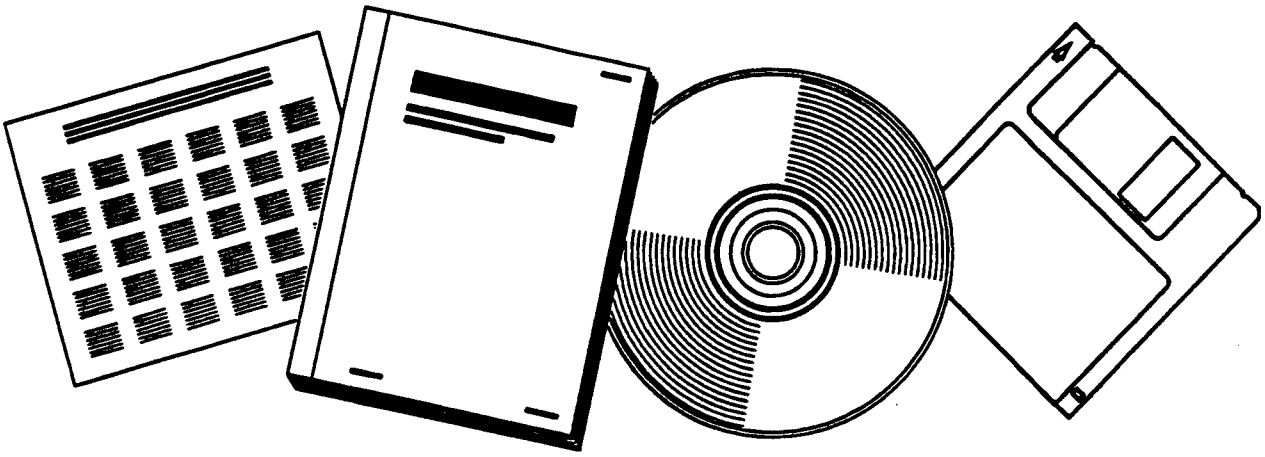

U.S. DEPARTMENT OF COMMERCE
National Technical Information Service

Exploratory Crash Tests of an FRP End-Terminal: FOIL Test Numbers 96F007, 96F016, 96F024, and 96F027

PUBLICATION NO. FHWA-RD-97-070

PB98-107014

JULY 1997

U.S. Department of Transportation
Federal Highway Administration

Research and Development
Turner-Fairbank Highway Research Center
6300 Georgetown Pike
McLean, VA 22101-2296

REPRODUCED BY: NTIS
U.S. Department of Commerce
National Technical Information Service
Springfield, Virginia 22161

FOREWORD

This report documents the test procedures used and the test results from four vehicle crash tests performed at the Federal Outdoor Impact Laboratory (FOIL) located at the Turner-Fairbank Highway Research Center (TFHRC). One of the most difficult problems to solve in the area of roadside safety hardware is how to terminate guardrail systems. Under a Small Business Innovation Research (SBIR) project, the Federal Highway Administration (FHWA) and Technology Development Associates (TDA) began exploring the use of composite materials in guardrail terminals. An "off-the-shelf" fiberglass reinforced plastic (FRP) box-section used for construction applications was targeted as a candidate for use in a guardrail terminal because preliminary pendulum tests showed that the FRP box-section had good energy-absorbing characteristics. The FRP box-section's ability to absorb energy and its availability led to research using full-scale vehicles impacting a guardrail terminal designed with the FRP box-section as the main component of the system. The results from these tests showed that the FRP box-section has potential as a guardrail terminal; however, it did not meet the safety performance criteria outlined in the National Cooperative Highway Research Program (NCHRP) report 350 that was used for the test setup procedures.

This report (FHWA-RD-97-070) contains test data, photographs taken with high-speed film, and a summary of the test results. The tests involved the FRP box-section terminal and a Ford Festiva traveling at 100 km/h.

This report will be of interest to all State departments of transportation, FHWA headquarters, region and division personnel, and highway safety researchers interested in the crashworthiness of roadside safety hardware.

A. George Ostensen, Director
Office of Safety and Traffic
Operations Research and Development

NOTICE

This document is disseminated under the sponsorship of the Department of Transportation in the interest of information exchange. The United States Government assumes no liability for its contents or use thereof. This report does not constitute a standard, specification, or regulation.

The United States Government does not endorse products or manufacturers. Trade and manufacturers' names appear in this report only because they are considered essential to the object of the document.

Technical Report Documentation Page

1. Report No. FHWA-RD-97-070 PB98-107014	Recipient's Catalog No.
4. Title and Subtitle EXPLORATORY CRASH TESTS OF AN FRP END-TERMINAL: FOIL TEST NUMBERS 96F007, 96F016, 96F024, AND 96F027	5. Report Date July 1997
	6. Performing Organization Code
7. Author(s) Christopher M. Brown	8. Performing Organization Report No.
9. Performing Organization Name and Address MiTech Incorporated 9430 Key West Avenue Suite 100 Rockville, MD 20850	10. Work Unit No. (TRAIS) 3A5F3142
	11. Contract or Grant No. DTFH61-94-C-00008
12. Sponsoring Agency Name and Address Office of Safety and Traffic Operations R&D Federal Highway Administration 6300 Georgetown Pike McLean, VA 22101-2296	13. Type of Report and Period Covered Test Report, Mar.-Dec. 1996
	14. Sponsoring Agency Code

15. Supplementary Notes
Contracting Officer's Technical Representative (COTR)- Richard King, HSR-20

16. Abstract

This report contains the results from four vehicle crash tests performed at the Federal Outdoor Impact Laboratory (FOIL) located at the Turner-Fairbank Highway Research Center (TFHRC) in McLean, Virginia. The tests conducted involved a fiberglass reinforced plastic (FRP) box-section terminal and a Ford Festiva traveling at 100 km/h. The purpose of these tests was to evaluate the safety performance of the FRP terminal and to provide data for future computer simulation models of the FRP terminal. The National Cooperative Highway Research Program (NCHRP) report 350 was used for the test setup procedures and the safety performance evaluation of the terminal. In addition to the instrumentation outlined in NCHRP 350, several transducers were added to provide computer simulation engineers with data from certain vehicle components. The results from these tests showed that the FRP box-section has potential as a guardrail terminal; however, it did not meet the safety performance criteria outlined in NCHRP 350. The data from on-board transducers will provide information for developing and validating finite element models (FEM) of roadside safety hardware. Results from the tests are presented as test summaries of data; graphs of data from the transducers affixed to the vehicles;and photographs taken before, during, and after the tests.

17. Key Words Fiberglass reinforced plastic, FRP, box-section, accelerometers, transducer, FOIL, Ford Festiva		18. Distribution Statement No restrictions. This document is available to the public through the National Technical Information Service, Springfield, VA 22161.	
19. Security Classif. (of this report) Unclassified	20. Security Classif. (of this page) Unclassified	21. No. of Pages 125	22. Price

Form DOT F 1700.7 (8-72) Reproduction of completed page authorized

SI* (MODERN METRIC) CONVERSION FACTORS

APPROXIMATE CONVERSIONS TO S' UNITS

Symbol	When You Know	Multiply By	To Find	Symbol
		LENGTH		
in	inches	25.4	millimeters	mm
ft	feet	0.305	meters	m
yd	yards	0.914	meters	m
mi	miles	1.61	kilometers	km
		AREA		
in^2	square inches	645.2	square millimeters	mm^2
ft^2	square feet	0.093	square meters	m^2
yd^2	square yards	0.836	square meters	m^2
ac	acres	0.405	hectares	ha
mi^2	square miles	2.59	square kilometers	km^2
		VOLUME		
fl oz	fluid ounces	29.57	milliliters	mL
gal	gallons	3.785	liters	L
ft^3	cubic feet	0.028	cubic meters	m^3
yd^3	cubic yards	0.765	cubic meters	m^3

NOTE: Volumes greater than 1000 l shall be shown in m^3.

		MASS		
oz	ounces	28.35	grams	g
lb	pounds	0.454	kilograms	kg
T	short tons (2000 lb)	0.907	megagrams (or "metric ton")	Mg (or "t")
		TEMPERATURE (exact)		
°F	Fahrenheit temperature	5(F-32)/9 or (F-32)/1.8	Celcius temperature	°C
		ILLUMINATION		
fc	foot-candles	10.76	lux	lx
fl	foot-Lamberts	3.426	candela/m^2	cd/m^2
		FORCE and PRESSURE or STRESS		
lbf	poundforce	4.45	newtons	N
lbf/in^2	poundforce per square inch	6.89	kilopascals	kPa

APPROXIMATE CONVERSIONS FROM SI UNITS

Symbol	When You Know	Multiply By	To Find	Symbol
		LENGTH		
mm	millimeters	0.039	inches	in
m	meters	3.28	feet	ft
m	meters	1.09	yards	yd
km	kilometers	0.621	miles	mi
		AREA		
mm^2	square millimeters	0.0016	square inches	in^2
m^2	square meters	10.764	square feet	ft^2
m^2	square meters	1.195	square yards	yd^2
ha	hectares	2.47	acres	ac
km^2	square kilometers	0.386	square miles	mi^2
		VOLUME		
mL	milliliters	0.034	fluid ounces	fl oz
L	liters	0.264	gallons	gal
m^3	cubic meters	35.71	cubic feet	ft^3
m^3	cubic meters	1.307	cubic yards	yd^3
		MASS		
g	grams	0.035	ounces	oz
kg	kilograms	2.202	pounds	lb
Mg (or "t")	megagrams (or "metric ton")	1.103	short tons (2000 lb)	T
		TEMPERATURE (exact)		
°C	Celcius temperature	1.8C + 32	Fahrenheit temperature	°F
		ILLUMINATION		
lx	lux	0.0929	foot-candles	fc
cd/m^2	candela/m^2	0.2919	foot-Lamberts	fl
		FORCE and PRESSURE or STRESS		
N	newtons	0.225	poundforce	lbf
kPa	kilopascals	0.145	poundforce per square inch	lbf/in^2

(Revised September 1993)

* SI is the symbol for the International System of Units. Appropriate rounding should be made to comply with Section 4 of ASTM E380.

TABLE OF CONTENTS

	Page
BACKGROUND	1
SCOPE	1
TEST MATRIX	2
VEHICLE	2
TEST ARTICLE	3
DATA SYSTEMS	3
Speed trap	11
Transducer data package	11
High-speed photography	11
DATA ANALYSIS	13
Speed trap	13
Transducer data package	13
High-speed photography	13
TEST RESULTS	14
CONCLUSIONS	15
APPENDIX A. PRE- AND POST-TEST PHOTOGRAPHS AND DATA PLOTS	24
REFERENCES	117

LIST OF FIGURES

Figure		Page
1.	Photographs of a typical test installation	4
2.	Photographs of the nose section and end-anchorage	5
3.	Photographs of the downstream end of the terminal	6
4.	Technical drawing for the system tested in test 96F027	7
5.	Overview of an FRP system installed at the FOIL	10
6.	FMVSS 208 transducer placements	12
7.	Test photographs during impact, test 96F007	16
8.	Test photographs during impact, test 96F016	17
9.	Test photographs during impact, test 96F024	18
10.	Test photographs during impact, test 96F027	19
11.	Summary of test 96F007	20
12.	Summary of test 96F016	21
13.	Summary of test 96F024	22
14.	Summary of test 96F027	23
15.	Pretest photographs, test 96F007	24
16.	Post-test photographs, test 96F007	26
17.	Pretest photographs, test 96F016	28
18.	Post-test photographs, test 96F016	30
19.	Pretest photographs, test 96F024	32
20.	Post-test photographs, test 96F024	34
21.	Pretest photographs, test 96F027	36
22.	Post-test photographs, test 96F027	38
23.	Acceleration vs. time, x-axis, test 96F007	40
24.	Acceleration vs. time, x-axis extended, test 96F007	41
25.	Velocity vs. time, x-axis, test 96F007	42
26.	Displacement vs. time, x-axis, test 96F007	43
27.	Occupant velocity and displacement vs. time, test 96F007	44
28.	Force vs. displacement, test 96F007	45
29.	Energy vs. displacement, test 96F007	46
30.	Acceleration vs. time, y-axis, test 96F007	47
31.	Occupant velocity and displacement vs. time, y-axis, test 96F007	48
32.	Acceleration vs. time, z-axis, test 96F007	49
33.	Pitch rate and angle vs. time, test 96F007	50
34.	Roll rate and angle vs. time, test 96F007	51
35.	Yaw rate and angle vs. time, test 96F007	52
36.	Acceleration vs. time, top of engine, test 96F007	53
37.	Acceleration vs. time, bottom of engine, test 96F007	54
38.	Acceleration vs. time, left control arm, test 96F007	55
39.	Acceleration vs. time, right control arm, test 96F007	56
40.	Acceleration vs. time, instrument panel, test 96F007	57
41.	Acceleration vs. time, right rear seat, test 96F007	58
42.	Acceleration vs. time, x-axis, test 96F016	59
43.	Acceleration vs. time, x-axis extended, test 96F016	60
44.	Velocity vs. time, x-axis, test 96F016	61
45.	Displacement vs. time, test 96F016	62
46.	Occupant velocity and displacement vs. time, x-axis, test 96F016	63
47.	Force vs. displacement, test 96F016	64

Figure | Page

48. Energy vs. displacement, test 96F016 65
49. Acceleration vs. time, y-axis, test 96F016 66
50. Occupant velocity and displacement vs. time, y-axis, test 96F016 67
51. Acceleration vs. time, z-axis, test 96F016 68
52. Pitch rate and angle vs. time, test 96F016 69
53. Roll rate and angle vs. time, test 96F016 70
54. Yaw rate and angle vs. time, test 96F016 71
55. Acceleration vs. time, top of engine, test 96F016 . . . 72
56. Acceleration vs. time, bottom of engine, test 96F016 . . 73
57. Acceleration vs. time, right control arm, test 96F016 . 74
58. Acceleration vs. time, instrument panel, test 96F016 . . 75
59. Acceleration vs. time, left rear seat, test 96F016 . . . 76
60. Acceleration vs. time, right rear seat, test 96F016 . . 77
61. Acceleration vs. time, x-axis, test 96F024 78
62. Acceleration vs. time, x-axis extended, test 96F024 . . 79
63. Velocity vs. time, x-axis, test 96F024 80
64. Displacement vs. time, x-axis, test 96F024 81
65. Occupant velocity and displacement vs. time, x-axis, test 96F024 82
66. Force vs. displacement, test 96F024 83
67. Energy vs. displacement, test 96F024 84
68. Acceleration vs. time, y-axis, test 96F024 85
69. Occupant velocity and displacement vs. time, y-axis, test 96F024 86
70. Acceleration vs. time, z-axis, test 96F024 87
71. Pitch rate and angle vs. time, test 96F024 88
72. Roll rate and angle vs. time, test 96F024 89
73. Yaw rate and angle vs. time, test 96F024 90
74. Acceleration vs. time, top of engine, test 96F024 . . . 91
75. Acceleration vs. time, bottom of engine, test 96F024 . . 92
76. Acceleration vs. time, left control arm, test 96F024 . . 93
77. Acceleration vs. time, right control arm, test 96F024 . 94
78. Acceleration vs. time, instrument panel, test 96F024 . . 95
79. Acceleration vs. time, left rear seat, test 96F024 . . . 96
80. Acceleration vs. time, right rear seat, test 96F024 . . 97
81. Acceleration vs. time, x-axis, test 96F027 98
82. Acceleration vs. time, x-axis extended, test 96F027 . . 99
83. Velocity vs. time, x-axis, test 96F027 100
84. Displacement vs. time, x-axis, test 96F027 101
85. Occupant velocity and displacement vs. time, x-axis, test 96F027 102
86. Force vs. displacement, test 96F027 103
87. Energy vs. displacement, test 96F027 104
88. Acceleration vs. time, y-axis, test 96F027 105
89. Occupant velocity and displacement vs. time, y-axis, test 96F027 106
90. Acceleration vs. time, z-axis, test 96F027 107
91. Pitch rate and angle vs. time, test 96F027 108
92. Roll rate and angle vs. time, test 96F027 109
93. Yaw rate and angle vs. time, test 96F027 110
94. Acceleration vs. time, top of engine, test 96F027 . . . 111
95. Acceleration vs. time, bottom of engine, test 96F027 . . 112

Figure | Page

96. Acceleration vs. time, right control arm, test 96F027 . 113
97. Acceleration vs. time, left control arm, test 96F027 . . 114
98. Acceleration vs. time, instrument panel, test 96F027 . . 115
99. Acceleration vs. time, right rear seat, test 96F027 . . 116

LIST OF TABLES

Table		Page
1.	Test matrix	2
2.	Vehicle parameters	2
3.	Camera configuration and placement	11
4.	Summary of the FRP composite terminal tests	14

BACKGROUND

One of the most difficult problems to solve in the area of roadside safety hardware is how to terminate guardrail systems. Under a Small Business Innovation Research (SBIR) project (phase II) the Federal Highway Administration (FHWA) and Technology Development Associates (TDA) began exploring the use of composite materials in guardrail terminals. More specifically, an "off-the-shelf" fiberglass reinforced plastic (FRP) box-section used for construction applications was targeted as a candidate for use in a guardrail terminal. Some preliminary pendulum tests showed that the FRP box-section had good energy-absorbing characteristics. The FRP box-section's ability to absorb energy, and its availability, led to further exploratory research using full-scale vehicles impacting a guardrail terminal designed with the FRP box-section as the main component of the system. The design principle of the terminal was to absorb the energy from a vehicle striking the terminal end-on, by tearing or ripping the FRP box-section with the bolts used to transition the fiberglass to standard w-beam rail element. Because this design is anticipated for use on the National Highway System (NHS), the National Cooperative Highway Research Program (NCHRP) Report 350 was used for the test setup procedures and the safety performance evaluation of the FRP terminal.[1]

SCOPE

This report documents the test procedures used and the test results from four vehicle crash tests performed at the Federal Outdoor Impact Laboratory (FOIL) located at the Tuner-Fairbank Highway Research Center (TFHRC) in McLean, Virginia. The crash tests were setup and conducted in accordance with the NCHRP 350 test designation 3-30. The tests conducted involved an FRP box-section terminal and a Ford Festiva traveling at 100 km/h. The purpose of these tests was to evaluate the safety performance of the FRP terminal and to provide data for future computer simulation models of the FRP terminal. One general concept of the terminal was tested; however, after analysis of each test, minor changes were made to the terminal design to enhance the safety performance during the subsequent tests. In addition to the instrumentation outlined in NCHRP 350, several transducers were added to provide computer simulation engineers with data from certain vehicle components. The vehicle component transducers were affixed to the vehicle in accordance with Federal Motor Vehicle Safety Standard 208 (FMVSS 208).[2] The results from these tests showed that the FRP box-section has potential as a guardrail terminal; however, it did not meet the safety performance criteria outlined in NCHRP 350. The data from on-board transducers will provide computer simulation engineers with information for developing and validating finite element models (FEM) of roadside safety hardware.

TEST MATRIX

Four vehicle crash tests were performed on the FRP terminal. The tests were set up following NCHRP test designation 3-30. Table 1 summarizes the nominal test conditions and matrix for the FRP terminal tests. The 820-kg vehicle used for these tests was the Ford Festiva two-door sedan.

Table 1. Test matrix.

Test Number	Date	Vehicle Weight (kg)	Impact angle	Nominal Speed (km/h)	Impact Location: Vehicle FRP Terminal	
96F007	3-13-96	820	0°	100	¼-point	Lead post
96F016	8-15-96	820	0°	100	¼-point	Lead post
96F024	10-22-96	820	0°	100	¼-point	Lead post
96F027	12-20-96	820	0°	100	¼-point	Lead post

VEHICLE

The test vehicles used were Ford Festiva two-door hatchbacks with manual transmissions. The vehicles were weighed and their inertial properties measured using the FOIL inertial measurement device (IMD). The vehicles were stripped of certain components to allow for the installation of data acquisition equipment, a remote brake system, and guidance carriages. No components were removed from the engine compartment. After the vehicles were instrumented, they were reweighed and their inertial properties remeasured. The target test weight for the vehicles was 820 kg. An anthropomorphic dummy was not placed in the vehicle. Table 2 lists physical properties and dimensions of the test vehicle before and after instrumentation (curb and ballasted).

Table 2. Vehicle parameters.

Test Number	Mode	Yr	VIN#	Weight (kg)	c.g. height (mm)	c.g. behind axle (mm)	Pitch inertia (kg-m²)	Roll inertia (kg-m²)	Yaw inertia (kg-m²)
96F007	Curb	88	KNJBT06K3J6132884	787	546	830	957	151	1039
	Ballasted	88	KNJBT06K3J6132884	816	533	833	950	167	1029
96F016	Curb	88	KNJBT06K8J6132735	756	520	800	914	217	1029
	Ballasted	88	KNJBT06K8J6132735	835	500	838	933	184	1032
96F024	Curb	90	KNJPT05H4L6147716	762	584	810	860	129	983
	Ballasted	90	KNJPT05H4L6147716	816	558	860	918	172	1036

Table 2. Vehicle parameters (continued).									
Test Number	Mode	Yr	VIN#	Weight (kg)	c.g. height (mm)	c.g. behind axle (mm)	Pitch inertia (kg-m²)	Roll inertia (kg-m²)	Yaw inertia (kg-m²)
96F027	Curb	93	KNJPT05H1P6134198	777	558	830	845	189	1010
	Ballasted	93	KNJPT05H1P6134198	820	544	838	911	195	1045

TEST ARTICLE

The FRP end-terminal was comprised of the same basic components for each of the four tests. However, some differences did exist between each test installation. A basic FRP terminal installation was comprised of an FRP composite box-section, a square composite nose piece, two standard breakaway cable terminal (BCT) posts, several extra-long breakaway CRT wood posts, a thrie beam panel and thrie beam to w-beam transition panel, and a steel weldment mounted inside the FRP box-section and affixed to the first downstream section of steel guardrail. Photographs depicting a typical test installation are shown in figure 1. Figure 2 shows photographs of the nose section and end-anchorage. The photographs in figure 3, of the downstream end of the terminal, show the bolts that tie the steel rail elements to the fiberglass beam and that will provide energy absorption as they tear through the fiberglass. Figure 4 is the technical drawing for the system tested in test 96F027. The systems tested in tests 96F007, 96F016, and 96F024 varied slightly from the design shown. Test 96F007 had a 4.3-m FRP box-section, rather than the 6.1-m length used in the other tests. In addition, in tests 96F007 and 96F016, a thrie beam to w-beam transition was attached to the composite beam instead of the 3.8-m thrie beam rail element shown. The wedge-shaped cutters that were added to the shear bolt-slots in tests 96F024 and 96F027 (shown in the drawing) to enhance the tearing action of the composite beam were not utilized in tests 96F007 and 96F016. The systems tested in tests 96F024 and 96F027 had minor differences. A wood spacer placed between the composite nose section and nose-weldment was installed for test 96F024, and was not added in test 96F027. Also, test 96F027 utilized four Z-brackets attached to the third and fourth posts to provide lateral support to the FRP composite box-section. Figure 5 is an overview of an FRP system installed at the FOIL. High-speed camera positions are included in the drawing.

DATA SYSTEMS

Three data systems were used to record data from the four crash tests. The systems were a speed trap, a transducer data package, and high-speed photography.

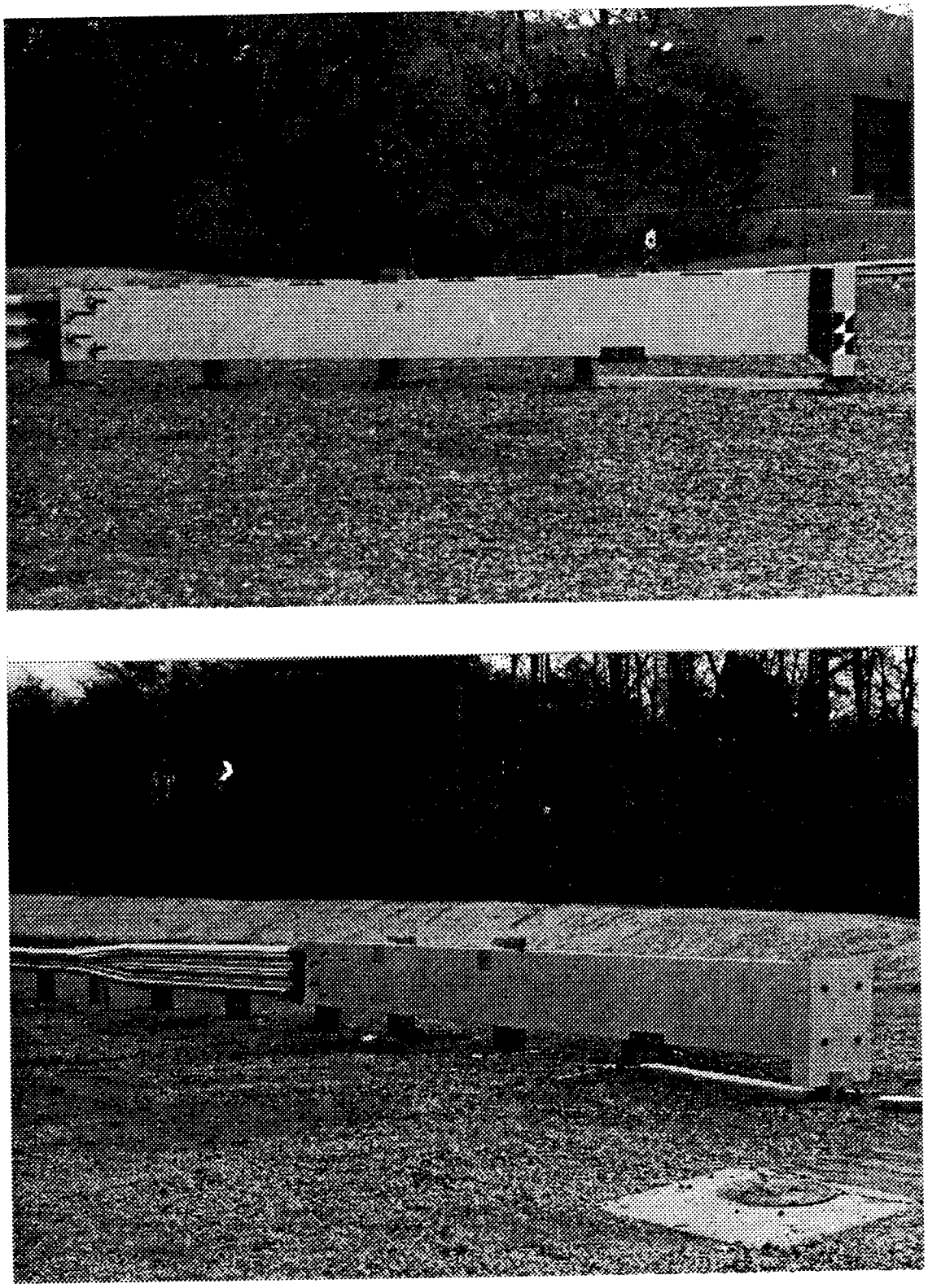

Figure 1. Photographs of a typical test installation.

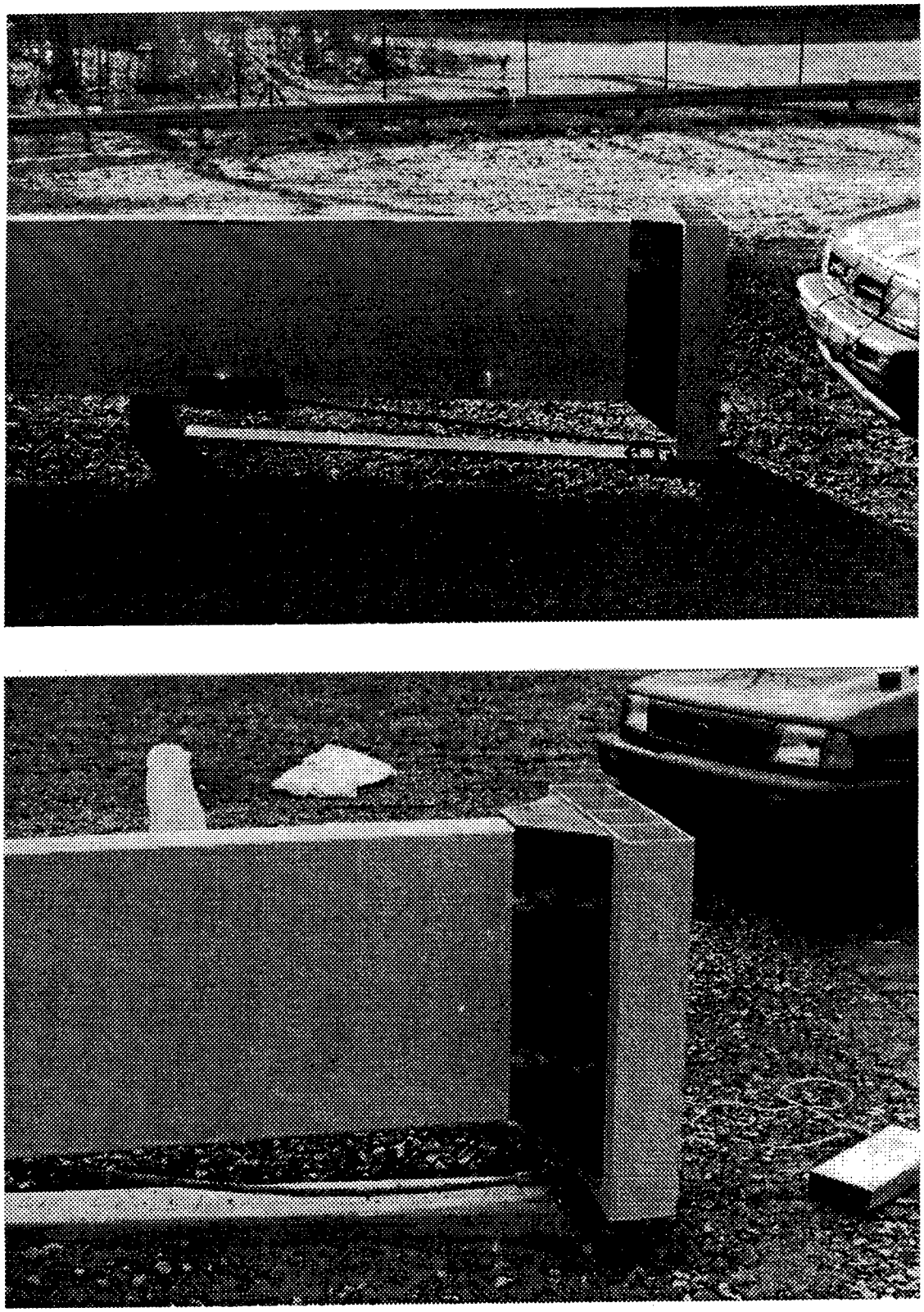

Figure 2. Photographs of the nose section and end-anchorage.

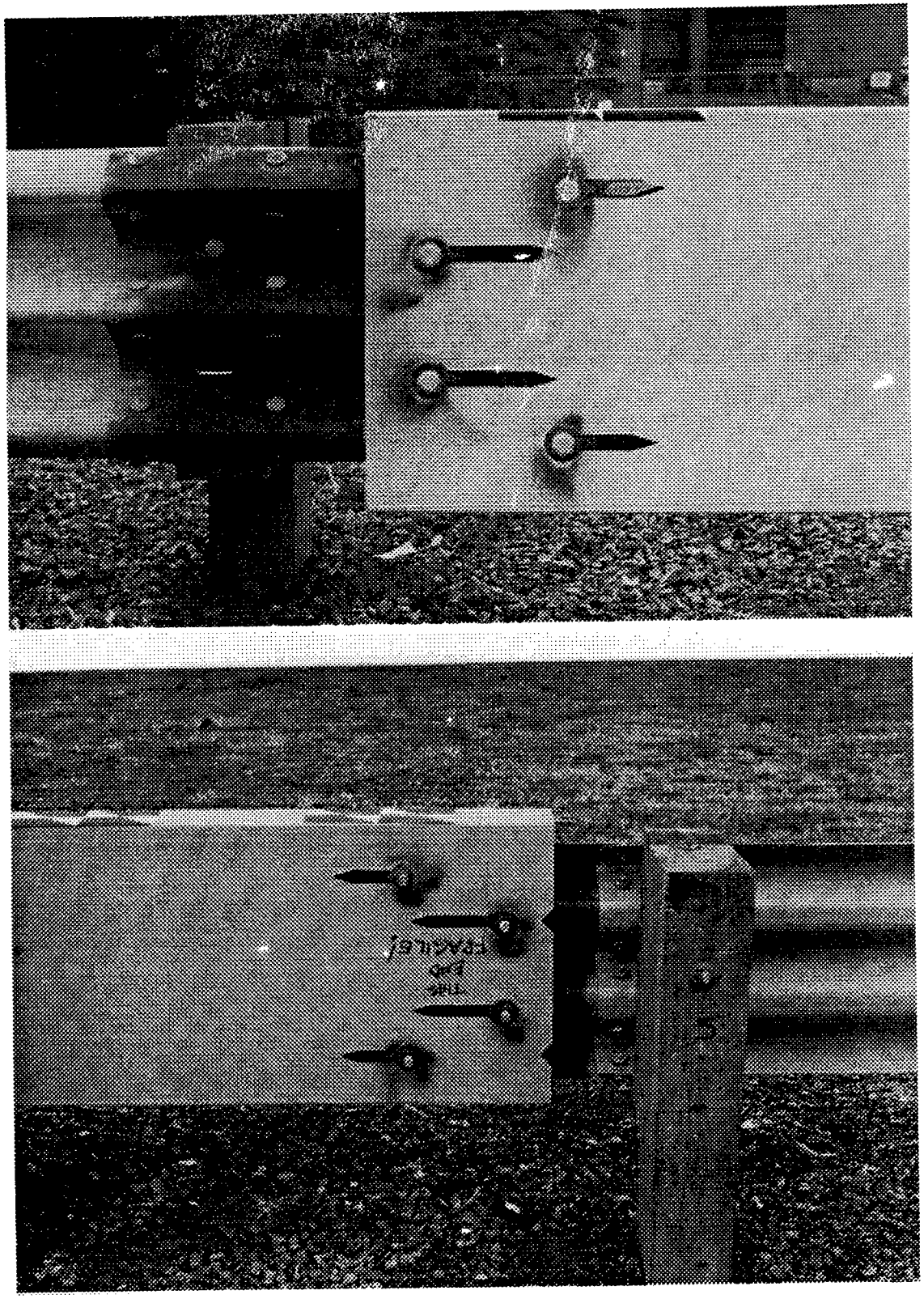

Figure 3. Photographs of the downstream end of the terminal.

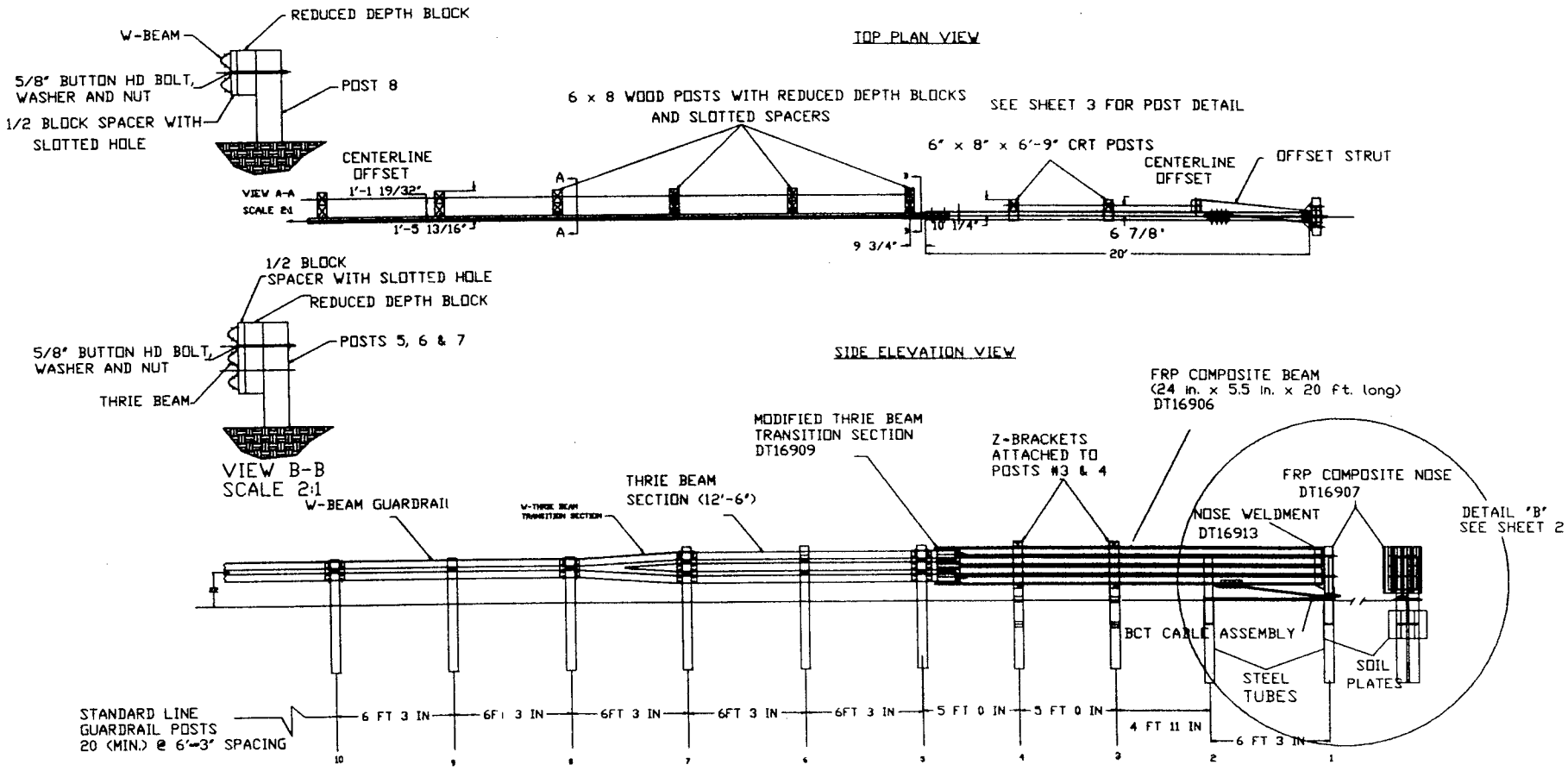

TECHNOLOGY DEVELOPMENT ASSOCIATES, INC.

992 OLD EAGLE SCHOOL ROAD, SUITE 910
WAYNE, PA 19087

1 in = 25.4 mm
1 ft = 0.305 m

Figure 4. Technical drawing for the system tested in test 96F027.

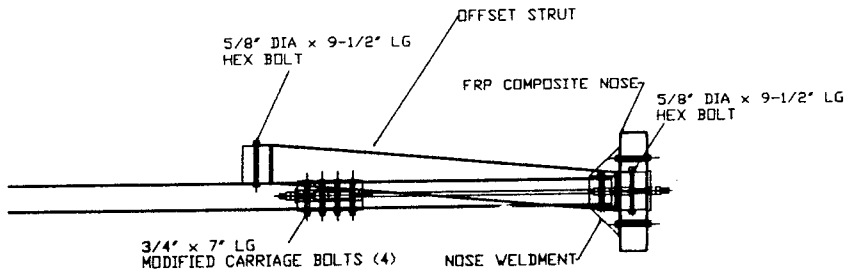

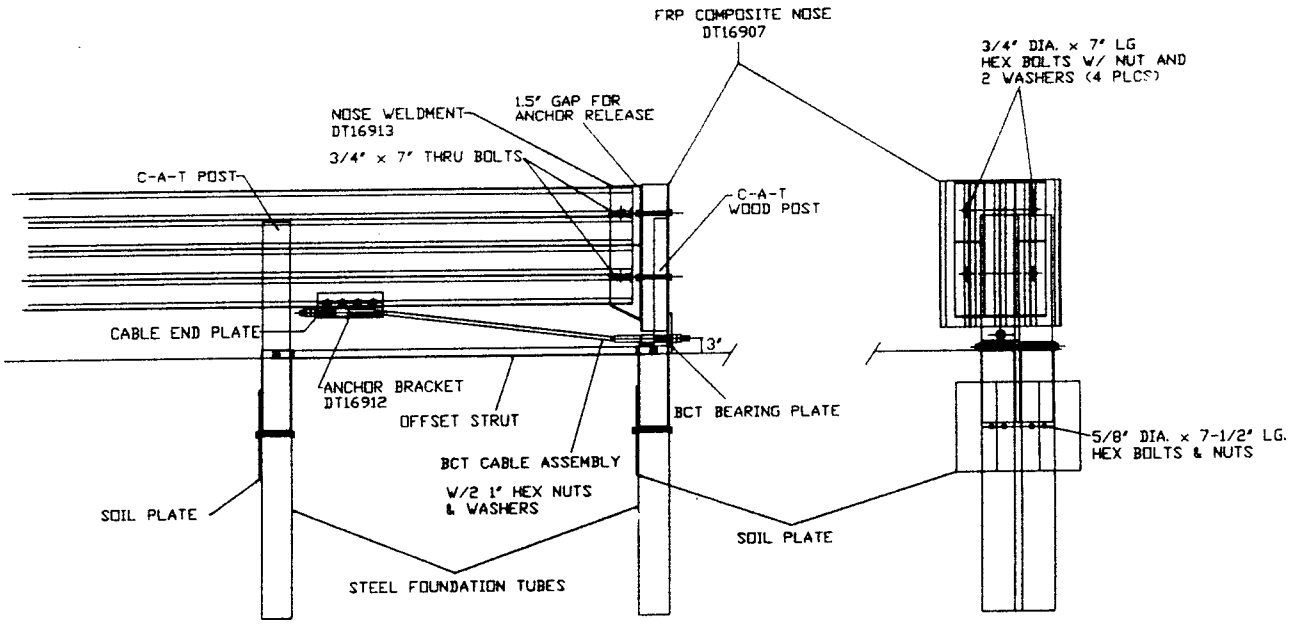

TECHNOLOGY DEVELOPMENT ASSOCIATES, INC.

992 OLD EAGLE SCHOOL ROAD, SUITE 910
WAYNE, PA 19087

1 in = 25.4 mm
1 ft = 0.305 m

Figure 4. Technical drawing for the system tested in test 96F027 (continued).

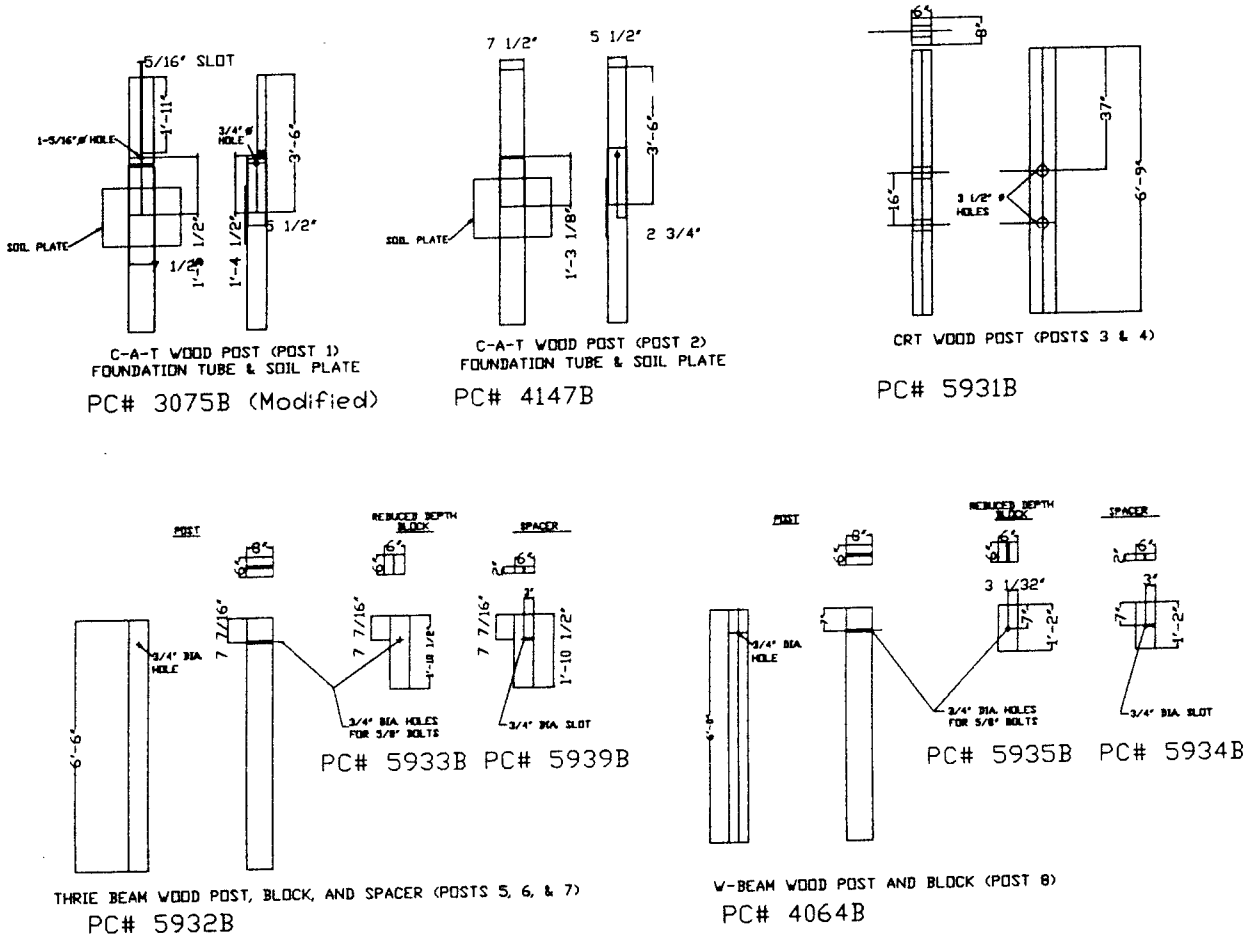

1 in = 25.4 mm
1 ft = 0.305 m

Figure 4. Technical drawing for the system tested in test 96F027 (continued).

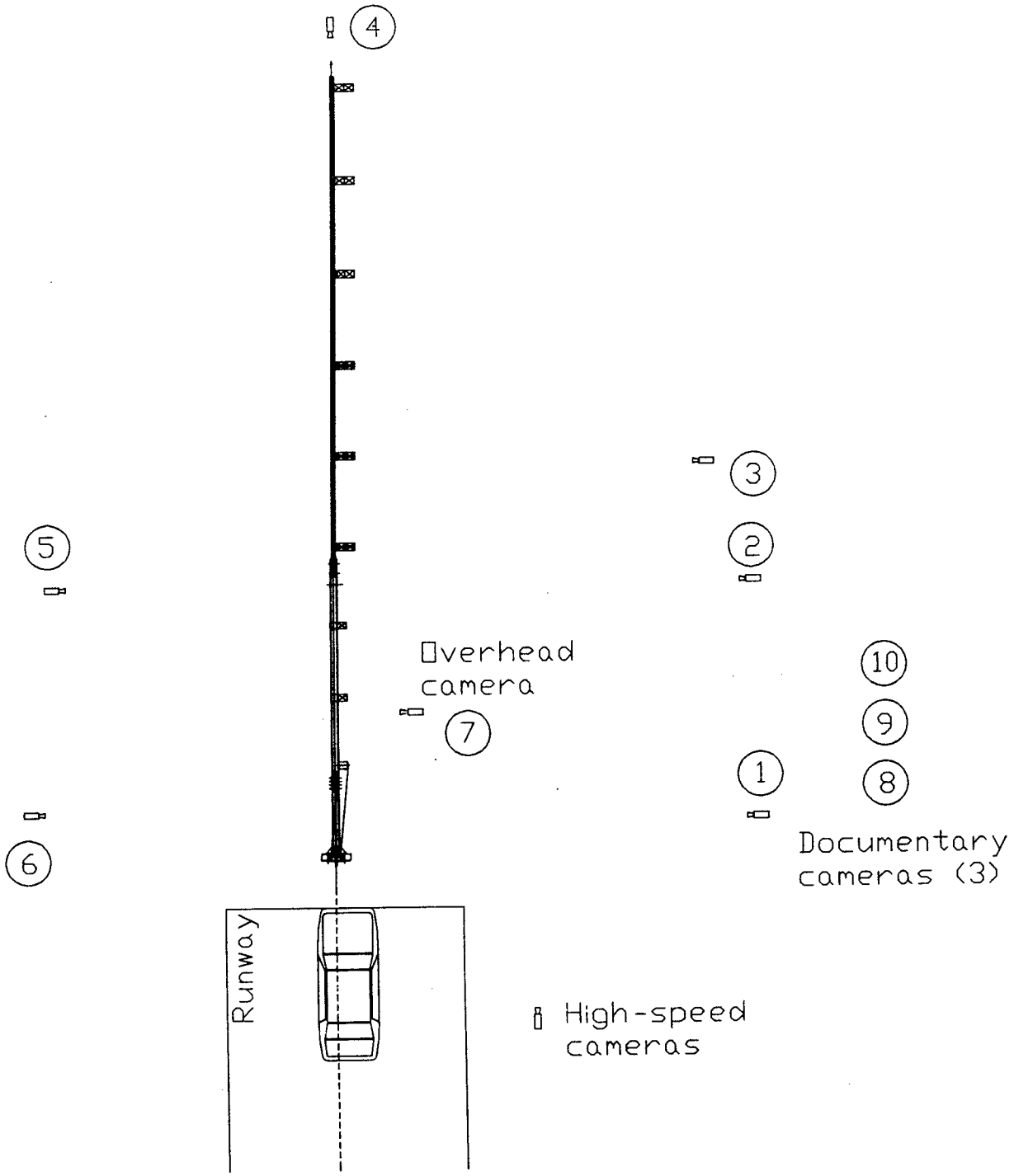

Figure 5. Overview of an FRP system installed at the FOIL.

Speed trap. A set of five contact switches were mounted to the FOIL runway just prior to the FRP terminal. As the vehicle passed over each of the contact switches, a 1.5V pulse was recorded. The five 1.5V pulses were later analyzed to determine the vehicle speed just prior to contact with the FRP terminal.

Transducer data package. Fourteen transducers consisting of 11 accelerometers and 3 rate transducers were affixed to the test vehicle. Four of the accelerometers and the three rate transducers were attached to the vehicle as close as possible to the vehicle center-of-gravity (c.g.). The remaining accelerometers were attached to various vehicle components as shown in FMVSS 208. Figure 6 is a sketch of the Ford Festiva with transducer locations.

High-speed photography. The test was photographed using seven high-speed cameras, one real-time camera, and two 35-mm still cameras. All high-speed cameras were loaded with Kodak 2253 color daylight film and the real-time camera was loaded with Kodak 7239 color film. One 35-mm camera was loaded with black and white print film and the other was loaded with 35-mm color slide film. The camera placements are summarized in table 3. The camera numbers in table 3 are also shown in figure 5.

Table 3. Camera configuration and placement.

Camera Number	Type	Film Speed (frames/s)	Lens (mm)	Location
1	Locam II	500	50	90° to impact rt. side
2	Photec	500	80	90° to shear bolts
3	Locam II	500	20	overall, rt. side
4	Locam II	500	25	180° to impact on berm
5	Locam II	500	75	90° to shear bolts
6	Locam II	500	50	90° to impact lft. side
7	Locam II	500	10	overhead, over terminal
8	Bolex	24	zoom	documentary
9	Canon A-1 (prints)	still	zoom	documentary
10	Canon A-1 (slides)	still	zoom	documentary

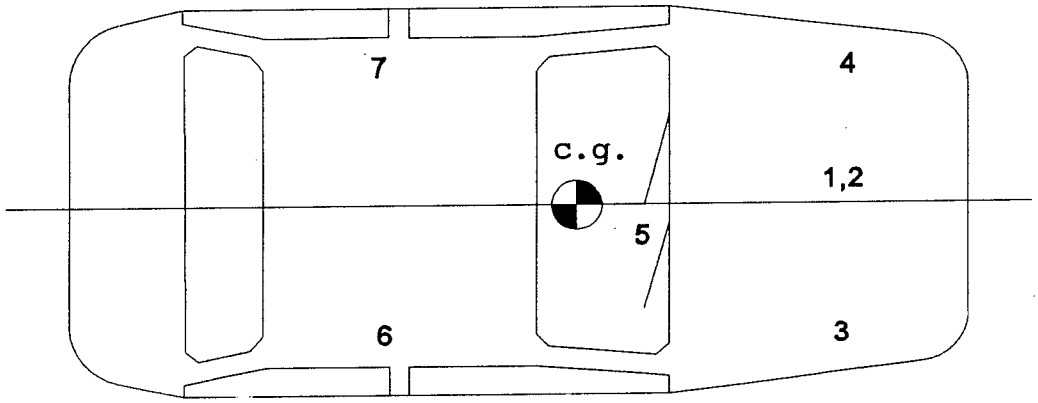

Location	Data	Full scale	(X,Y,Z) position* (mm)
1	Top of engine	2000 g	140;813;508
2	Bottom of engine	2000 g	178;813;13
3	Right control arm	2000 g	127;127;0
4	Left control arm	2000 g	127;1372;0
5	Top of instrument panel	2000 g	-495;800;660
6	Right side under rear seat	2000 g	-1727;445;178
7	Left side under rear seat	2000 g	-1727;1143;178
c.g.	Rate transducer	500 °/s	-813;787;152
c.g.	Longitudinal acceleration	100 g	-813;787;152
c.g.	Lateral acceleration	100 g	-813;787;152
c.g.	Vertical acceleration	100 g	-813;787;152
c.g.	Longitudinal acceleration	100 g	-813;787;152
* Referenced from the center of the right wheel hub.			

Figure 6. FMVSS 208 transducer placements.

DATA ANALYSIS

Data was gathered and analyzed from a speed trap, on-board transducers, and high-speed photography.

Speed trap. The speed trap consisted of a set of five contact switches fastened to the runway at 0.3-m intervals. The center of the speed trap was placed approximately 1.8 m from the FRP terminal impact point. As the vehicle passed over the switches, electronic pulses were recorded on analog tape. The tape was played back through a Data Translation Analog/Digital (A/D) converter inside a Compaq Systempro computer. The time intervals between the first pulse and each of the subsequent four pulses were then obtained using the analysis software provided with the A/D converter. The time-displacement data was imported into a computer spreadsheet and a linear regression was performed to determine the best-line fit of the data points. The impact velocity was then determined from the slope of the best-line fit of the time-displacement data.

Transducer data package. The data from all transducers were digitally recorded and converted to the ASCII format. The sampling rate during data acquisition was 4000 Hz for data recorded via the FOIL umbilical cable (c.g. accelerometers) and 12,500 Hz for data recorded via the ODAS III on-board system (rate transducers and FMVSS component accelerometers). The ASCII files were processed, which included removal of zero-bias, storing the region of interest, and digitally filtering the data to 300 Hz (Class 180). The 300-Hz data were imported into a spreadsheet for plotting and analysis. Evaluation criteria calculations were performed on the data as described in NCHRP Report 350.

High-speed photography. The crash event was recorded on 16-mm film by seven high-speed cameras. Primarily, the overhead camera was the only camera used for high-speed film analysis. Analysis of the crash event was performed using a NAC Film Motion Analyzer model 160-F in conjunction with an IBM PC-AT. The motion analyzer digitized the 16-mm film, reducing the image to Cartesian coordinates. Using the Cartesian coordinate data, a time-displacement history of the test was obtained. The time-displacement data were then imported into a computer spreadsheet and a linear regression was performed to determine the impact velocity of the vehicle. Using the Cartesian coordinate data and trigonometry, the impact, exit, pitch, yaw, and roll angle data were determined. Film analysis data were used in the event of electronic data channel failure. The speed trap data were used as the primary measurement for impact velocity.

TEST RESULTS

During each of the four composite end-terminal tests, the driver-side ¼-point of the Ford Festiva struck the FRP composite end-terminal at the centerline of the composite box-section as intended. The sequence of events was similar during each crash test. Within the first 0.006 s, the vehicle collapsed the composite nose section as its front end collapsed. The first BCT post fractured at the foundation tube and the tension in the anchor-cable was released. At that time, the load was born by the composite beam and the beam was ripped by the downstream weldment and bolts. The four weldment bolts reached the end of the slots at different times. The top and bottom bolts bottomed out at approximately 0.020 s; approximately 0.002 s later, the two inside or middle bolts reached the end of the slots. The end of the FRP section and the nose piece sustained significantly more damage in tests 96F016 and 96F027. The nose section was dislodged from the FRP section during test 96F016. The amount of crush stroke of the FRP composite varied between tests. The off-center load induced a high rate of yaw into the vehicles and the vehicles spun counterclockwise between 3/4 and 1 full rotation. The vehicle remained upright during all four tests. After the tests, each FRP box-section was cross-sectioned with a safety saw to observe the weldment and thrie beam inside the FRP beam. Significant amounts of fiberglass material had built up inside the box-section between the transition elements. No significant differences were noticed between tests. Table 4 summarizes the data from each test. Photographs taken of the collision event with high-speed film are shown in figures 7 through 10. NCHRP Report 350 summary pages are shown in figures 11 through 14. Pre- and post-test photographs of each test and data plots from each test recorded by the on-board transducers are shown in Appendix A.

Table 4. Summary of the FRP composite terminal tests.

DATA	96F007	96F016	96F024	96F027
Impact speed (km/h)	100.7	95.0	97.2	97.8
Impact energy (kJ)	320	291	297	303
Longitudinal OIV (m/s)	12.8	12.3	13.6	12.6
Time OIV occurred (s)	0.097	0.099	0.095	0.096
Longitudinal ridedown (g's)	14.9	5.5	11.7	9.1
Vehicle crush (mm)	502	514	400	355
FRP box-section stroke (mm)	1257.3	317.5	1130.3	533.4
Longitudinal 50-ms average g's	18.2	17.7	19.1	17.8
Peak g's: Longitudinal	35.0	32.1	44.4	37.2

Table 4. Summary of the FRP composite terminal tests (cont'd).				
DATA	**96F007**	**96F016**	**96F024**	**96F027**
Peak g's: Lateral	22.0	19.1	20	19.8
Lateral OIV (m/s)	2.2	4.3	2.4	3.8
Time OIV occurred (s)	0.428	0.509	0.455	0.416
Lateral ridedown (g's)	2.5	8.0	1.5	2.6

CONCLUSIONS

The results show that the ability of the FRP terminal to split and tear (greater crush stroke) does not correlate with better or lower occupant impact velocity (OIV). The results indicate that the test with the least amount of FRP composite shear (test 94F016) produced the lowest OIV (12.3 m/s), while the two tests with greater FRP composite shear produced the highest OIV. This suggests that a minimum FRP shear of 317.5 mm, coupled with the energy consumed by the vehicle crush, nose piece deformation, tension cable release, and fracture of the lead post, was enough energy dissipation to produce occupant impact velocities higher than the acceptable limits specified by NCHRP 350. The occupant impact velocity values for each test occurred at essentially the same time during the event. This further suggests that the crucial events are occurring before significant tearing of the FRP box-section. The differences in FRP box-section shear (crush stroke) may be a result of the nose piece's interaction with the vehicle's front end. The two tests that yielded the largest FRP crush stroke were the two tests with the least amount of damage to the up-stream end of the FRP box-section and nose piece. During tests 96F016 and 96F027, the vehicle started to penetrate under the nose piece, and the nose piece and box-section began to rise up the vehicle's hood. As the vehicle continued forward, the nose piece pivoted counterclockwise around the FRP beam. The up-stream end of the box-section was split and torn apart, and the nose piece was dislodged from the terminal or was ripped and fragmented. In the tests with larger FRP shear, the nose piece captured the vehicle's front end better, which allowed the vehicle to maintain the principal direction of force along the centerline of the FRP box-section. However, improvement of the current beam's ability to shear longer may not improve or lower the occupant risk values. An FRP composite beam with a lower force requirement for shear may help reduce the occupant risk.

Electronic data and high-speed film photographs were successfully obtained during each test. This data will provide simulation engineers with essential information for developing and validating computer-generated models of this end-terminal system.

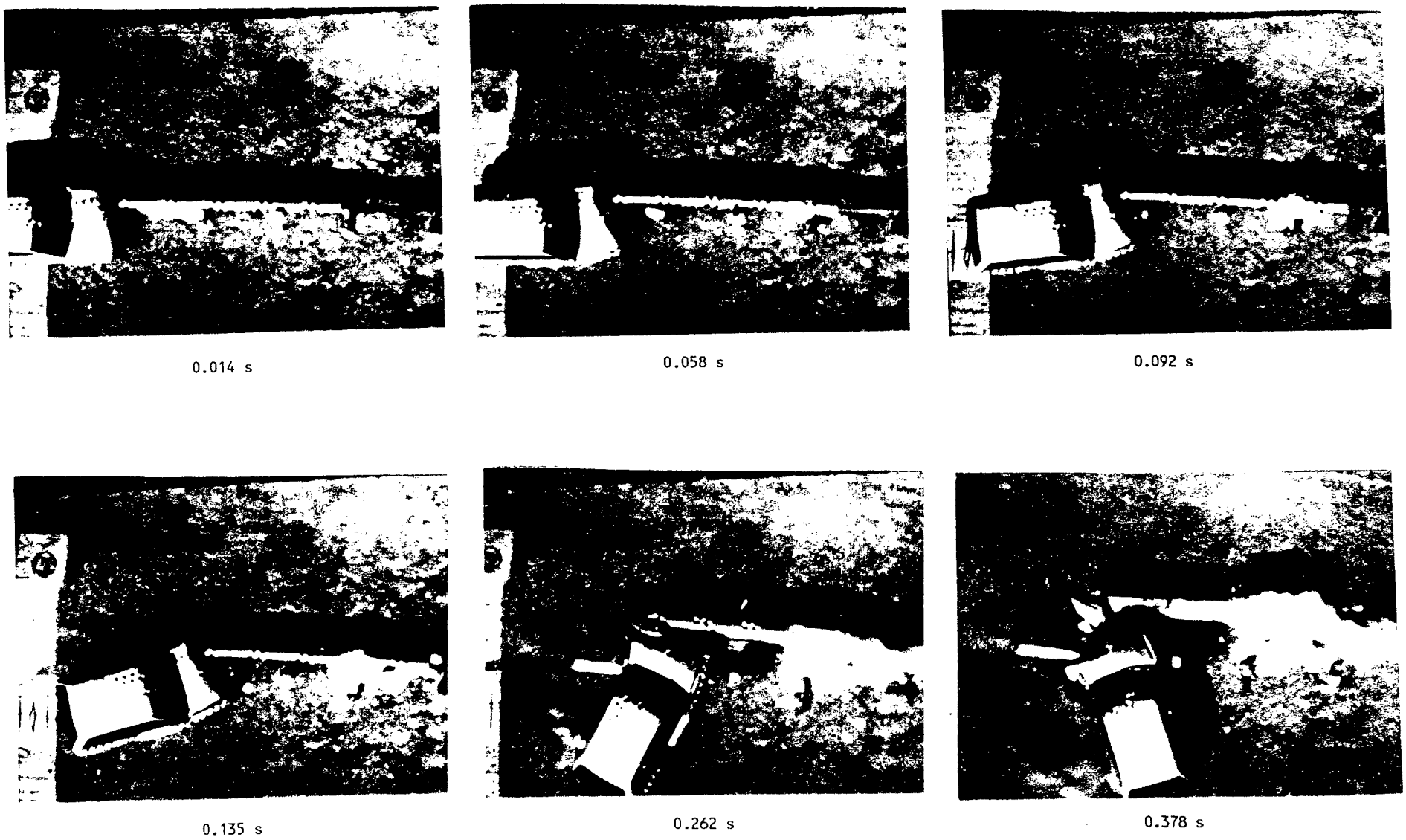

Figure 7. Test photographs during impact, test 96F007.

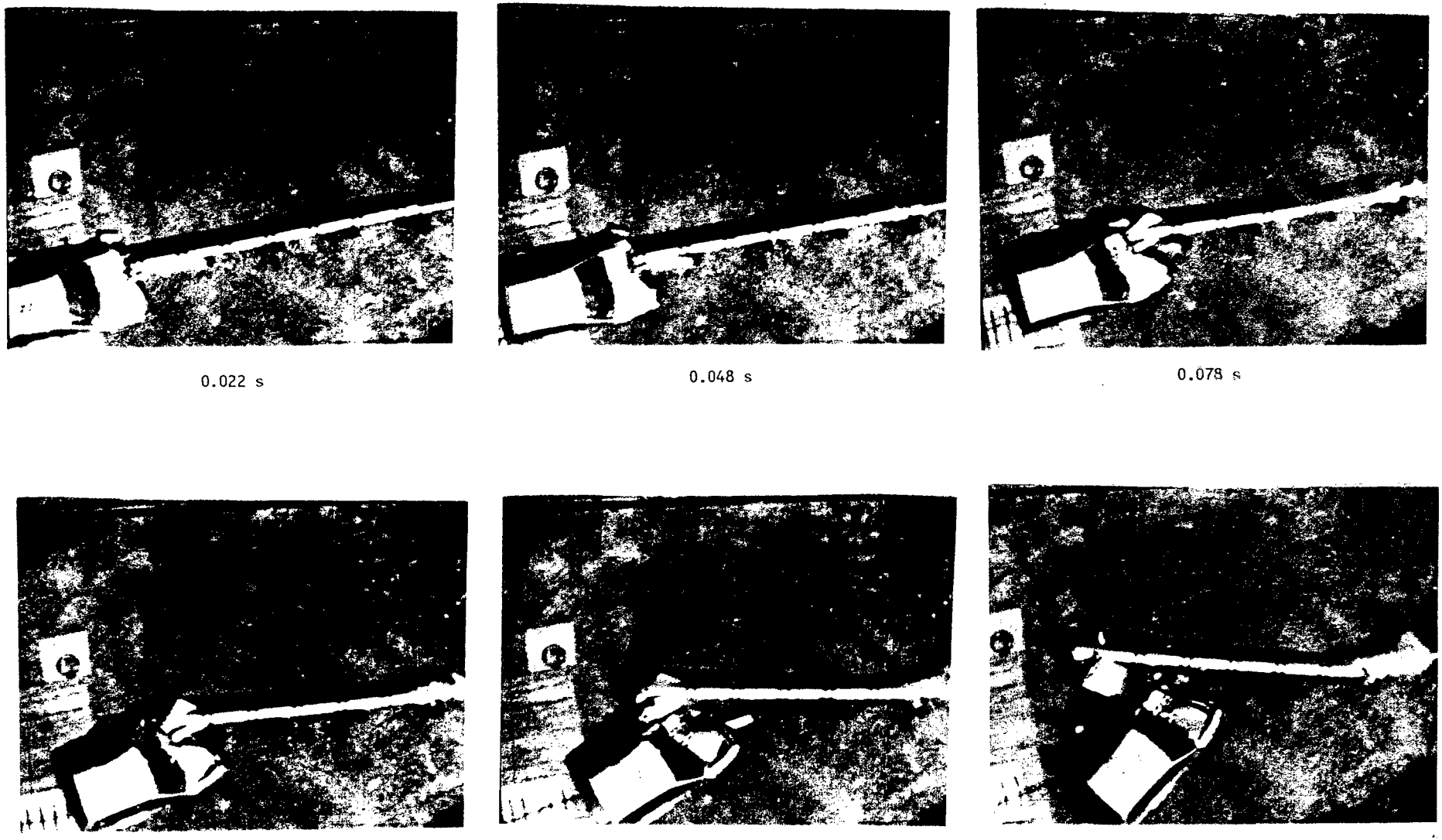

Figure 8. Test photographs during impact, test 96F016.

Figure 9. Test photographs during impact, test 96F024.

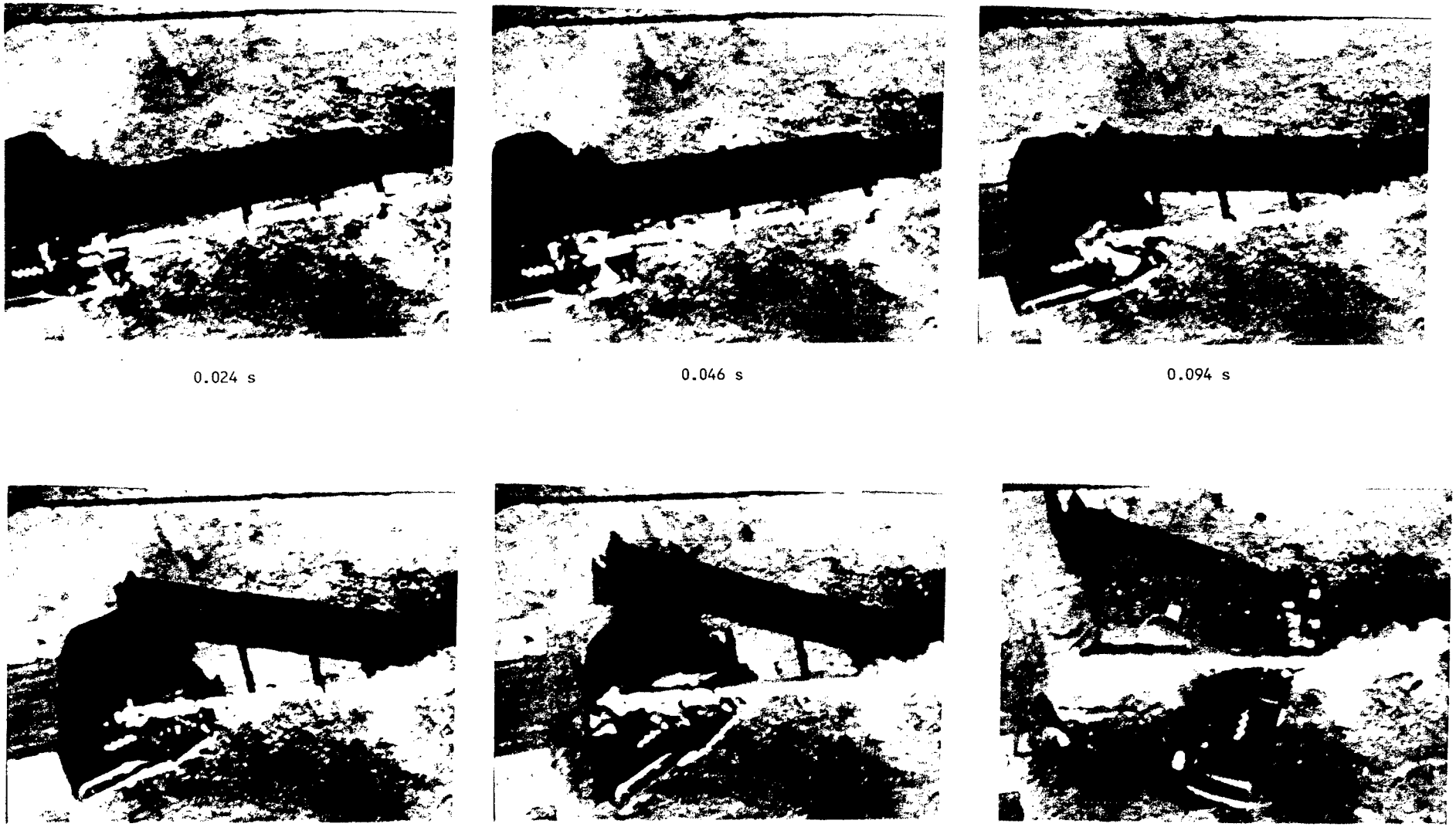

Figure 10. Test photographs during impact, test 96F027.

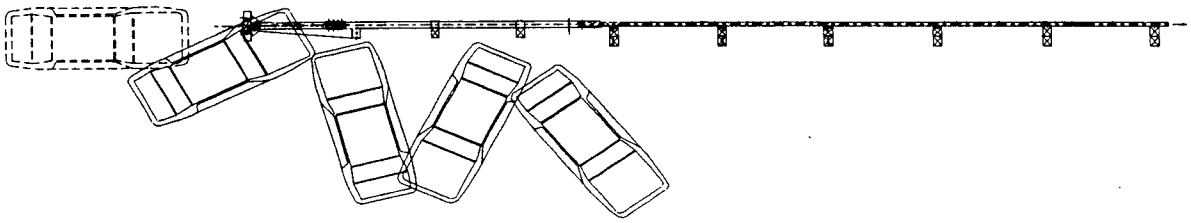

Test number.....96F007

Date.....March 13, 1996

Test vehicle.....1988 Ford Festiva

Vehicle weight.....816 kg

Test article.....FRP composite

Total length.....45 m
Terminal.....6.5 m
FRP box-section length.....4.3 m

Guardrail type.....12 gauge w-beam

Rail height.....685 mm

Foundation.....FOIL clay

Impact speed.....100.7 km/h

Impact angle.....0°

Impact location.....Driver 1/4-point

Vehicle analysis:	Observed	Design/Limit
Longitudinal:		
Occupant Delta V at 0.6 m.....	12.8 m/s	9/12 m/s
Ridedown acceleration.....	14.9 g's	15/20 g's
Lateral:		
Occupant Delta V at 0.3 m.....	2.2 m/s	9/12 m/s
Ridedown acceleration.....	2.5 g's	15/20 g's

Peak 50 ms acceleration:
Longitudinal.....18.2 g's
Lateral.....NA

Vehicle Damage:
Traffic Accident Data (TAD).....12-FL-5
Vehicle Damage Index (VDI).....12FYEW5

Vehicle crush.....502 mm

FRP crush stroke.....1257 mm

Figure 11. Summary of test 96F007.

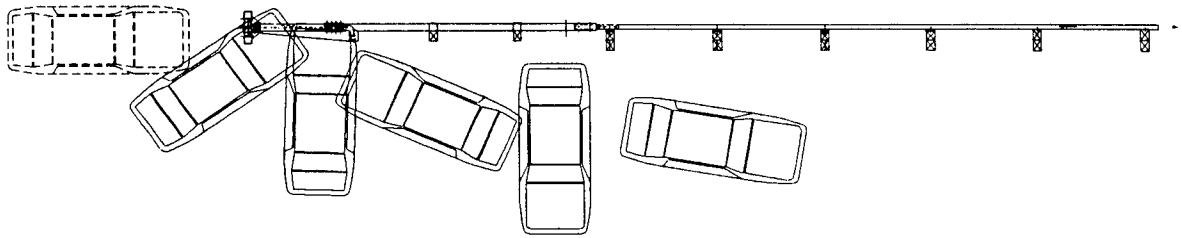

Test number.....96F016

Date.....August 15, 1996

Test vehicle.....1988 Ford Festiva

Vehicle weight.....835 kg
No dummy

Test article.....FRP composite

Total length.....45 m
Terminal.....8.3 m
FRP box-section length.....6.1 m

Guardrail type.....12 gauge w-beam

Rail height.....685 mm

Foundation.....FOIL clay

Impact speed..... .....95 km/h

Impact angle.....0°

Impact location.....Driver 1/4-point

Vehicle analysis:	Observed	Design/Limit
Longitudinal:		
Occupant Delta V at 0.6 m.....	12.3 m/s	9/12 m/s
Ridedown acceleration.....	5.5 g's	15/20 g's
Lateral:		
Occupant Delta V at 0.3 m.....	4.3 m/s	9/12 m/s
Ridedown acceleration.....	8.0 g's	15/20 g's

Peak 50 ms acceleration:
Longitudinal.....17.7 g's
Lateral.....NA

Vehicle Damage:

Traffic Accident Data (TAD).....12-FL-5
Vehicle Damage Index (VDI).....12FYEW5

Vehicle crush.....514 mm

FRP crush stroke.....318 mm

Figure 12. Summary of test 96F016.

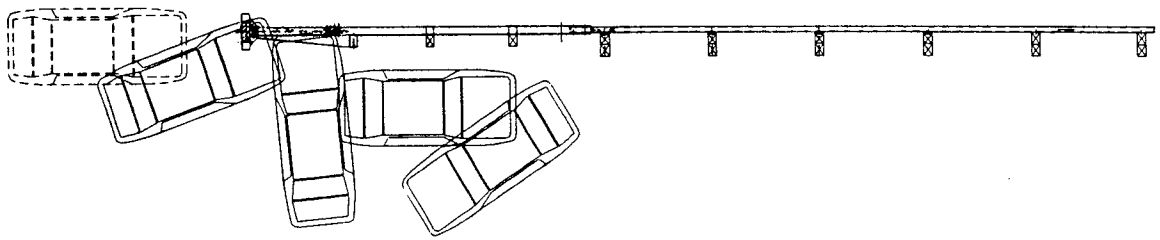

Test number.....96F024

Date.....October 22, 1996

Test vehicle.....1990 Ford Festiva

Vehicle weight.....816 kg
No dummy

Test article.....FRP composite

Total length.....45 m
Terminal.....12.2 m
FRP box-section length.....6.1 m

Guardrail type.....12 gauge w-beam

Rail height.....685 mm

Foundation.....FOIL clay

Impact speed.....97.2 km/h

Impact angle.....0°

Impact location.....Driver 1/4-point

Vehicle analysis:	Observed	Design/Limit
Longitudinal:		
Occupant Delta V at 0.6 m	13.6 m/s	9/12 m/s
Ridedown acceleration	11.7 g's	15/20 g's
Lateral:		
Occupant Delta V at 0.3 m	2.4 m/s	9/12 m/s
Ridedown acceleration	1.5 g's	15/20 g's

Peak 50 ms acceleration:
Longitudinal.....19.1 g's
Lateral.....NA

Vehicle Damage:
Traffic Accident Data (TAD).....12-FL-5
Vehicle Damage Index (VDI).....12FYEW5

Vehicle crush.....400 mm

FRP crush stroke.....1130 mm

Figure 13. Summary of test 96F024.

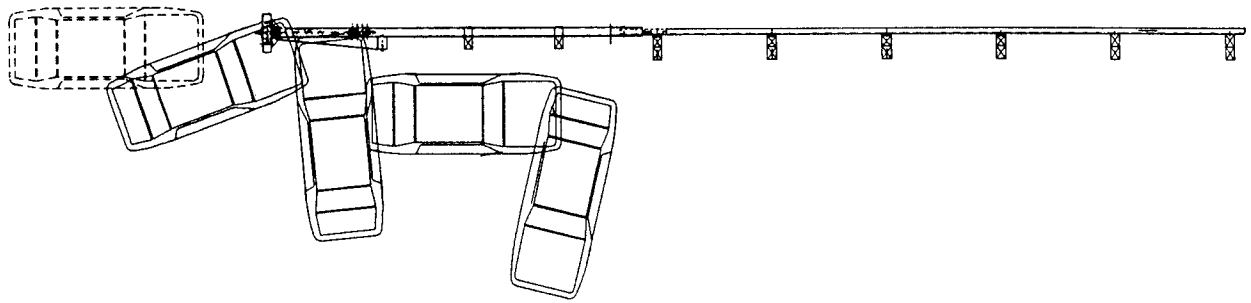

Test number.....96F027

Date.....December 20, 1996

Test vehicle.....1993 Ford Festiva

Vehicle weight.....820 kg
No dummy

Test article.....FRP composite

Total length.....45 m
Terminal.....12.2 m
FRP box-section length.....6.1 m

Guardrail type.....12 gauge w-beam

Rail height.....685 mm

Foundation.....FOIL clay

Impact speed.....97.8 km/h

Impact angle.....0°

Impact location.....Driver 1/4-point

Vehicle analysis:	Observed	Design/Limit
Longitudinal:		
Occupant Delta V at 0.6 m	12.6 m/s	9/12 m/s
Ridedown acceleration	9.1 g's	15/20 g's
Lateral:		
Occupant Delta V at 0.3 m	3.8 m/s	9/12 m/s
Ridedown acceleration	2.6 g's	15/20 g's

Peak 50 ms acceleration:
Longitudinal.....17.8 g's
Lateral.....NA

Vehicle Damage:
Traffic Accident Data (TAD).....12-FD-6
Vehicle Damage Index (VDI).....12FDAW6

Vehicle crush.....355 mm

FRP crush stroke.....533 mm

Figure 14. Summary of test 96F027.

APPENDIX A. PRE- AND POST-TEST PHOTOGRAPHS AND DATA PLOTS.

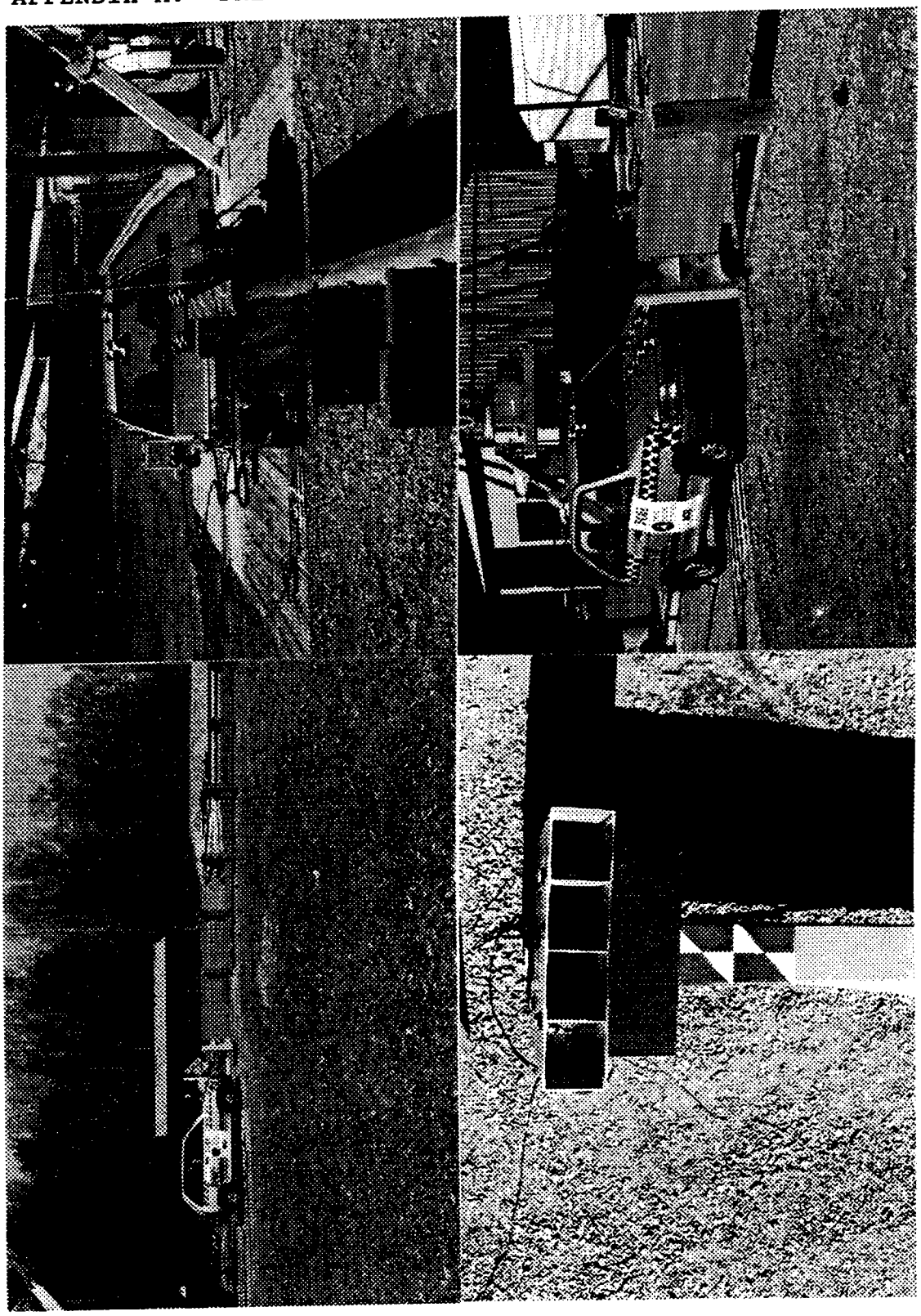

Figure 15. Pretest photographs, test 96F007.

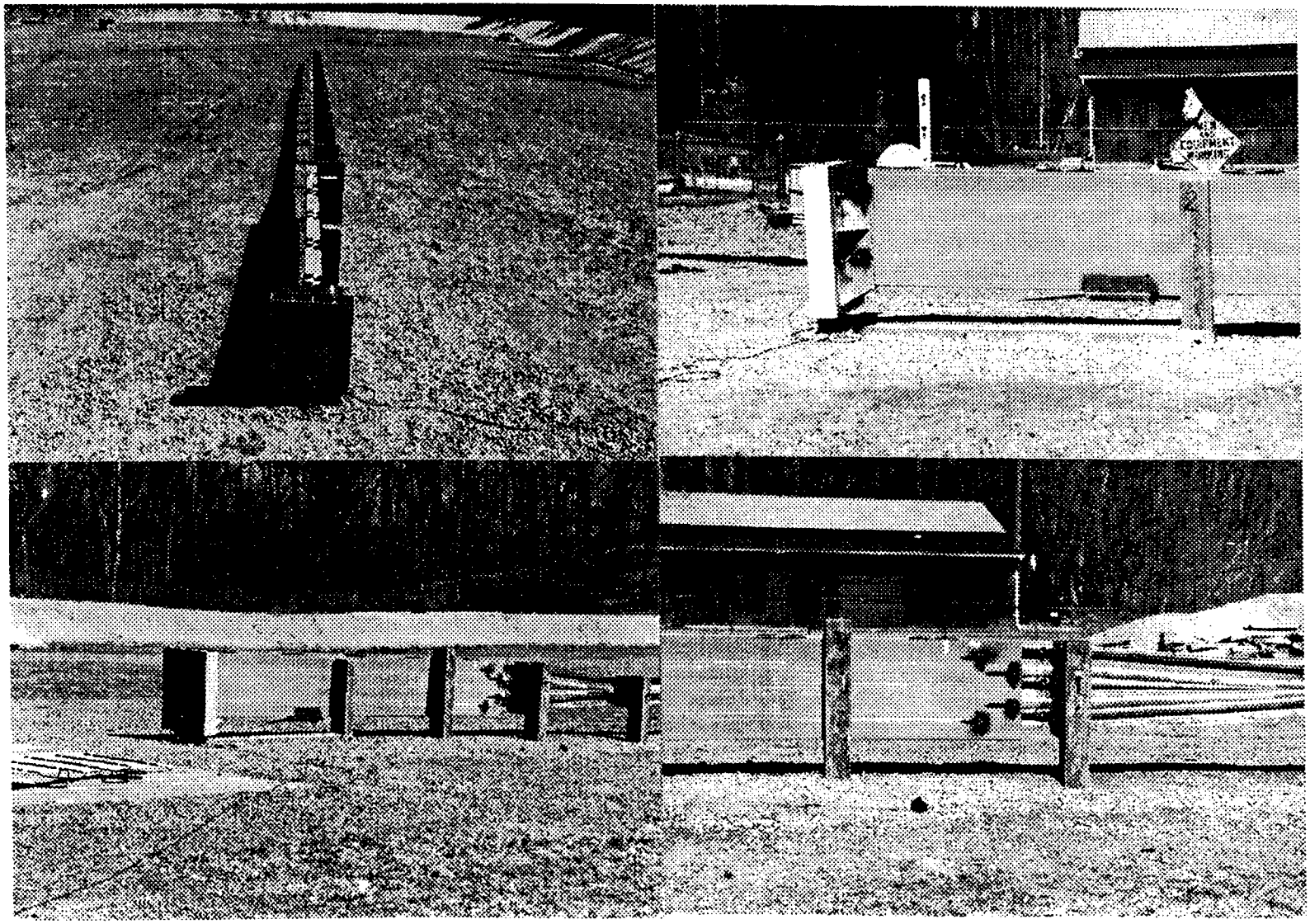

Figure 15. Pretest photographs, test 96F007 (continued).

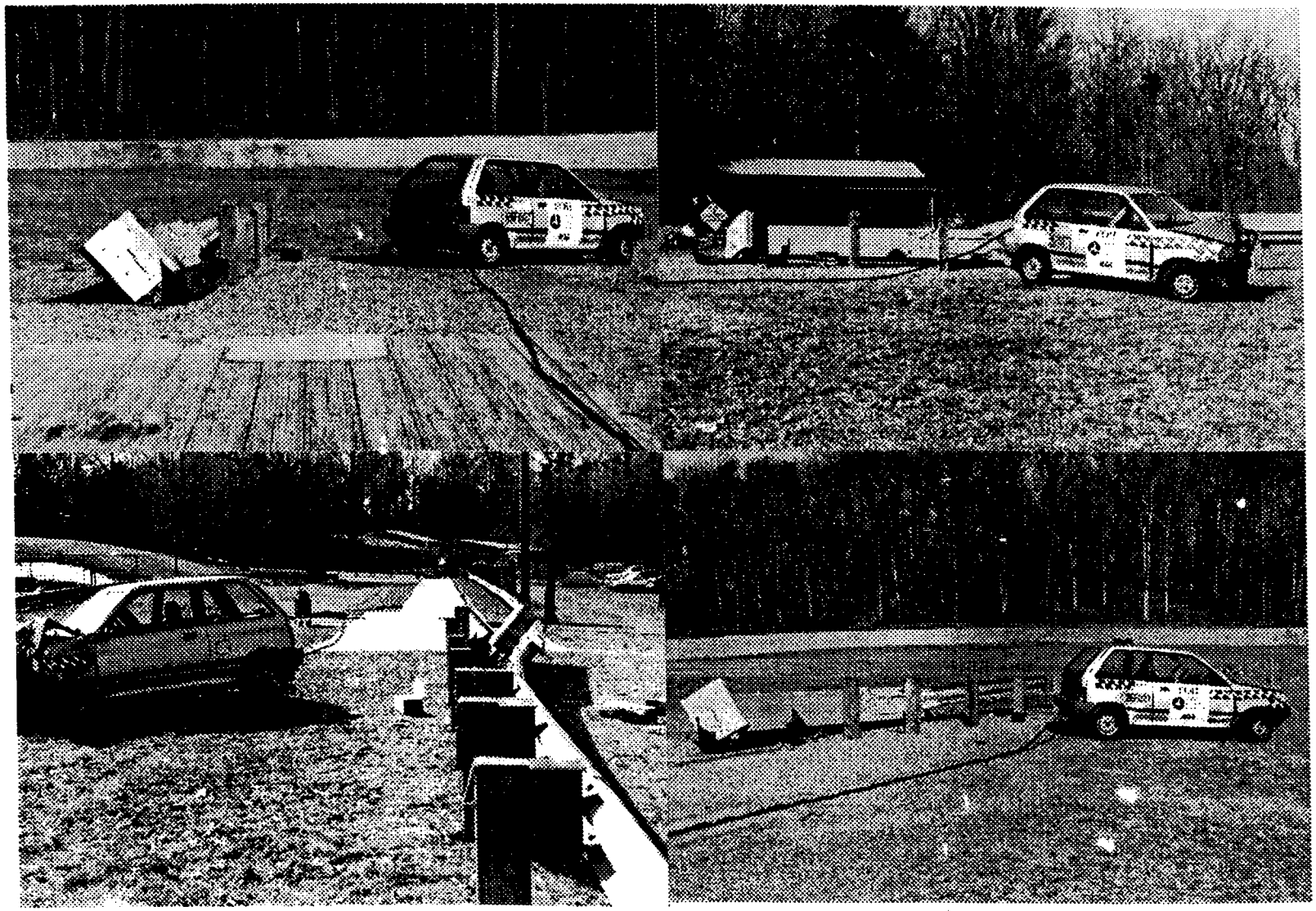

Figure 16. Post-test photographs, test 96F007.

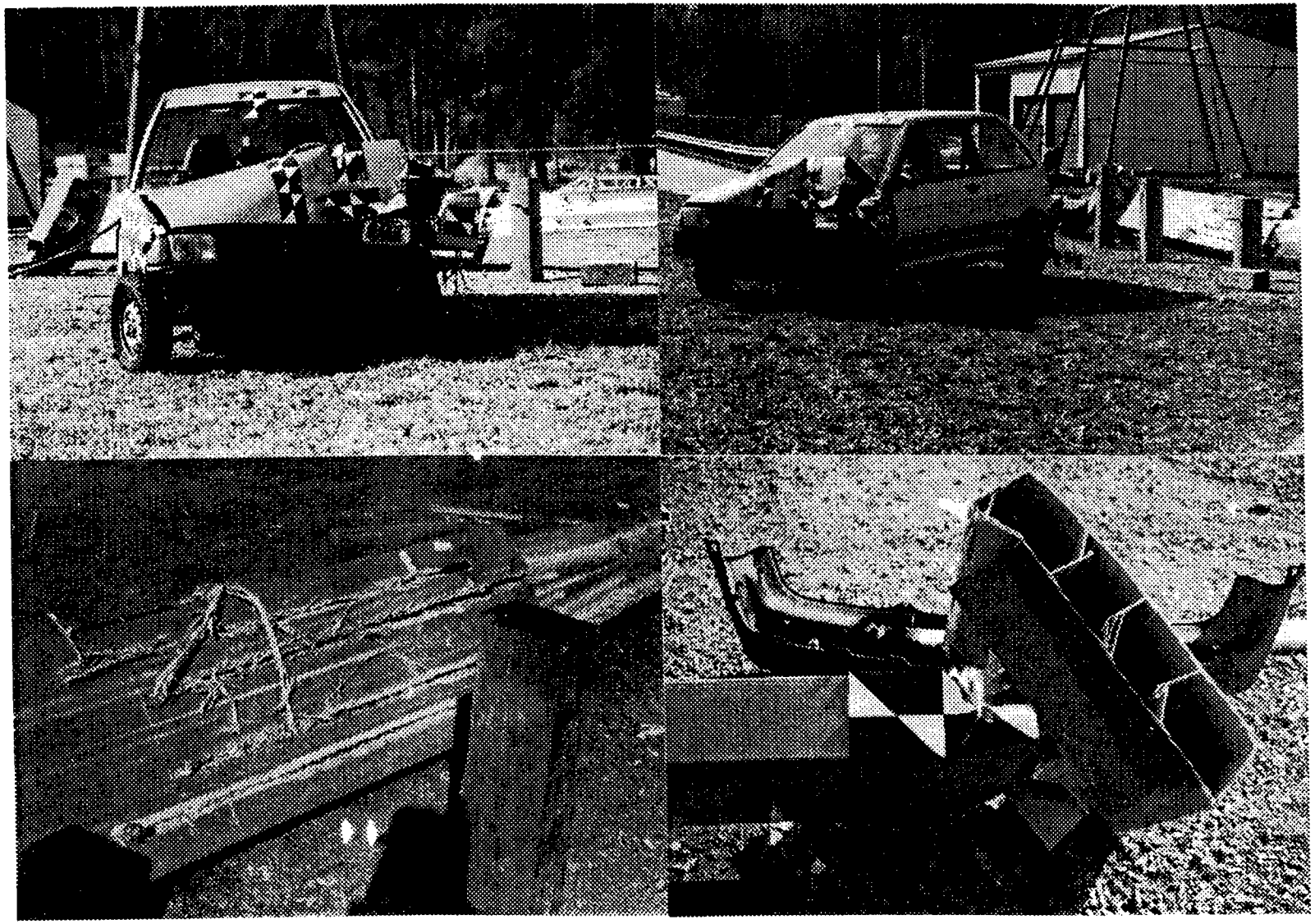

Figure 16. Post-test photographs, test 96F007 (continued).

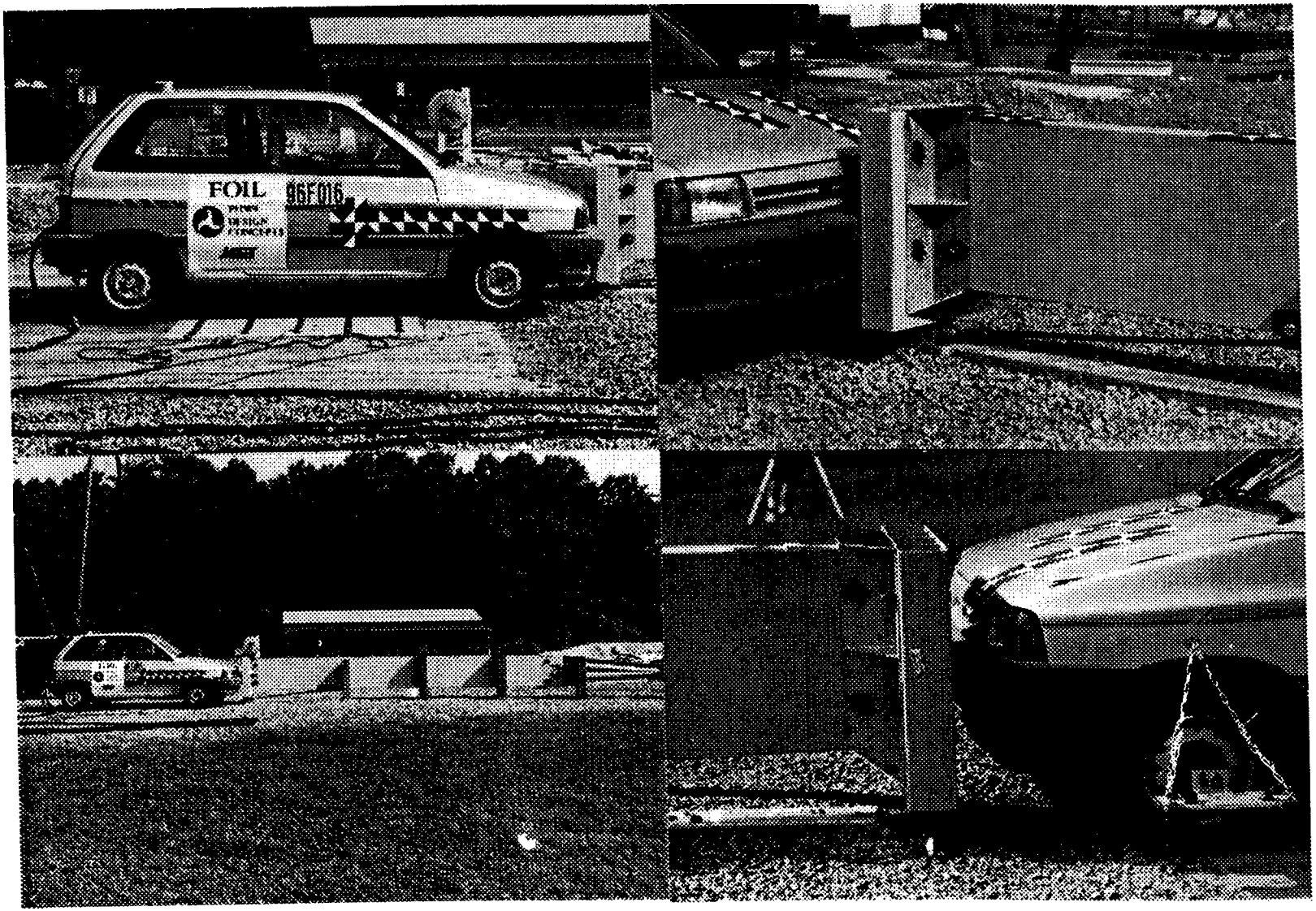

Figure 17. Pretest photographs, test 96F016.

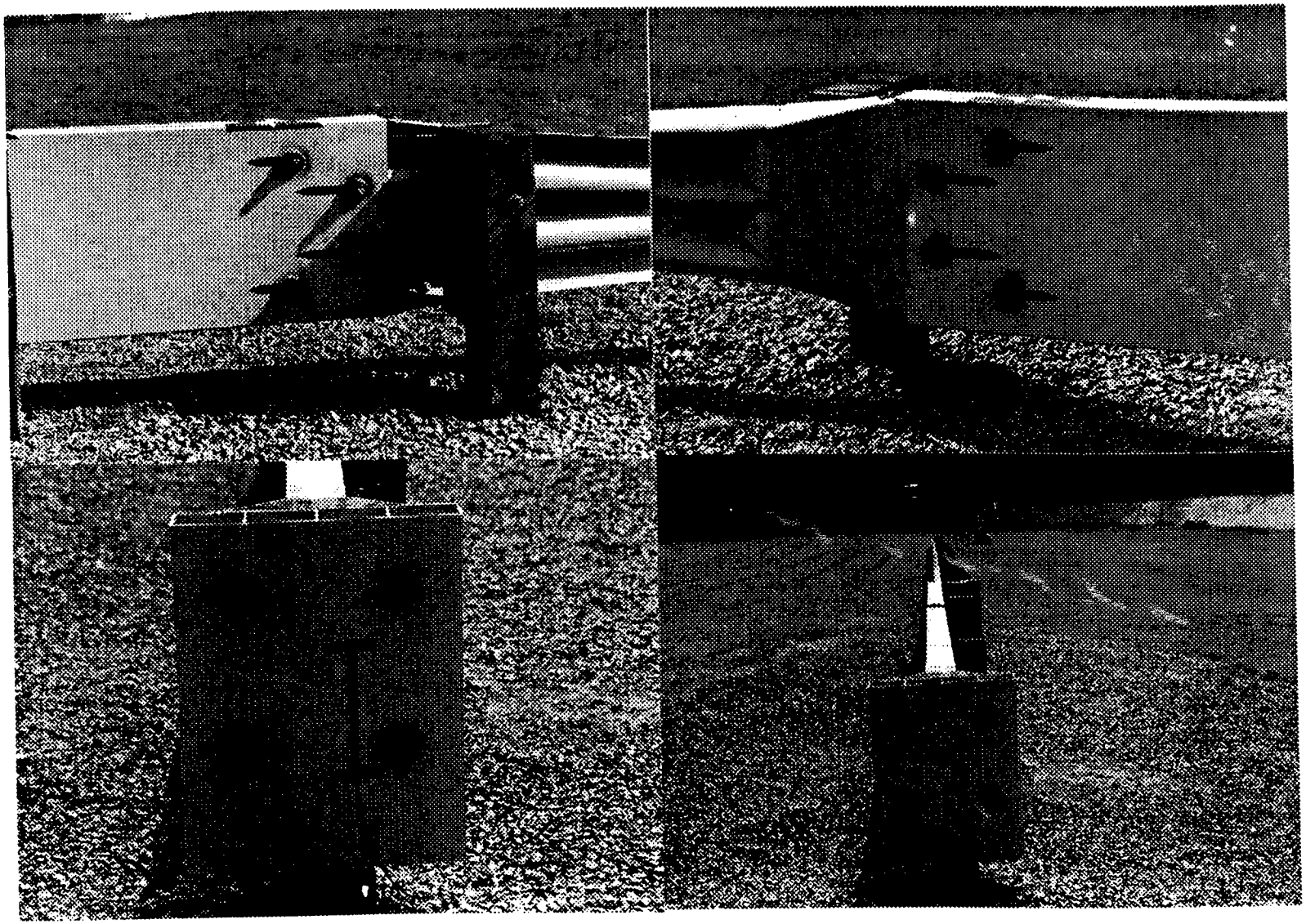

Figure 17. Pretest photographs, test 96F016 (continued).

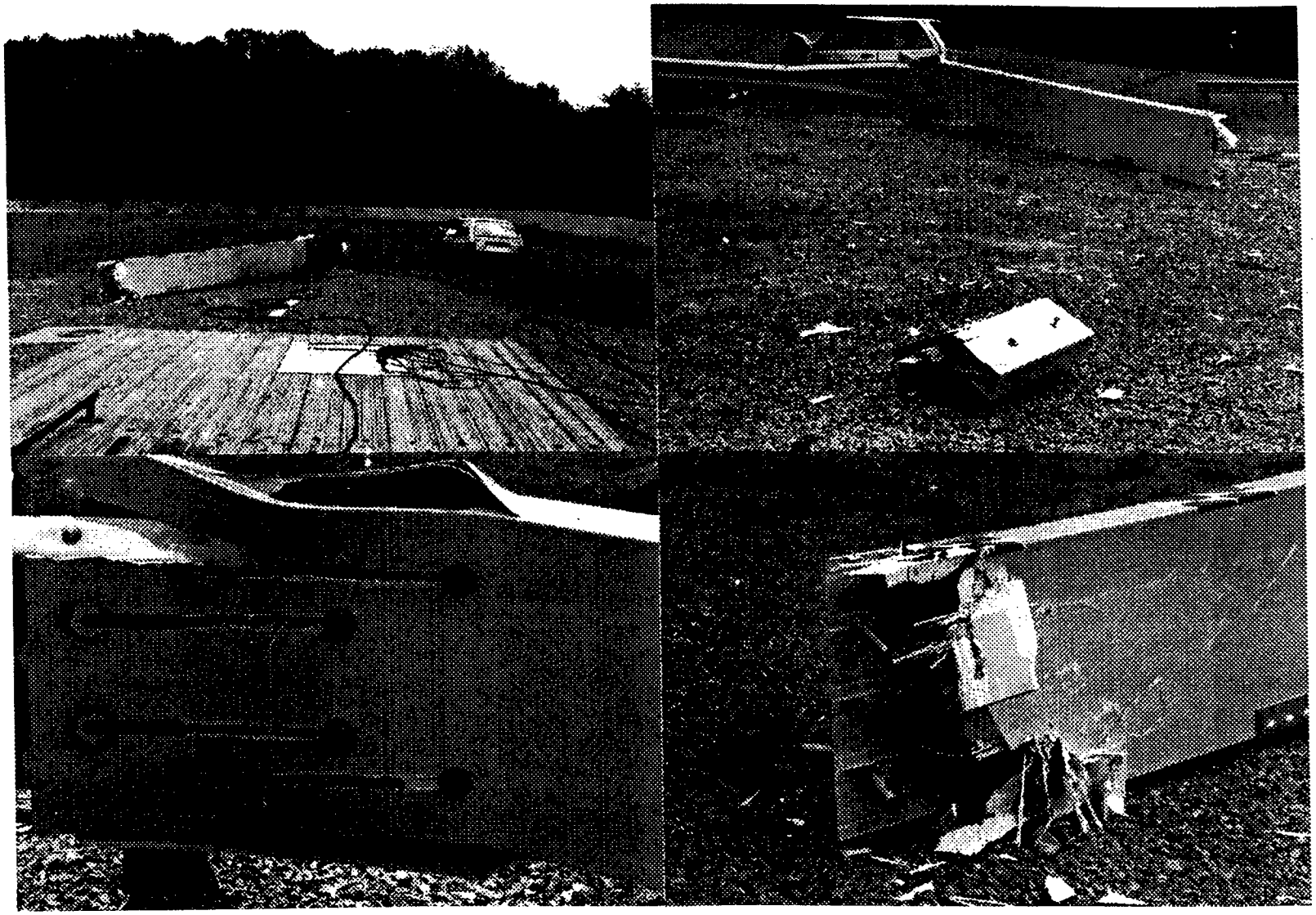

Figure 18. Post-test photographs, test 96F016.

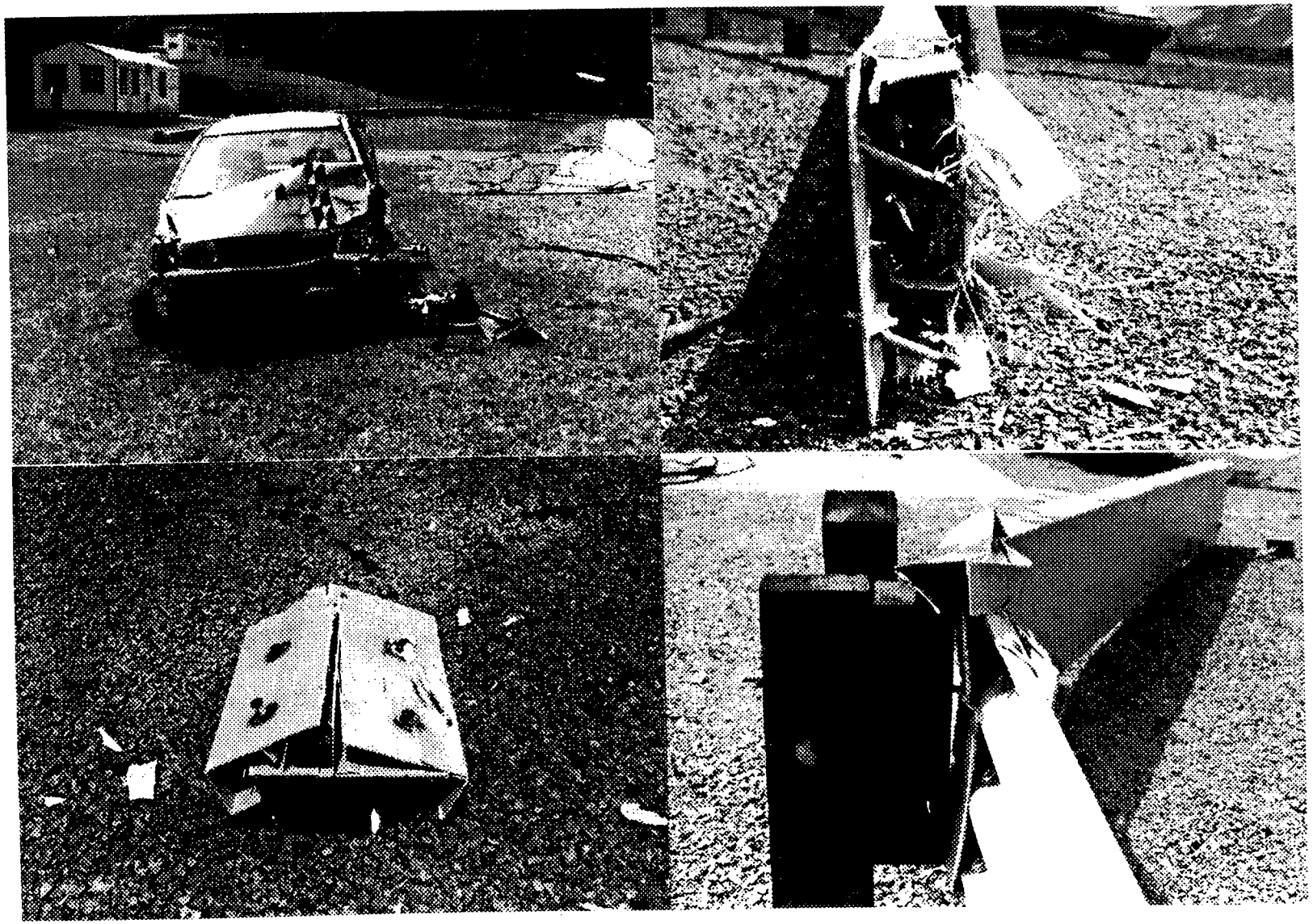

Figure 18. Post-test photographs, test 96F016 (continued).

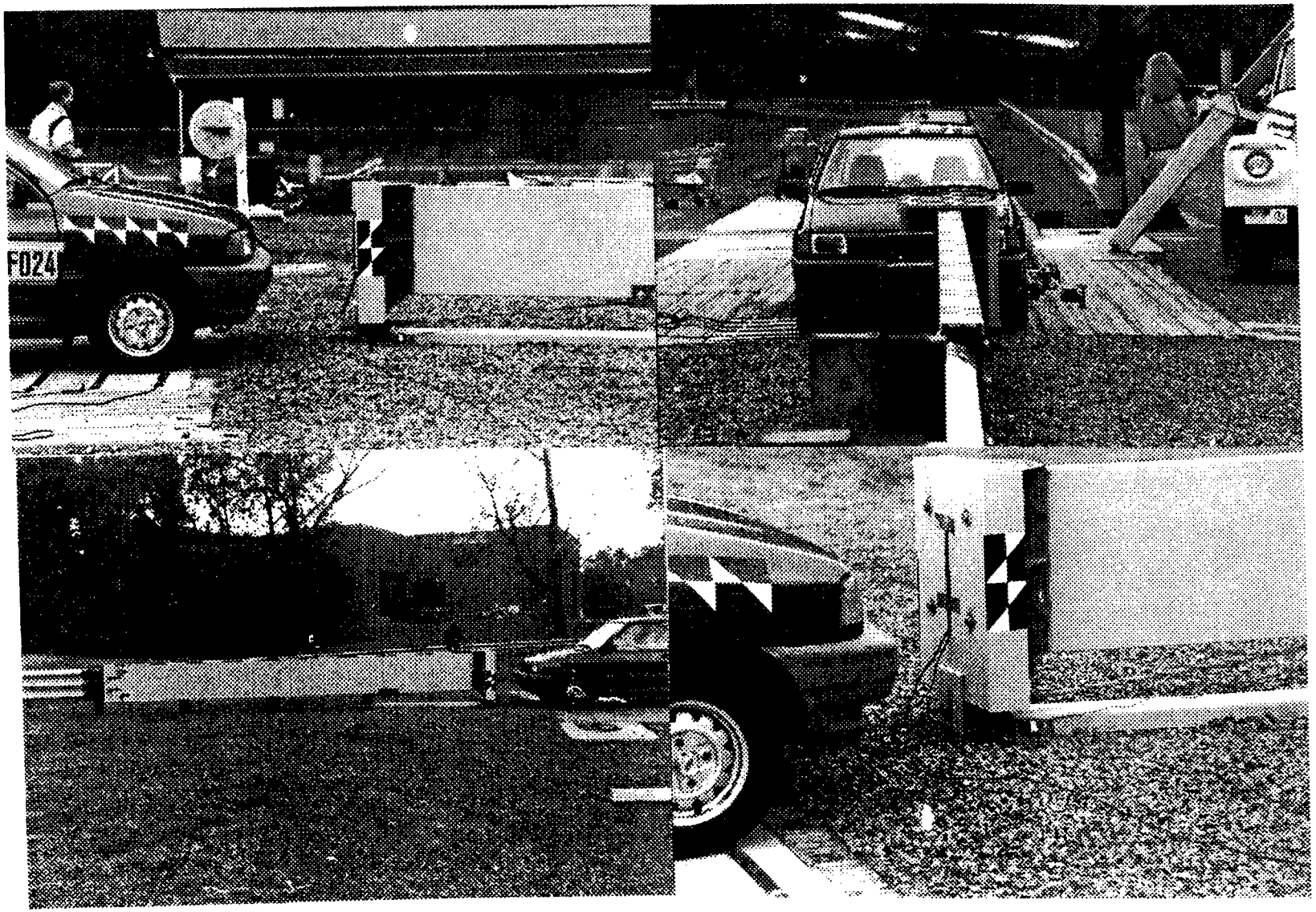

Figure 19. Pretest photographs, test 96F024.

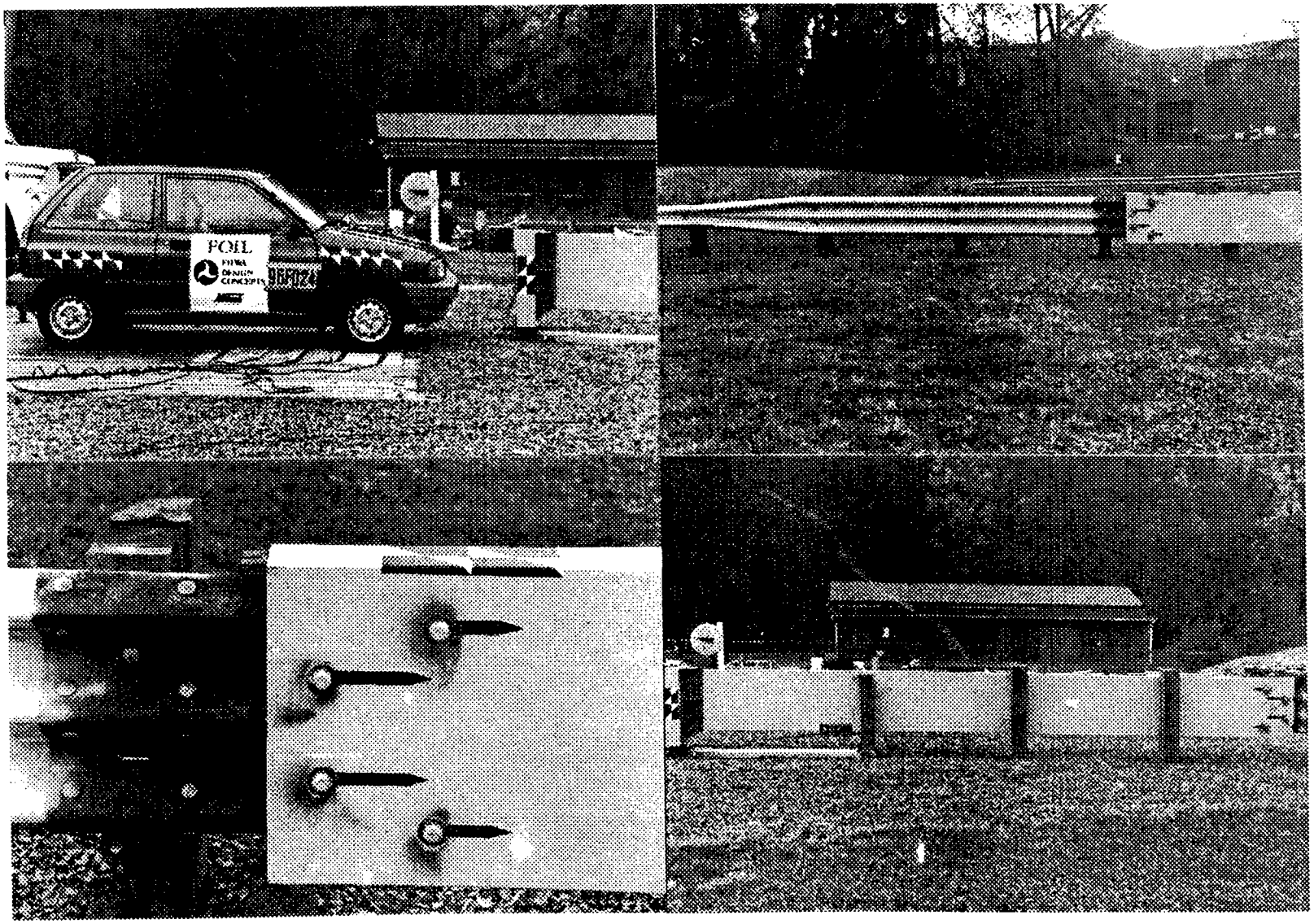

Figure 19. Pretest photographs, test 96F024 (continued).

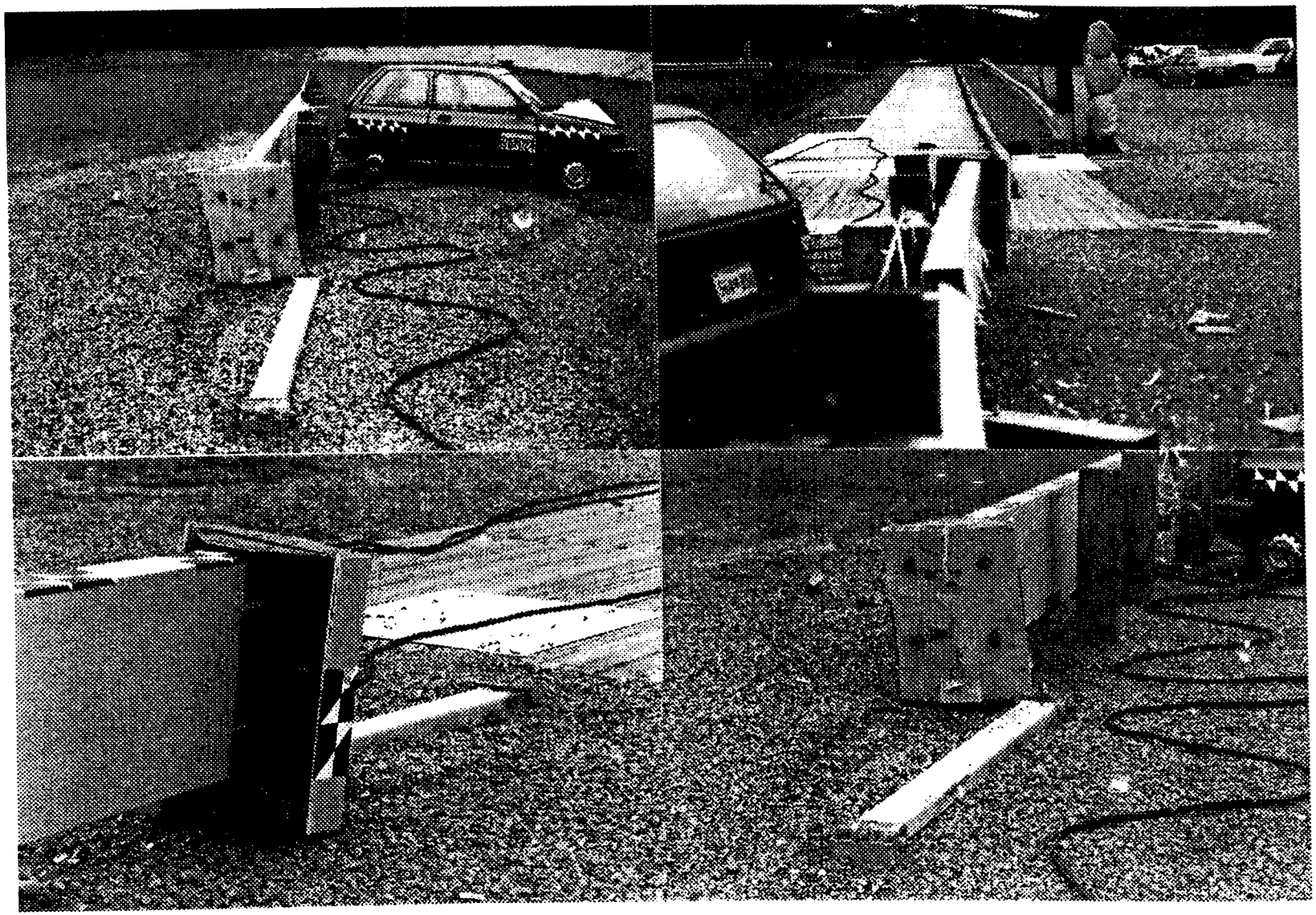

Figure 20. Post-test photographs, test 96F024.

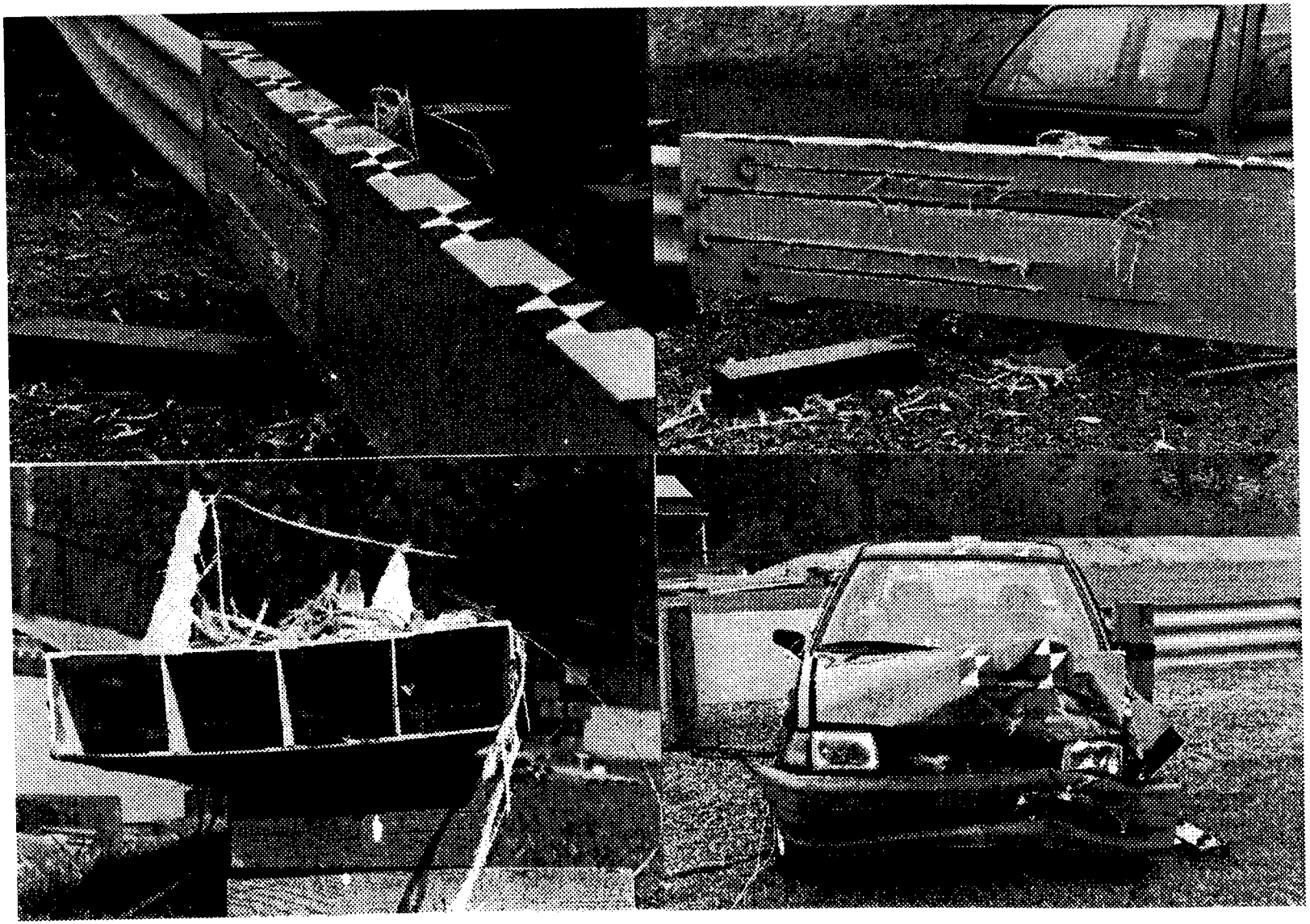

Figure 20. Post-test photographs, test 96F024 (continued).

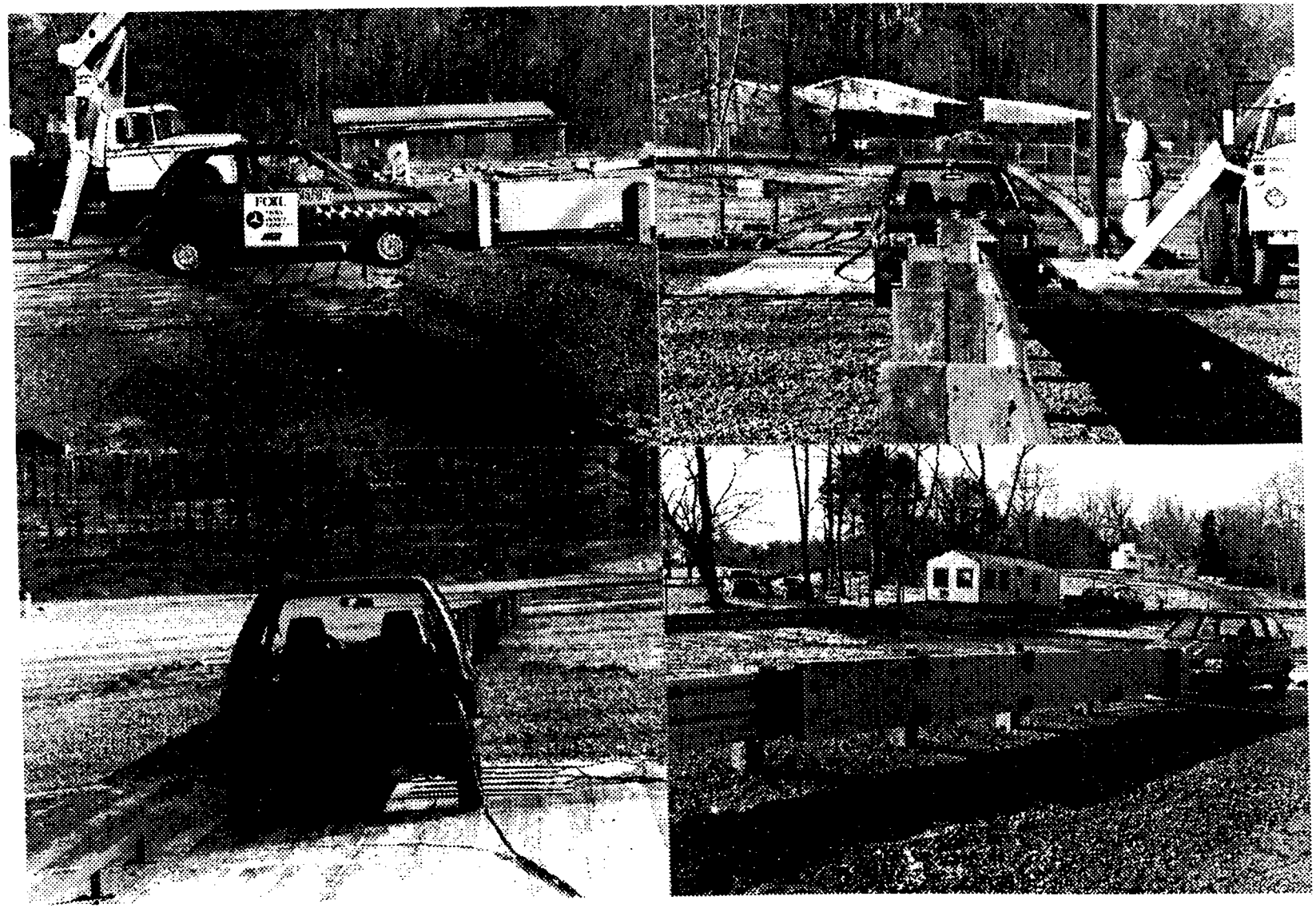

Figure 21. Pretest photographs, test 96F027.

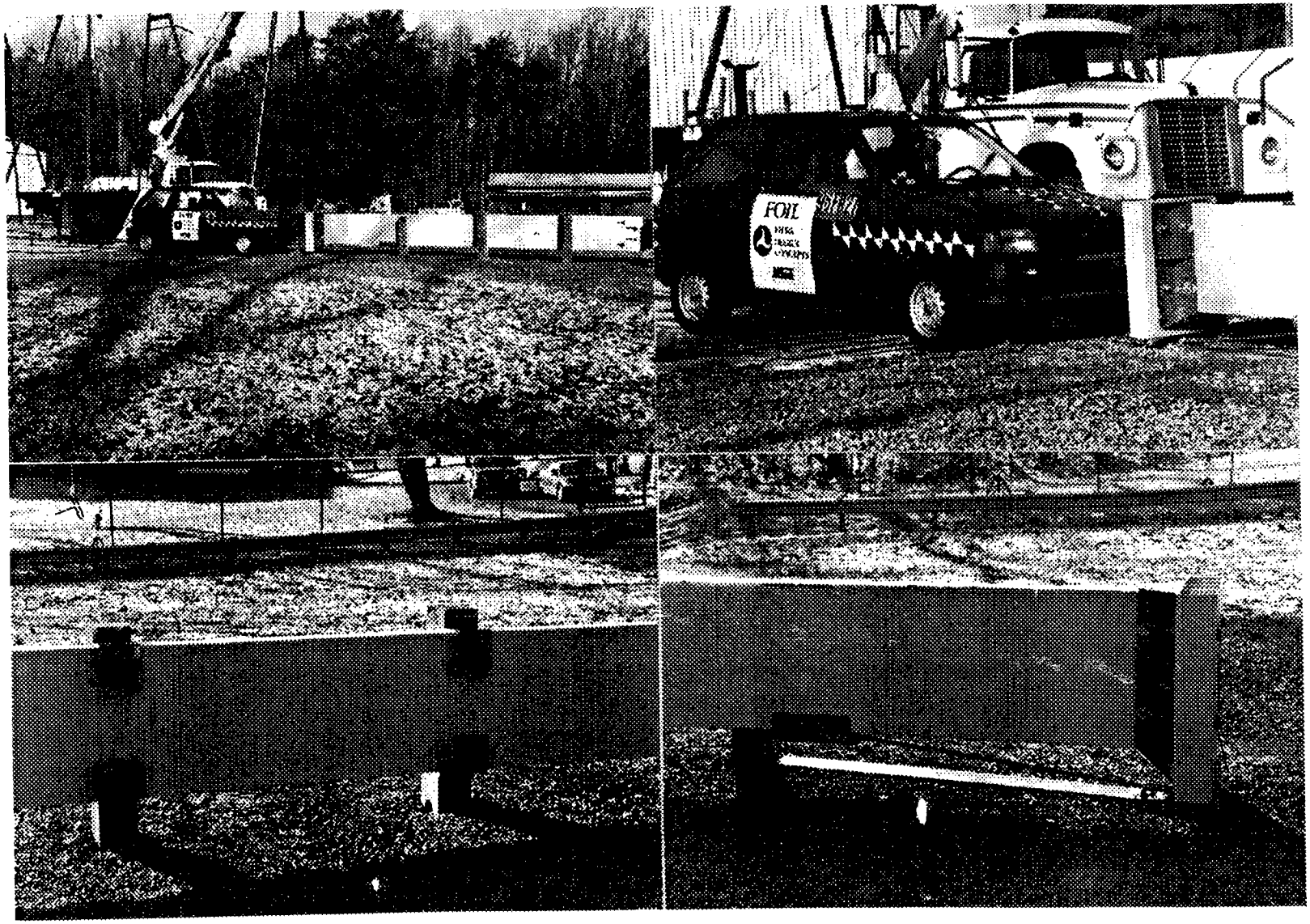

Figure 21. Pretest photographs, test 96F027 (continued).

Figure 22. Post-test photographs, test 96F027.

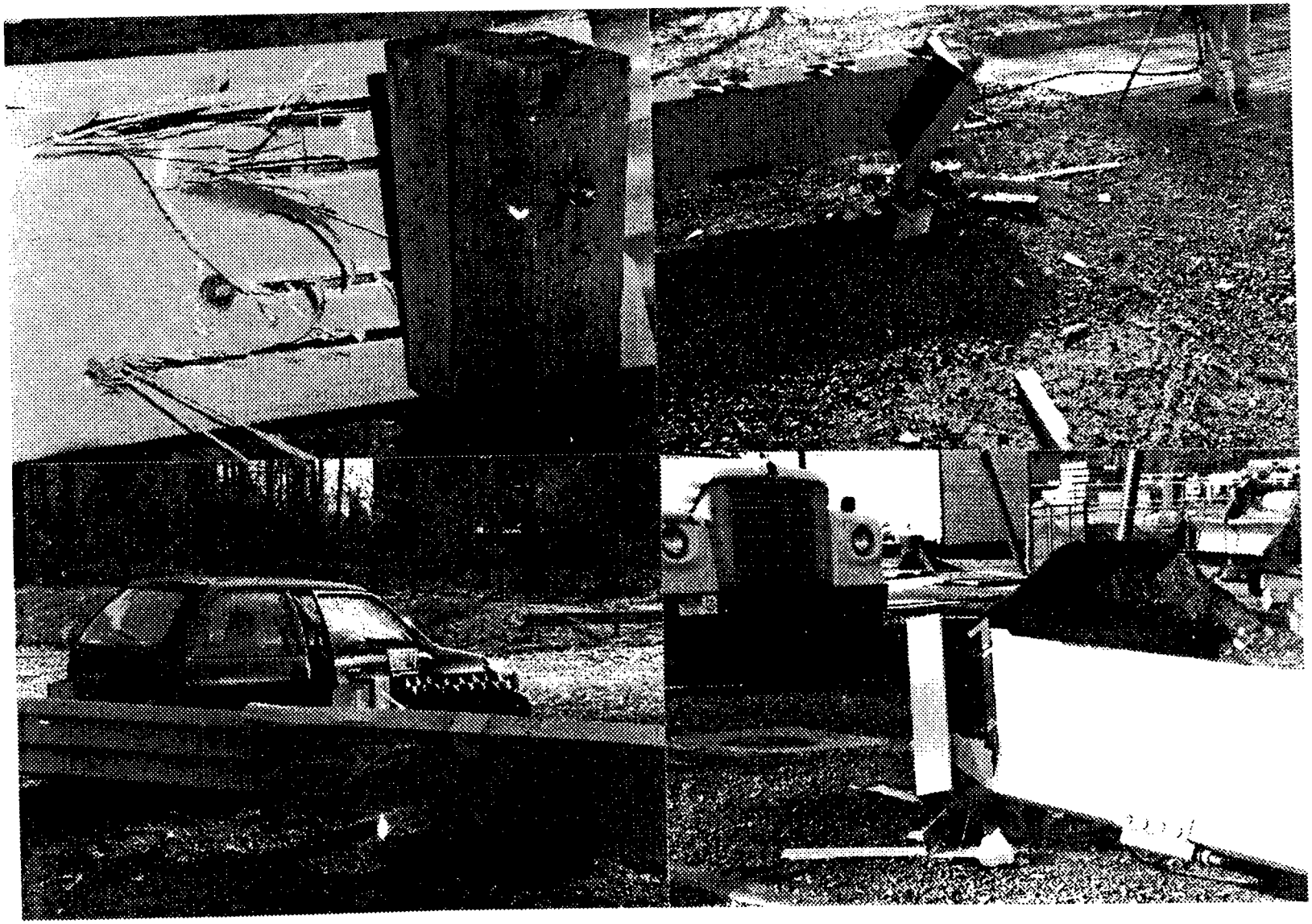

Figure 22. Post-test photographs, test 96F027(continued).

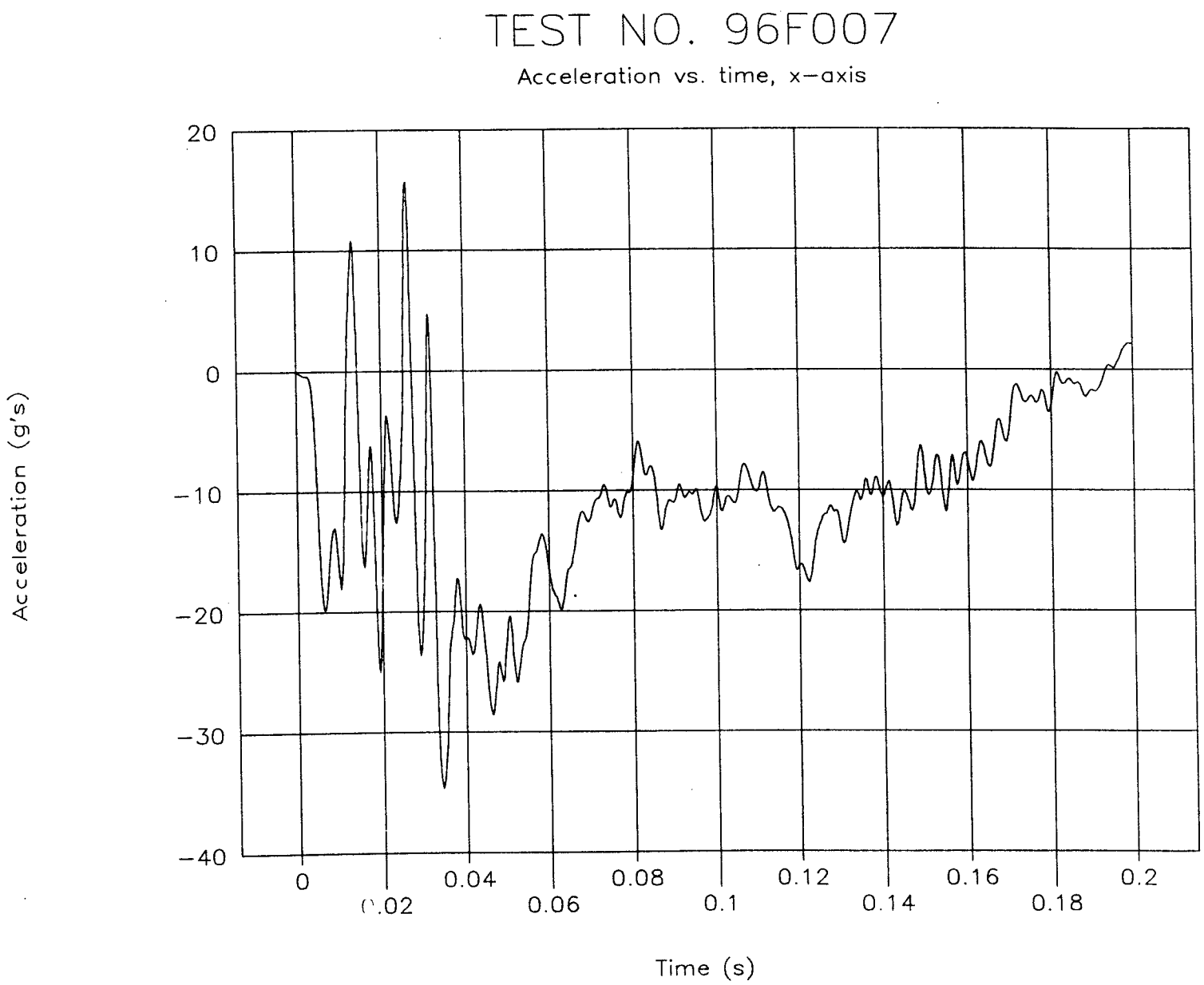

Figure 23. Acceleration vs. time, x-axis, test 96F007.

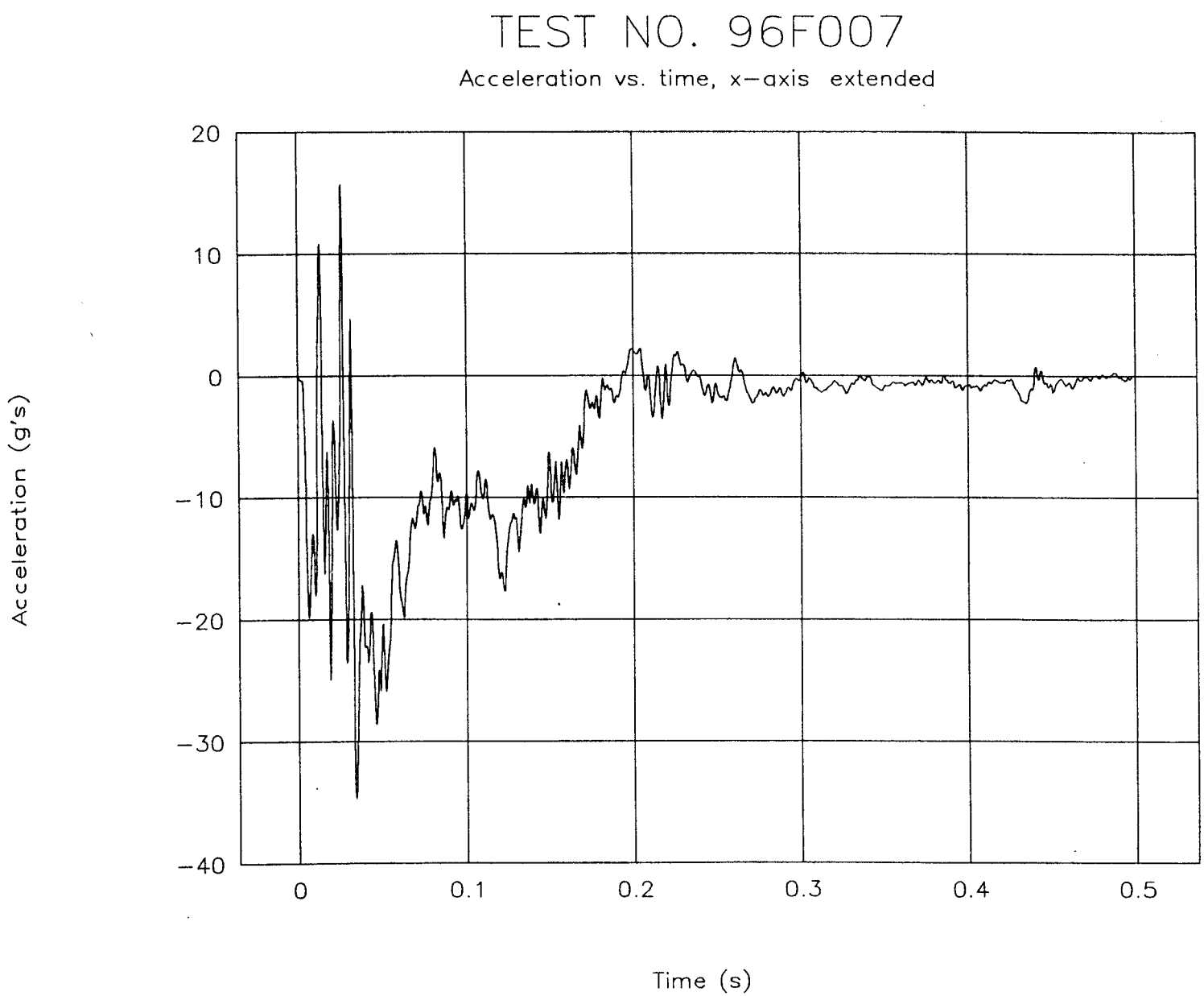

Figure 24. Acceleration vs. time, x-axis extended, test 96F007.

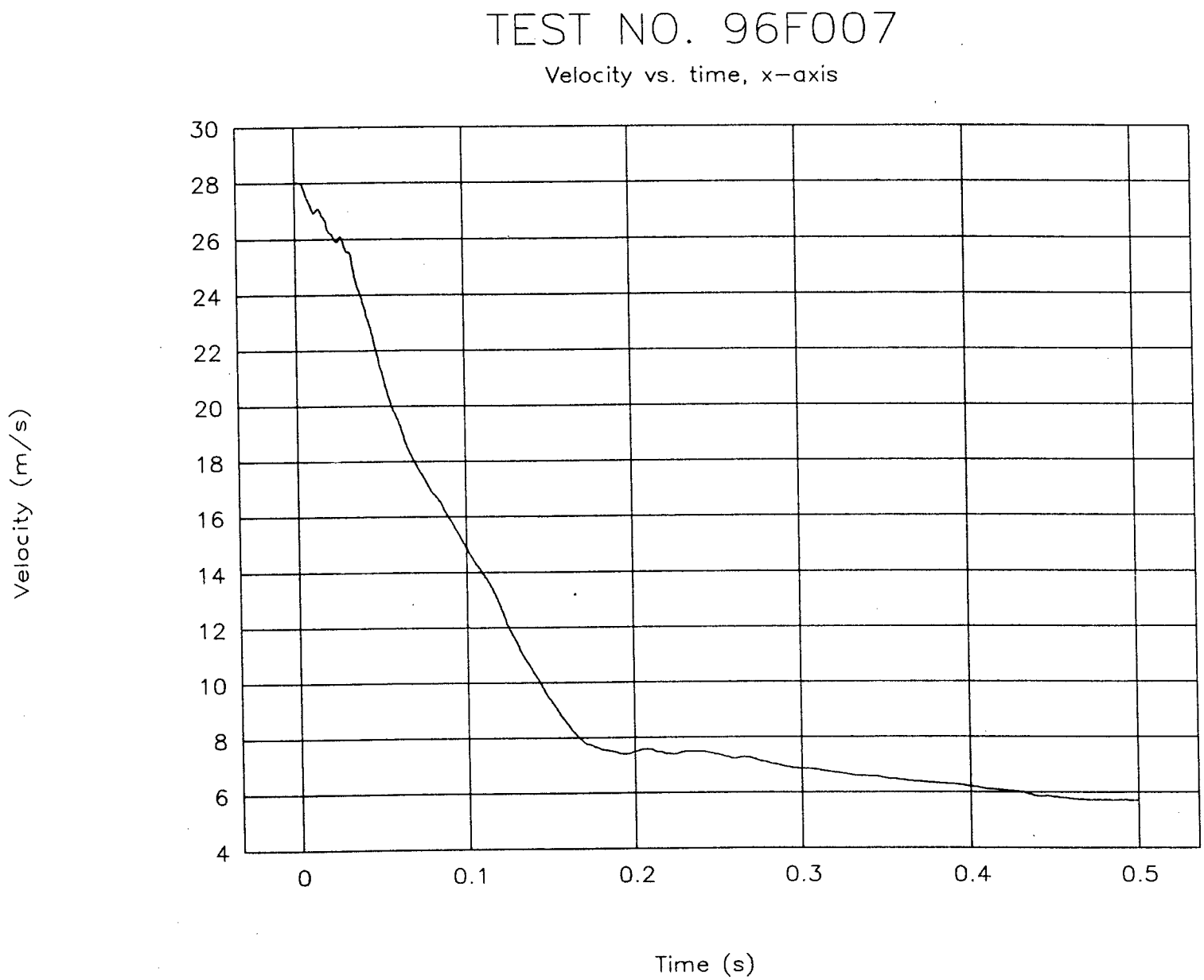

Figure 25. Velocity vs. time, x-axis, test 96F007.

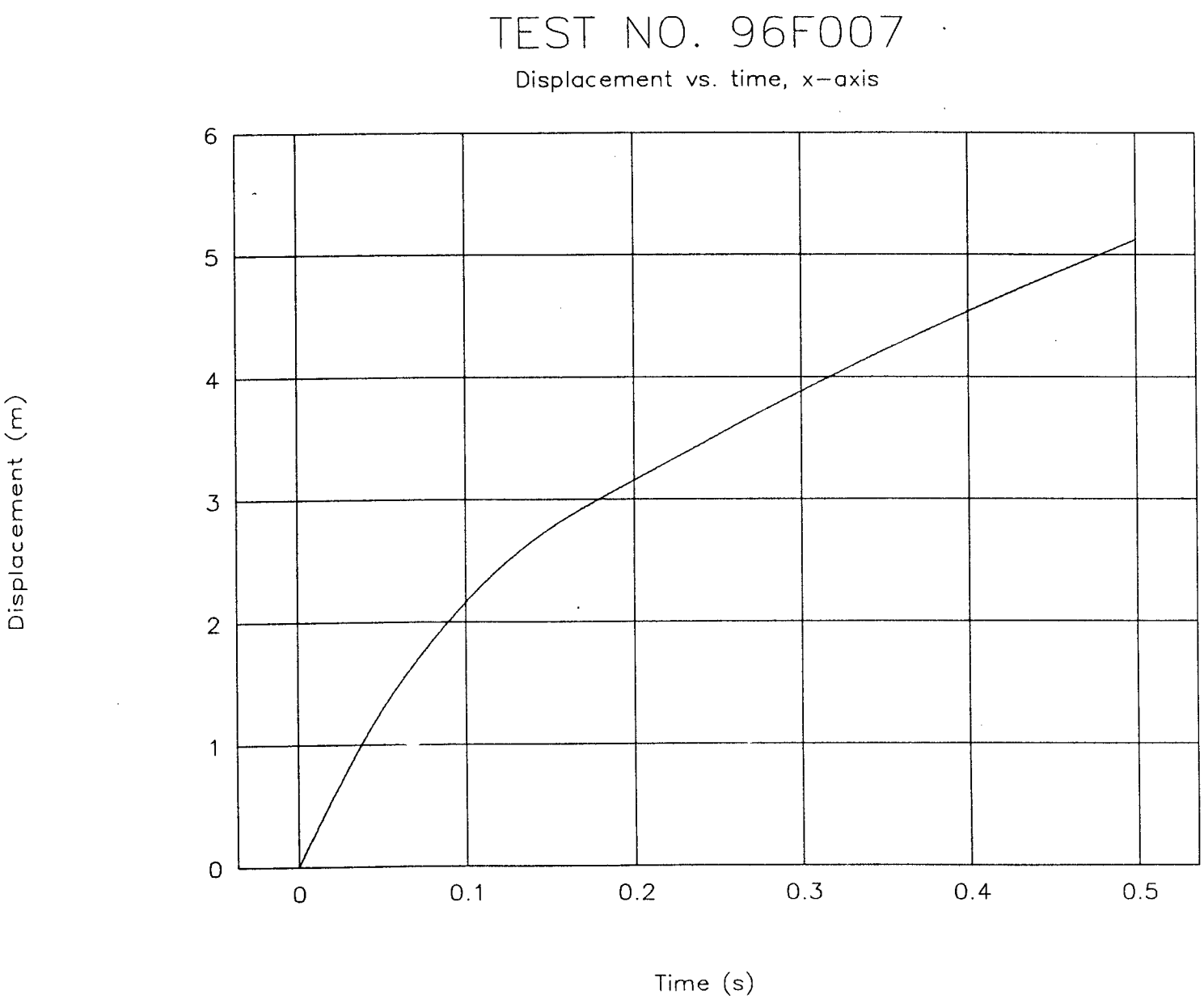

Figure 26. Displacement vs. time, x-axis, test 96F007.

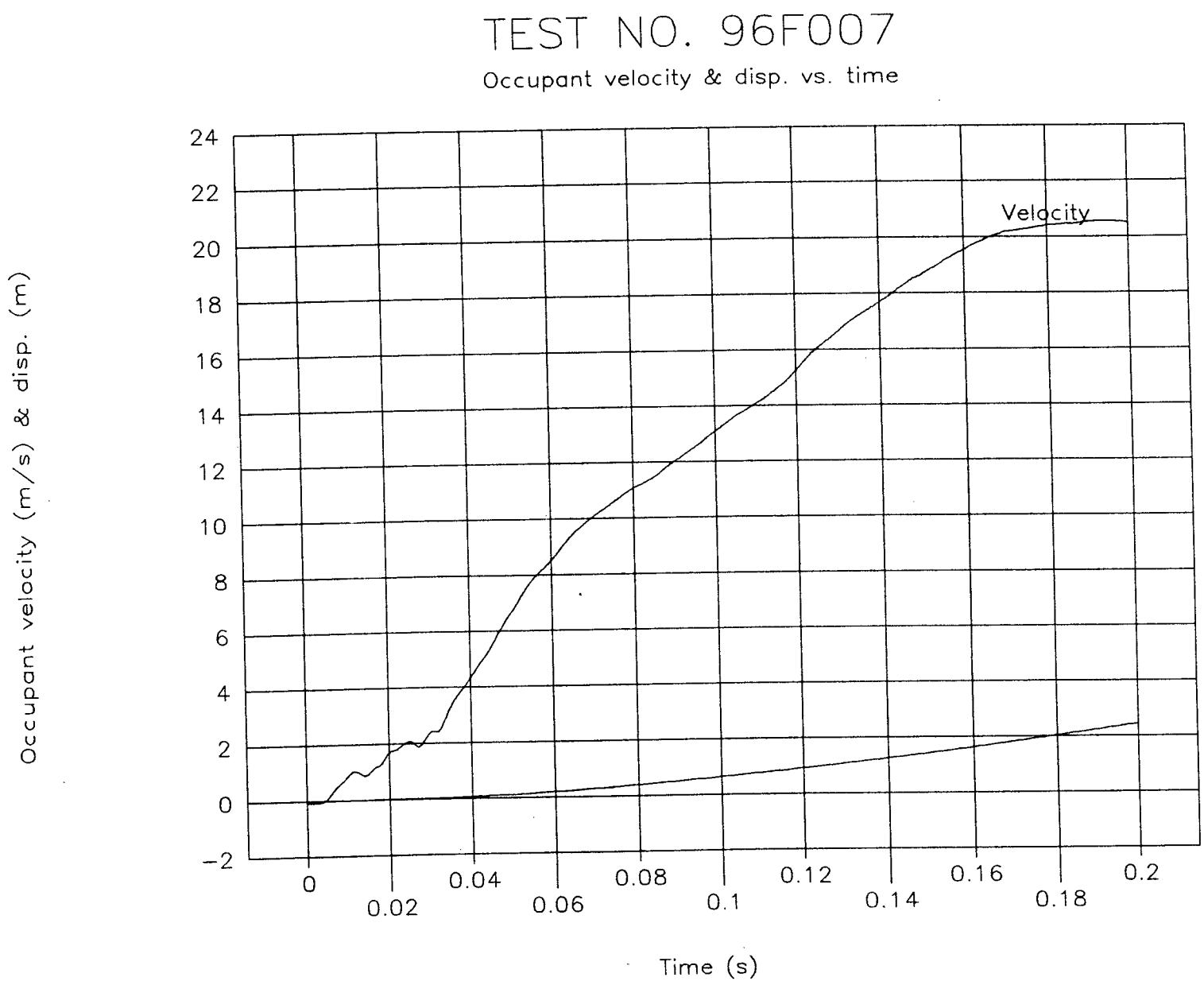

Figure 27. Occupant velocity and displacement vs. time, test 96F007.

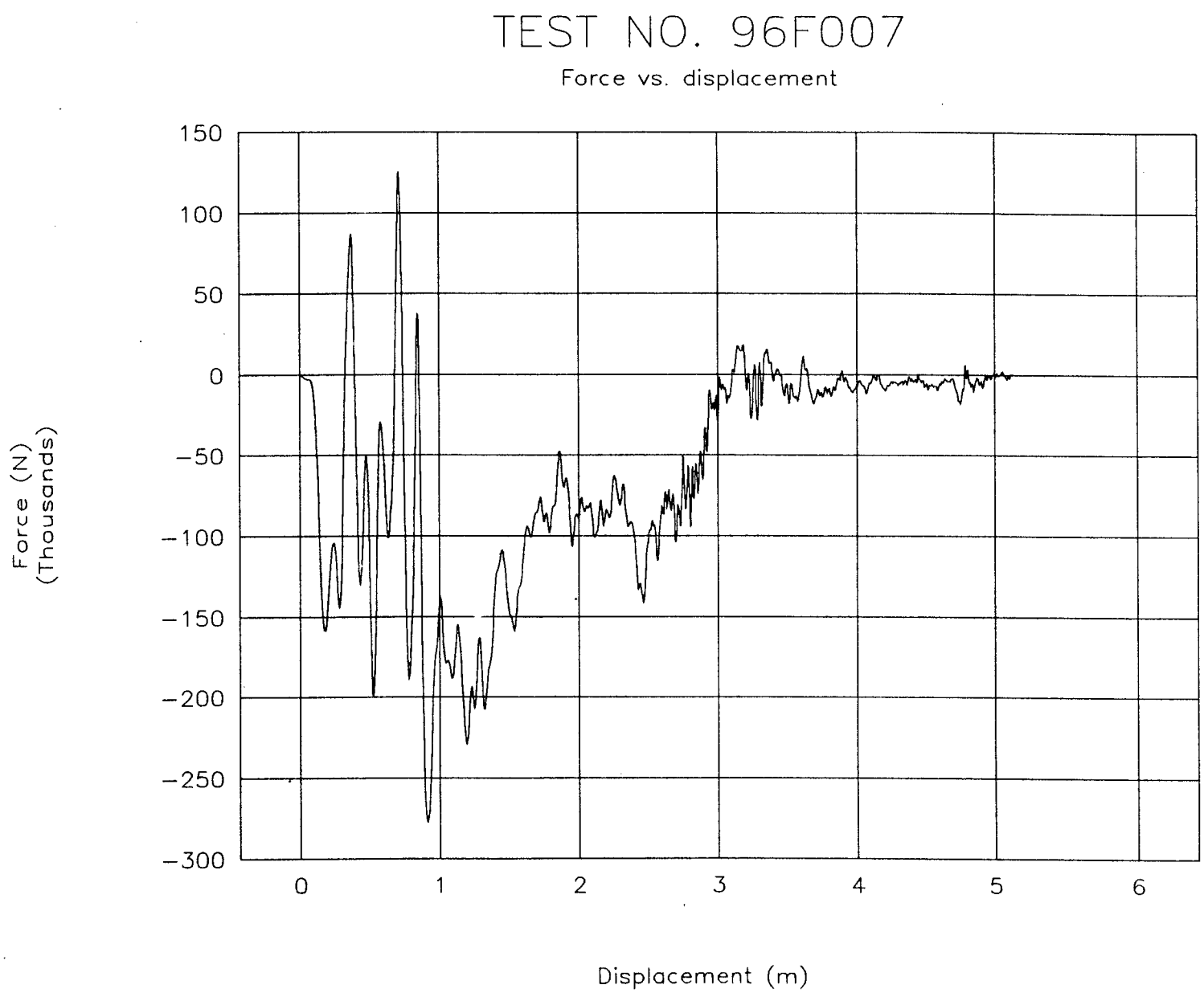

Figure 28. Force vs. displacement, test 96F007.

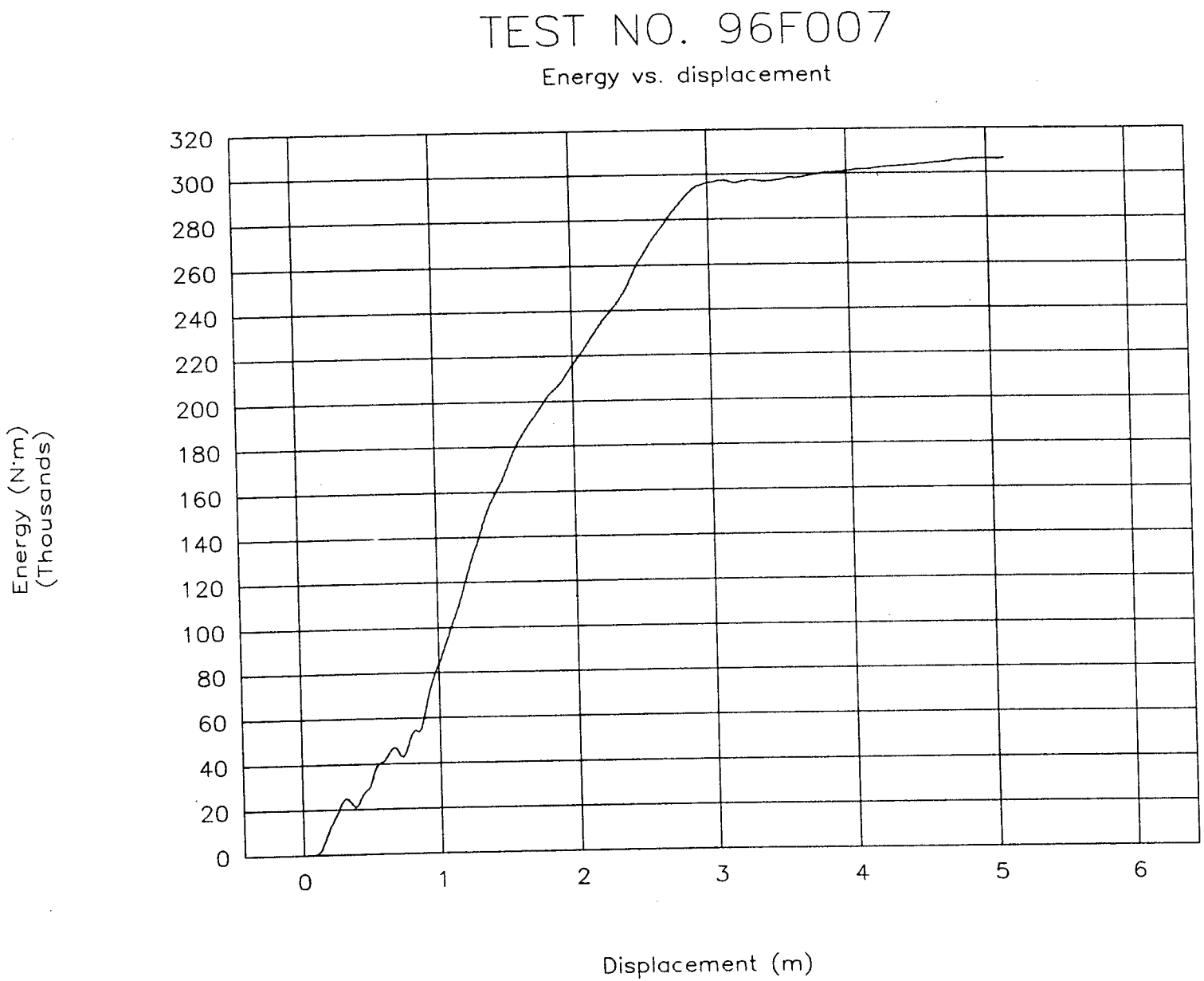

Figure 29. Energy vs. displacement, test 96F007.

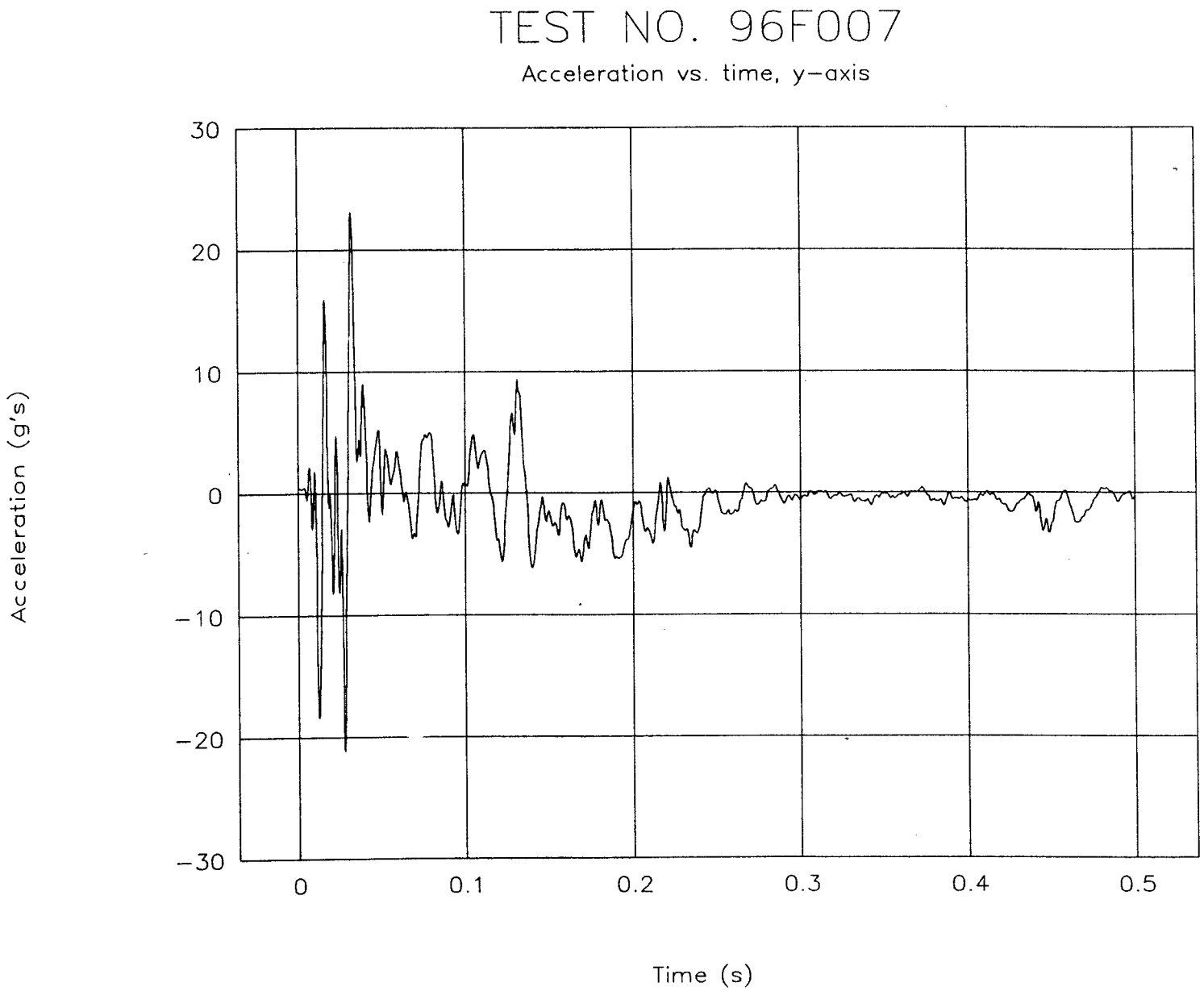

Figure 30. Acceleration vs. time, y-axis, test 96F007.

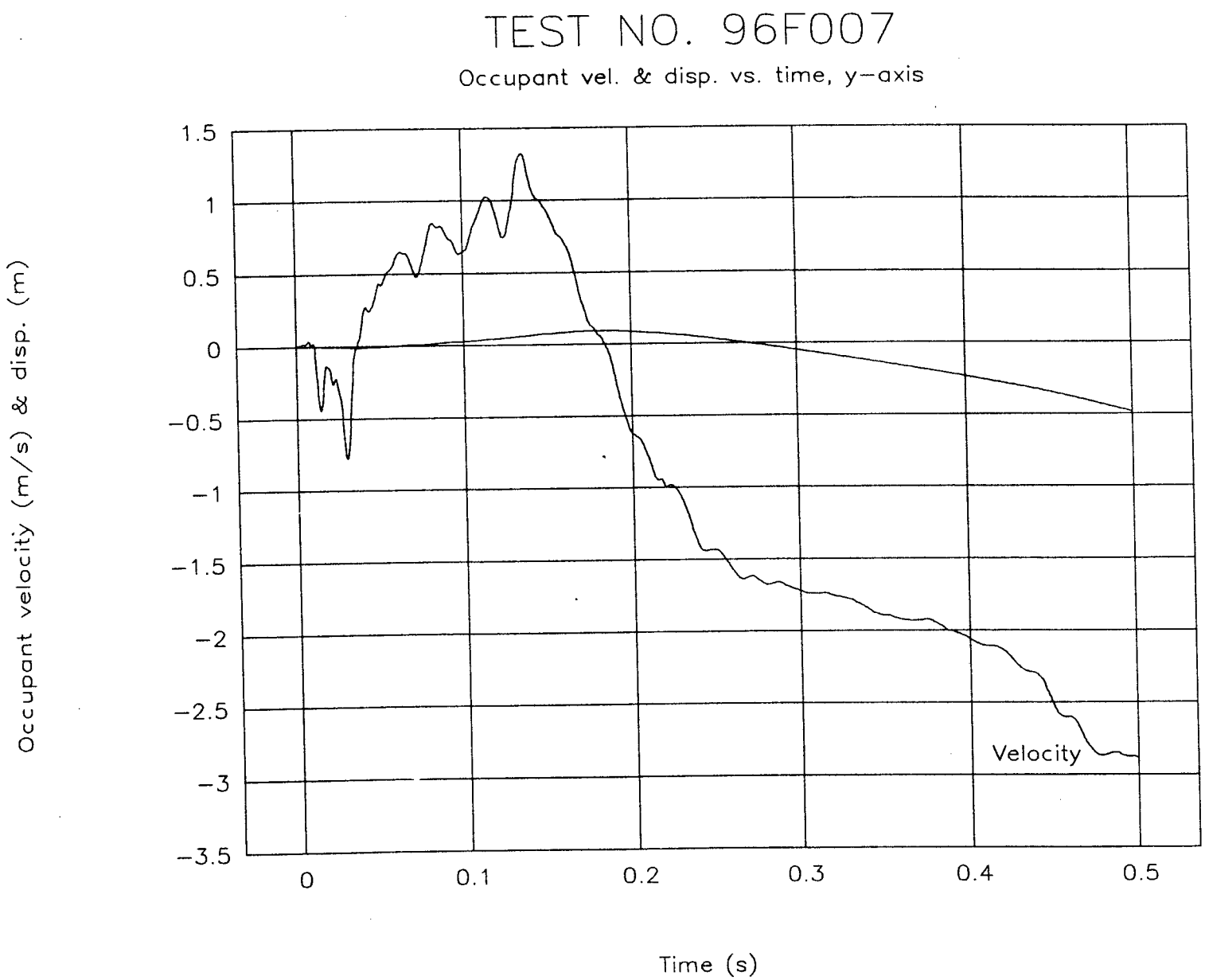

Figure 31. Occupant velocity and displacement vs. time, y-axis, test 96F007.

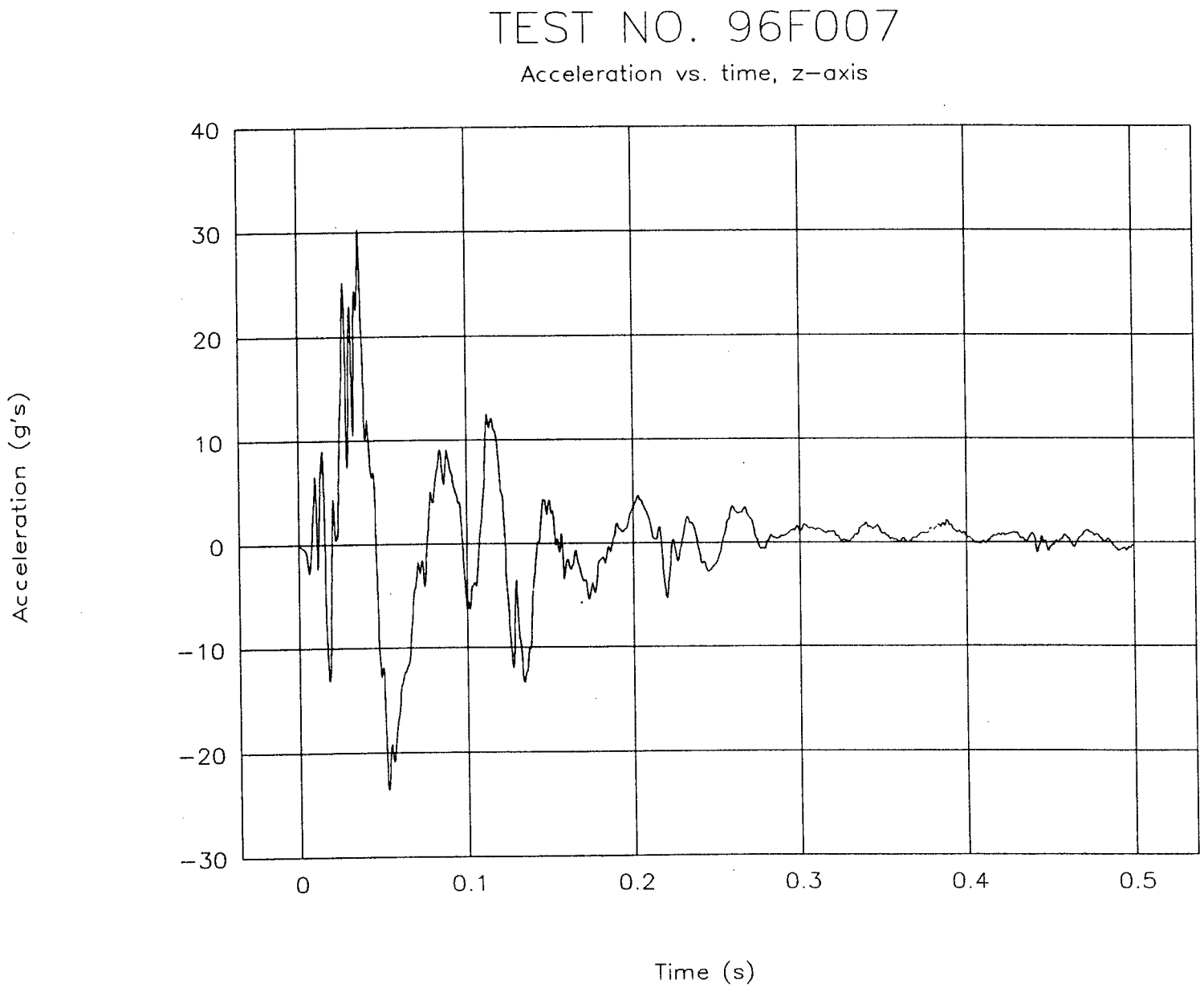

Figure 32. Acceleration vs. time, z-axis, test 96F007.

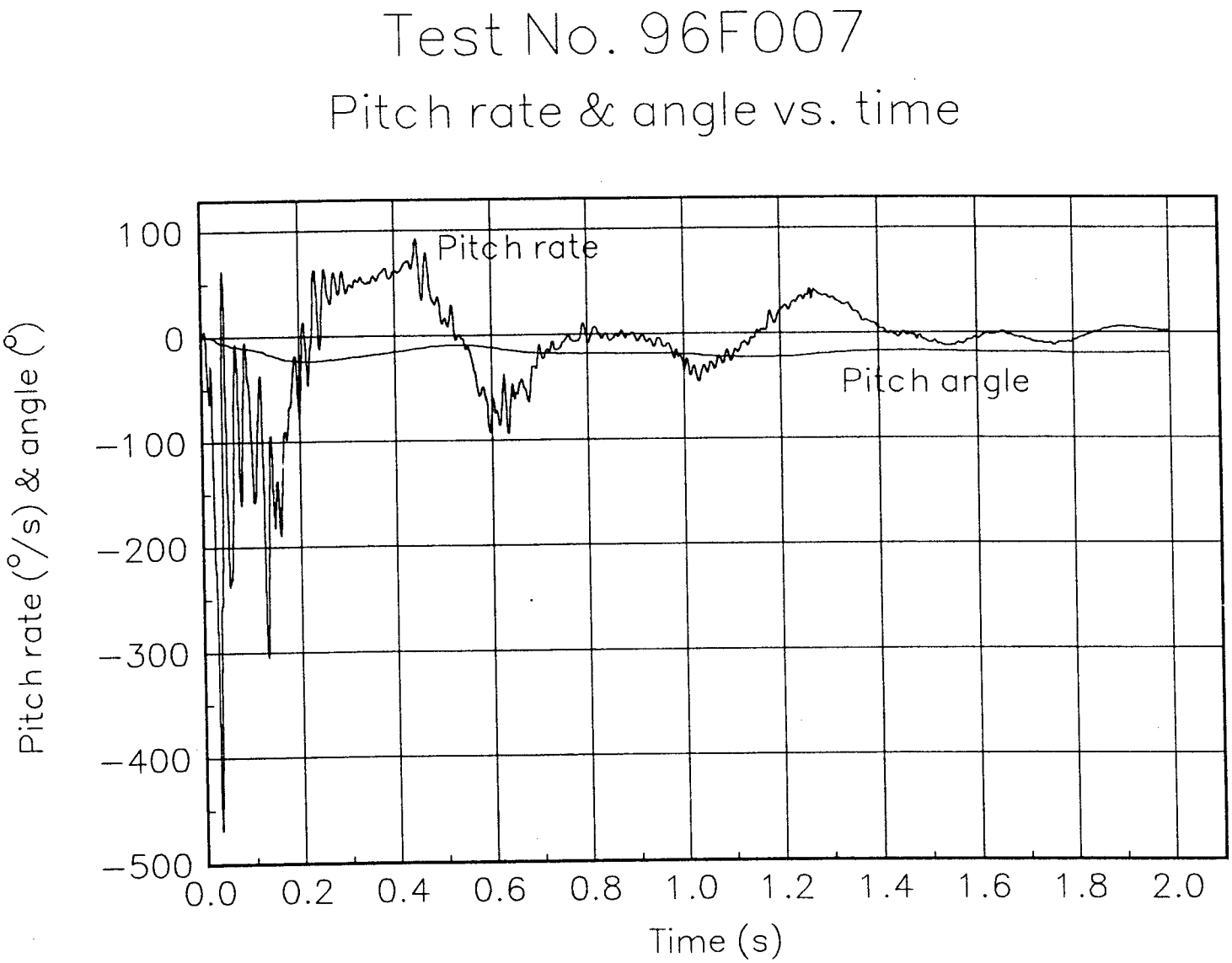

Figure 33. Pitch rate and angle vs. time, test 96F007.

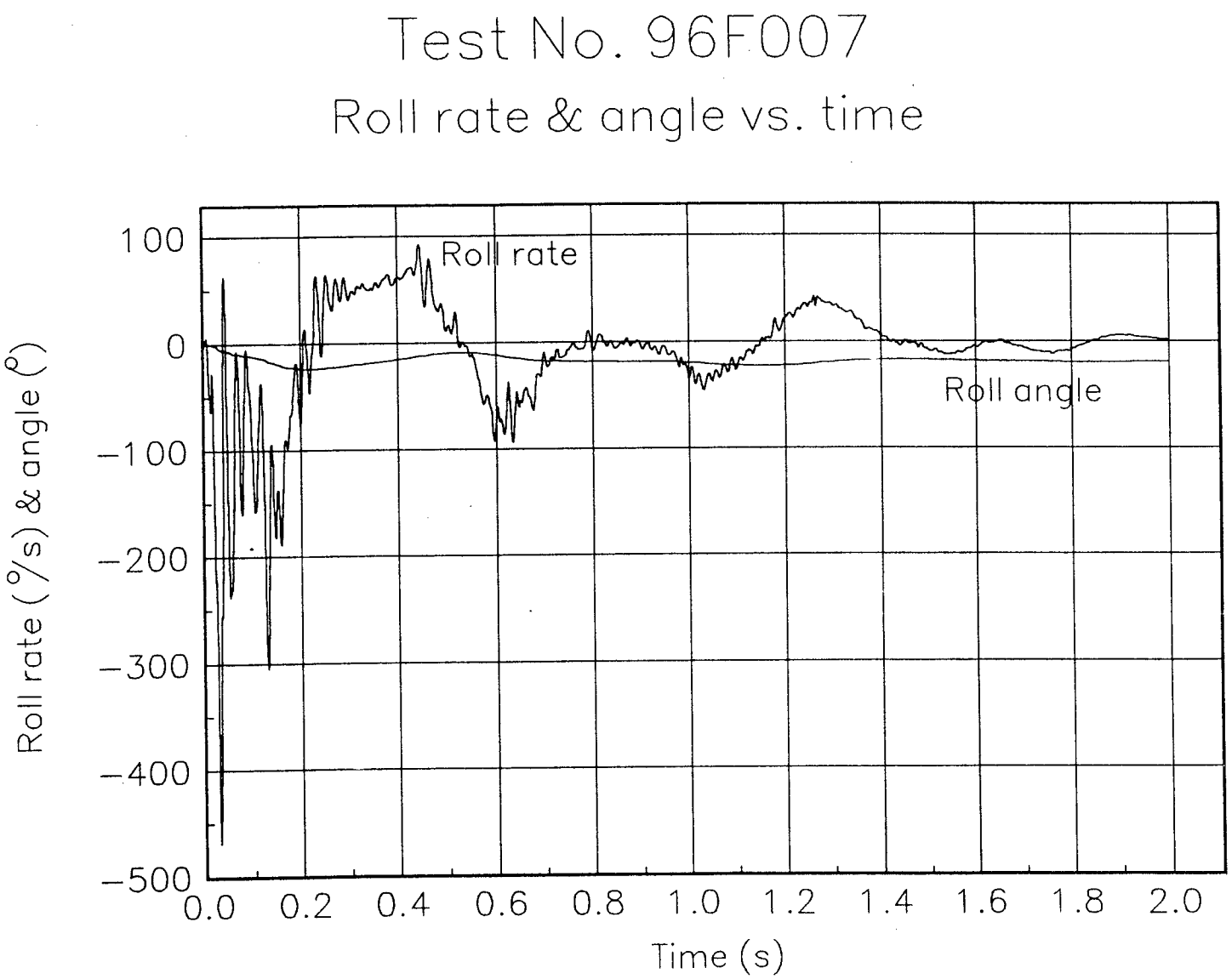

Figure 34. Roll rate and angle vs. time, test 96F007.

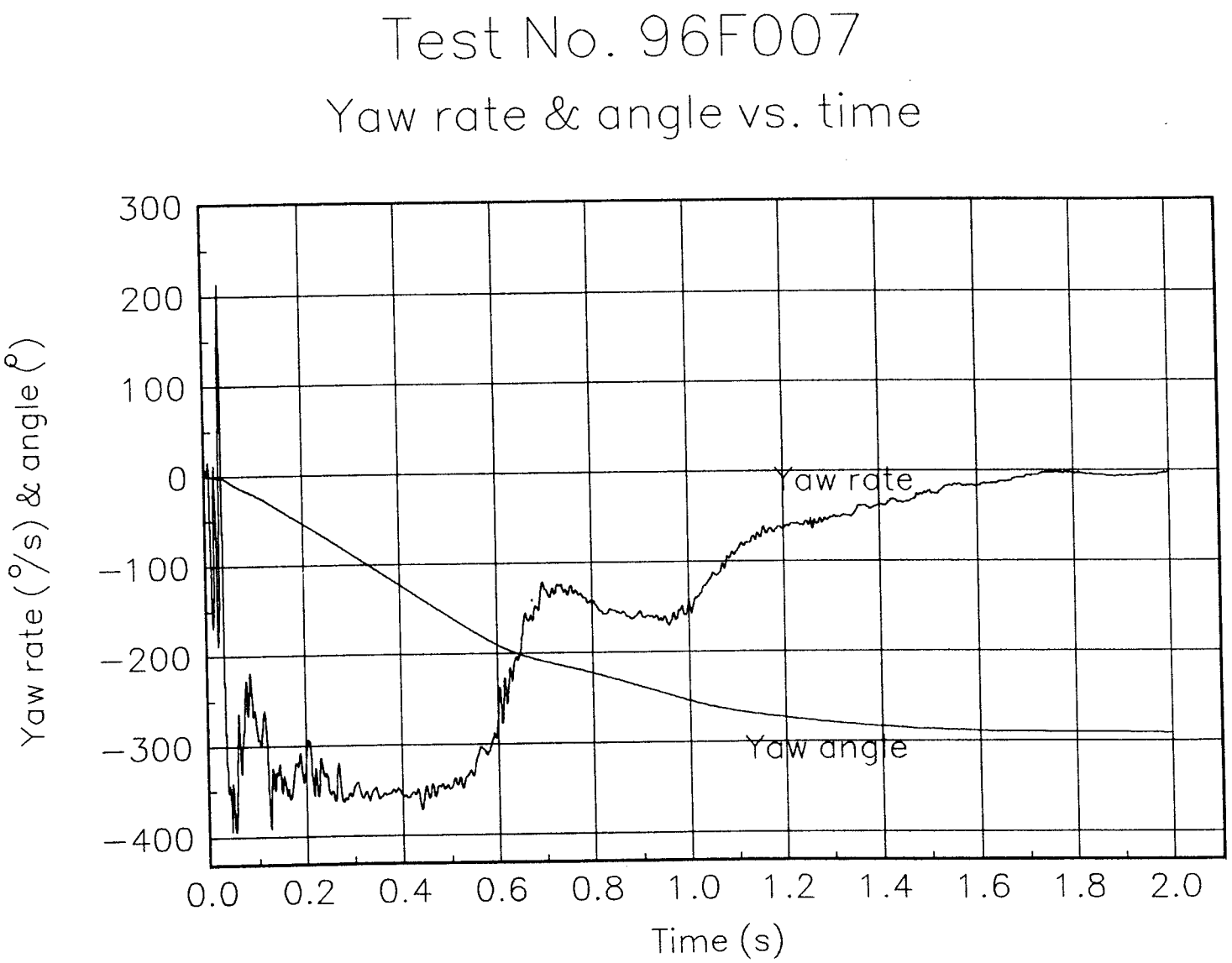

Figure 35. Yaw rate and angle vs. time, test 96F007.

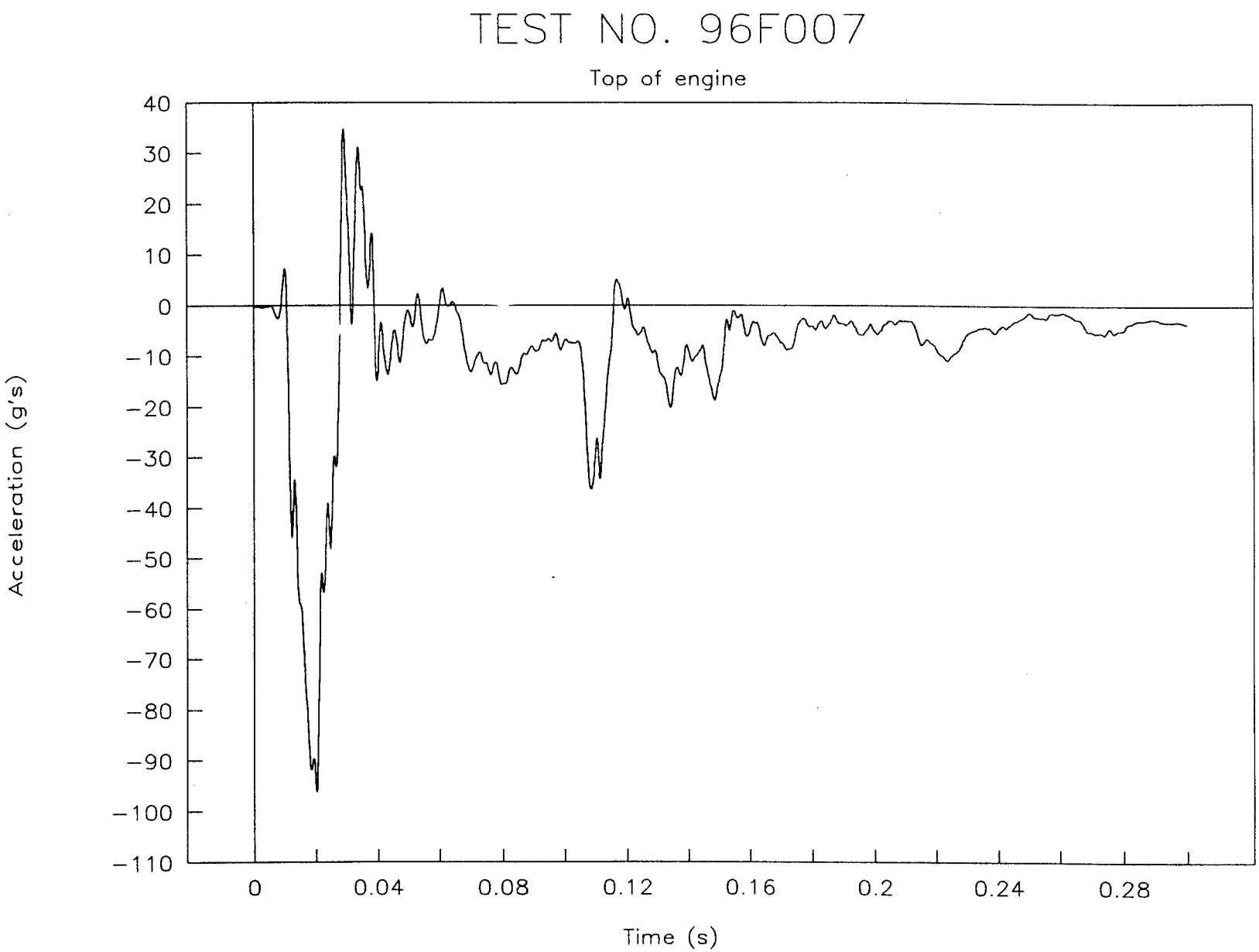

Figure 36. Acceleration vs. time, top of engine, test 96F007.

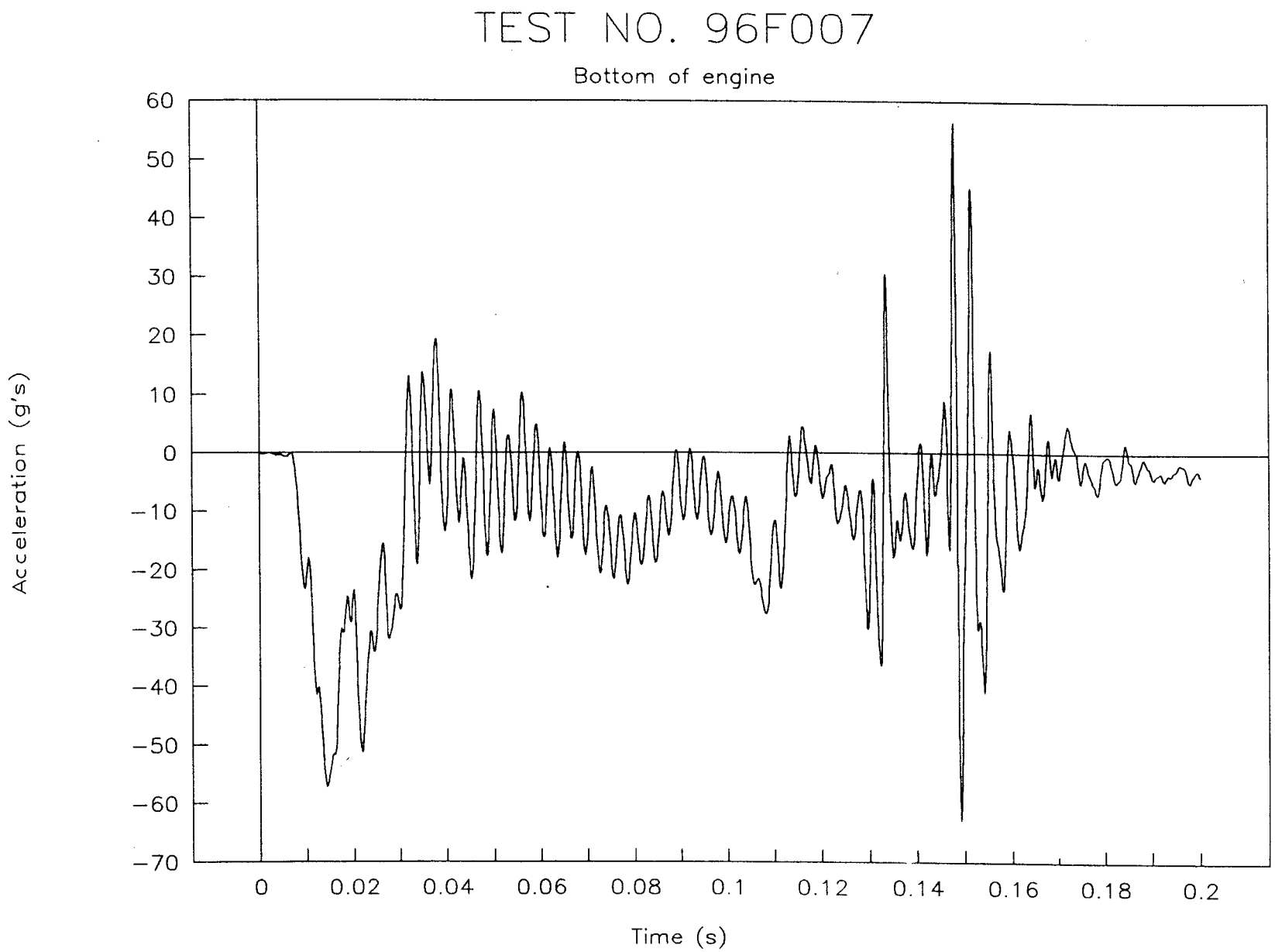

Figure 37. Acceleration vs. time, bottom of engine, test 96F007.

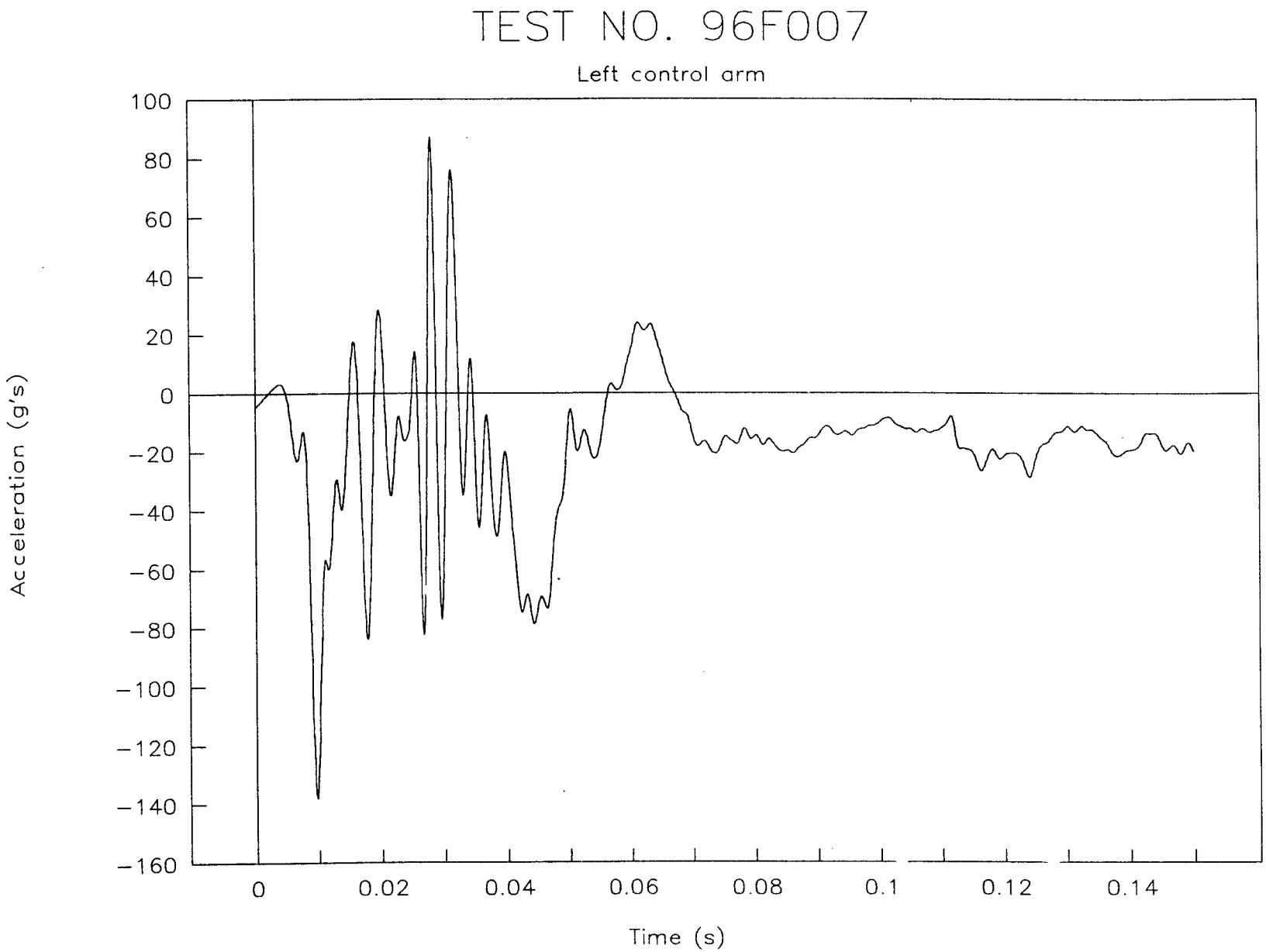

Figure 38. Acceleration vs. time, left control arm, test 96F007.

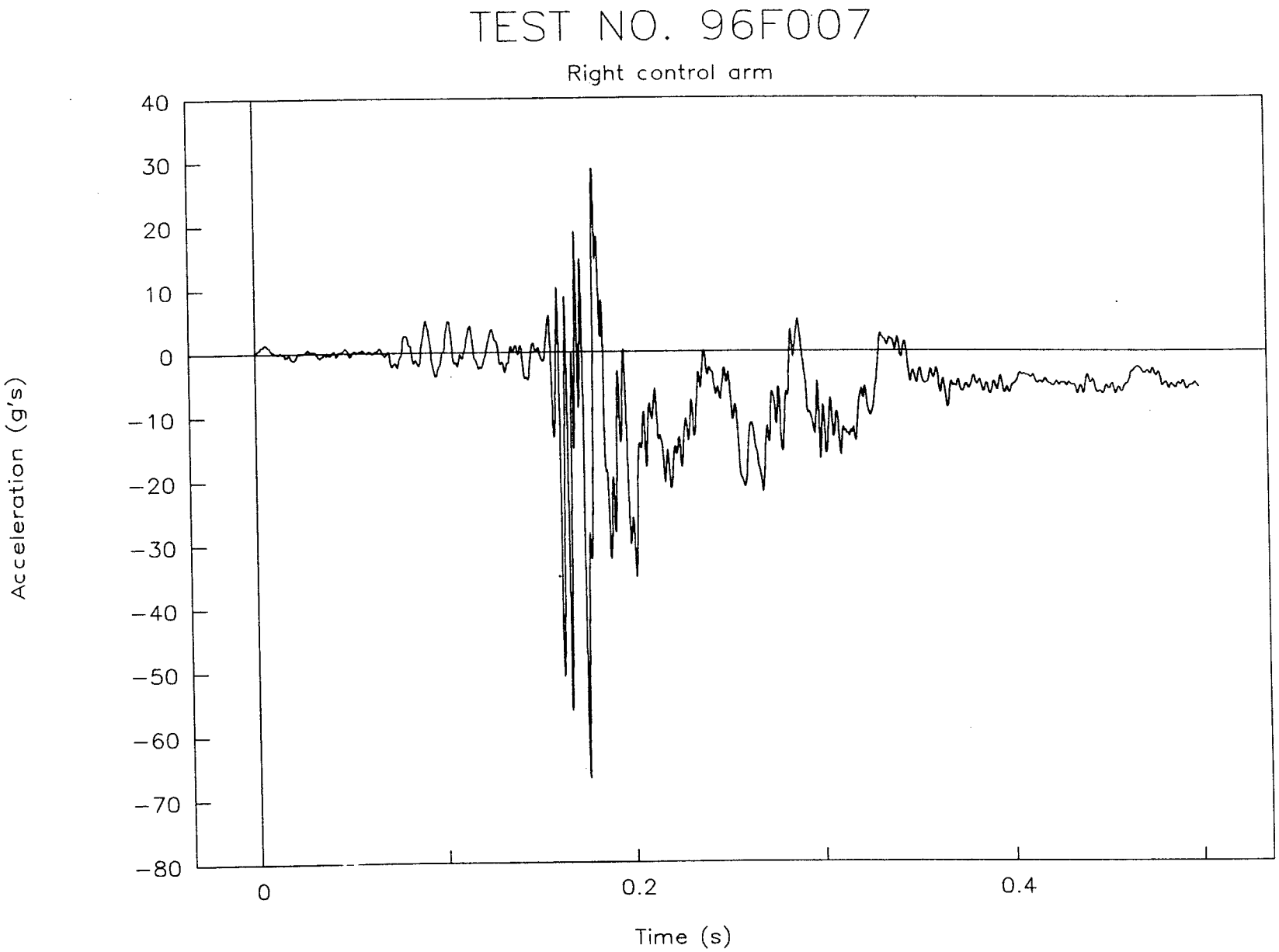

Figure 39. Acceleration vs. time, right control arm, test 96F007.

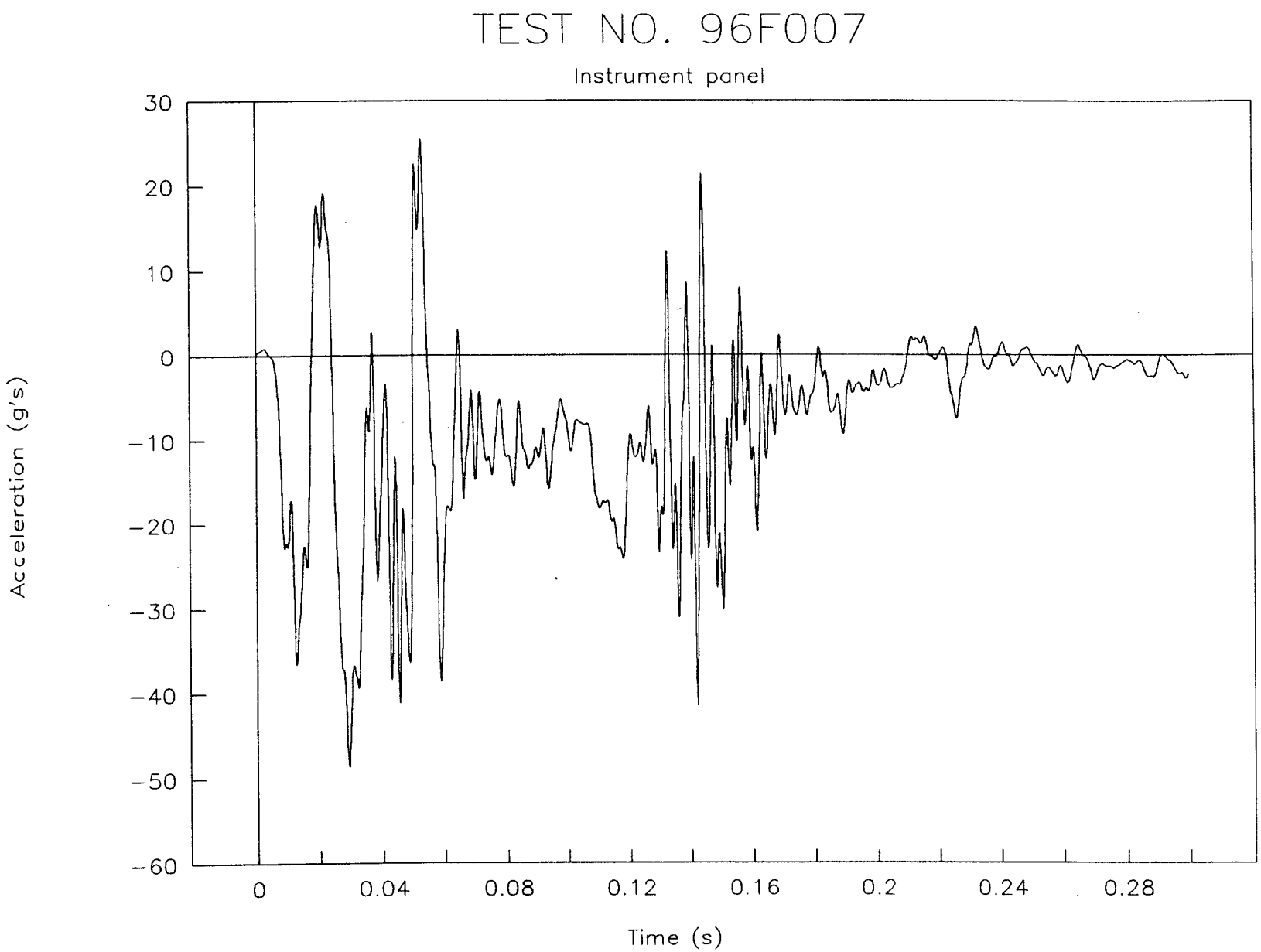

Figure 40. Acceleration vs. time, instrument panel, test 96F007.

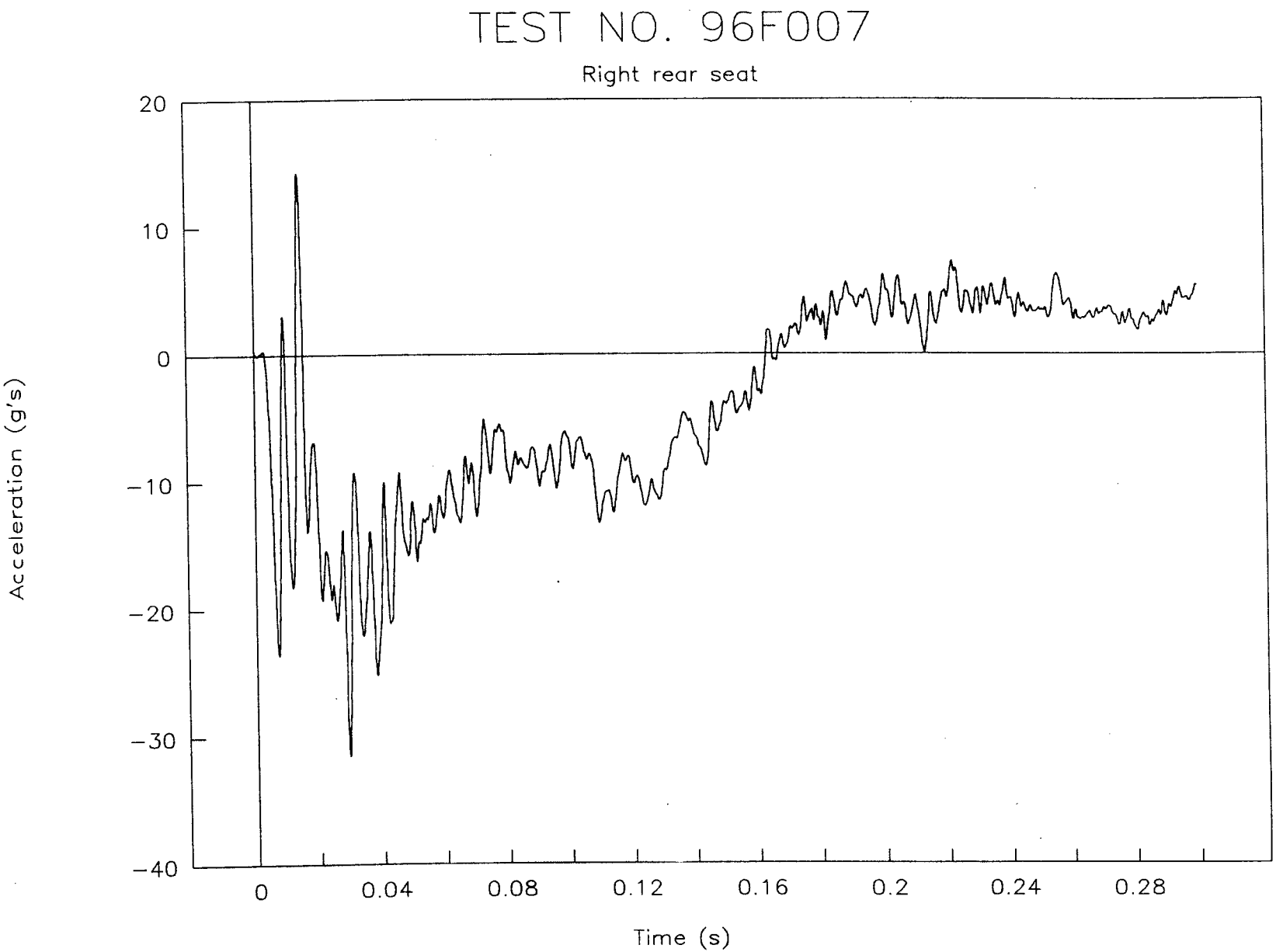

Figure 41. Acceleration vs. time, right rear seat, test 96F007.

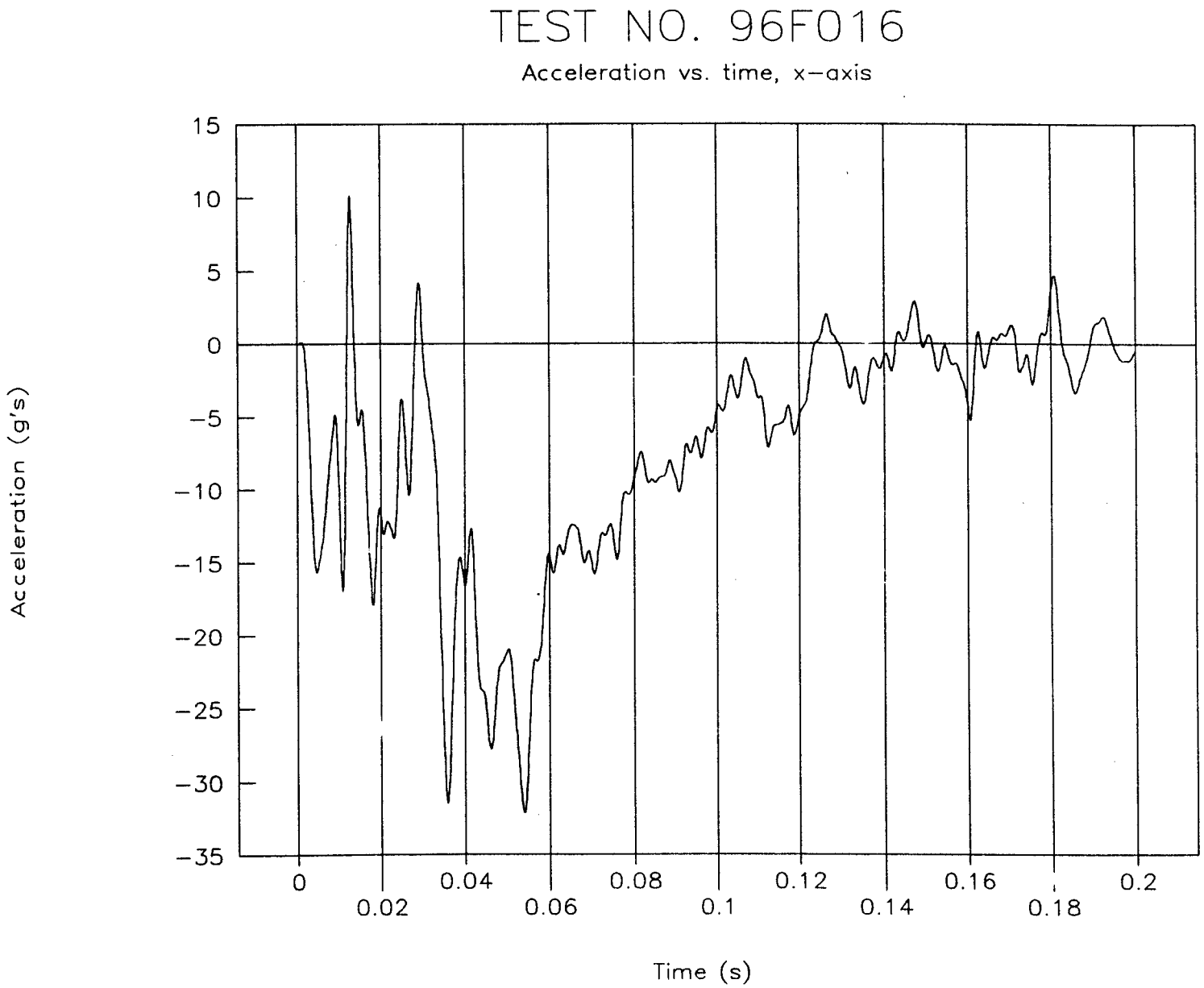

Figure 42. Acceleration vs. time, x-axis, test 96F016.

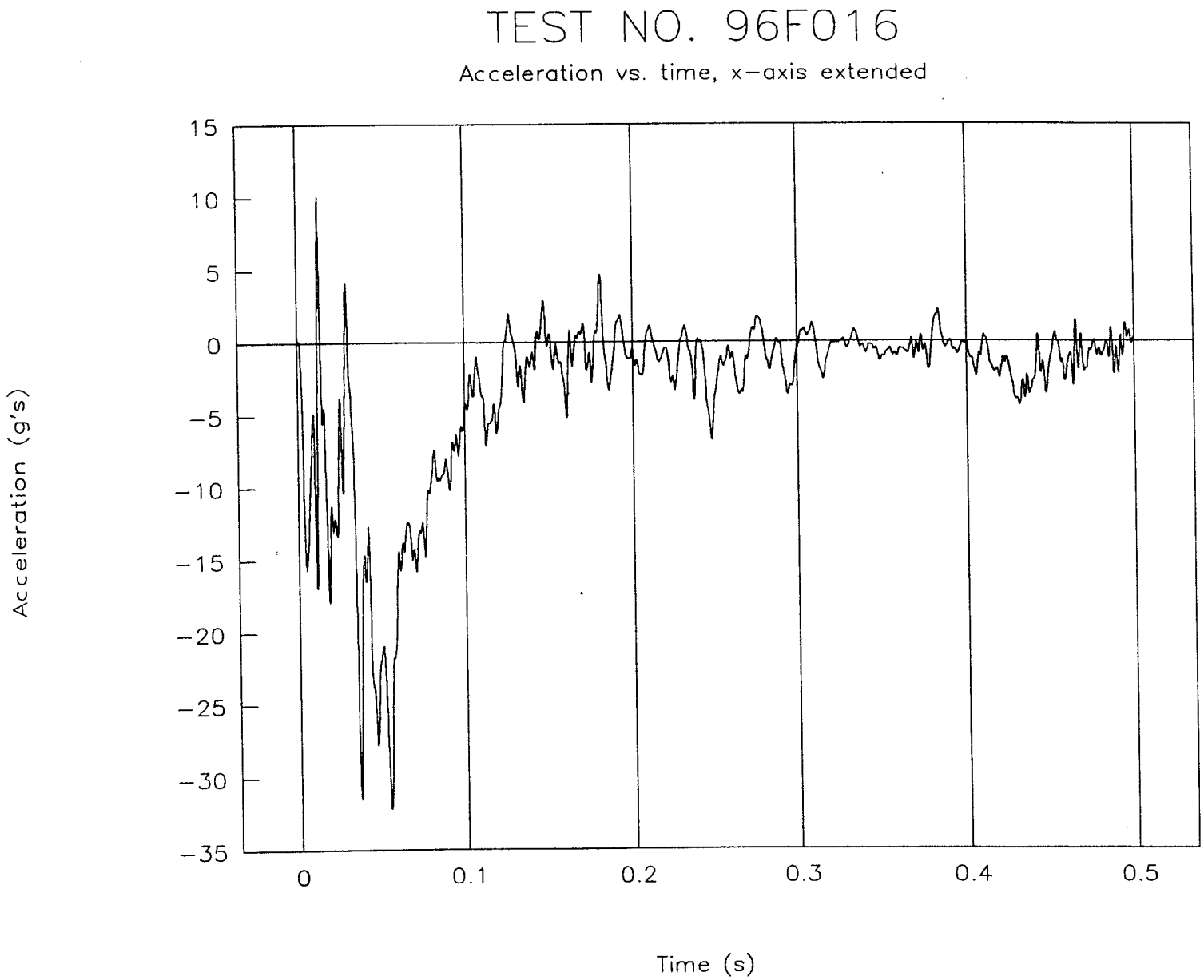

Figure 43. Acceleration vs. time, x-axis extended, test 96F016.

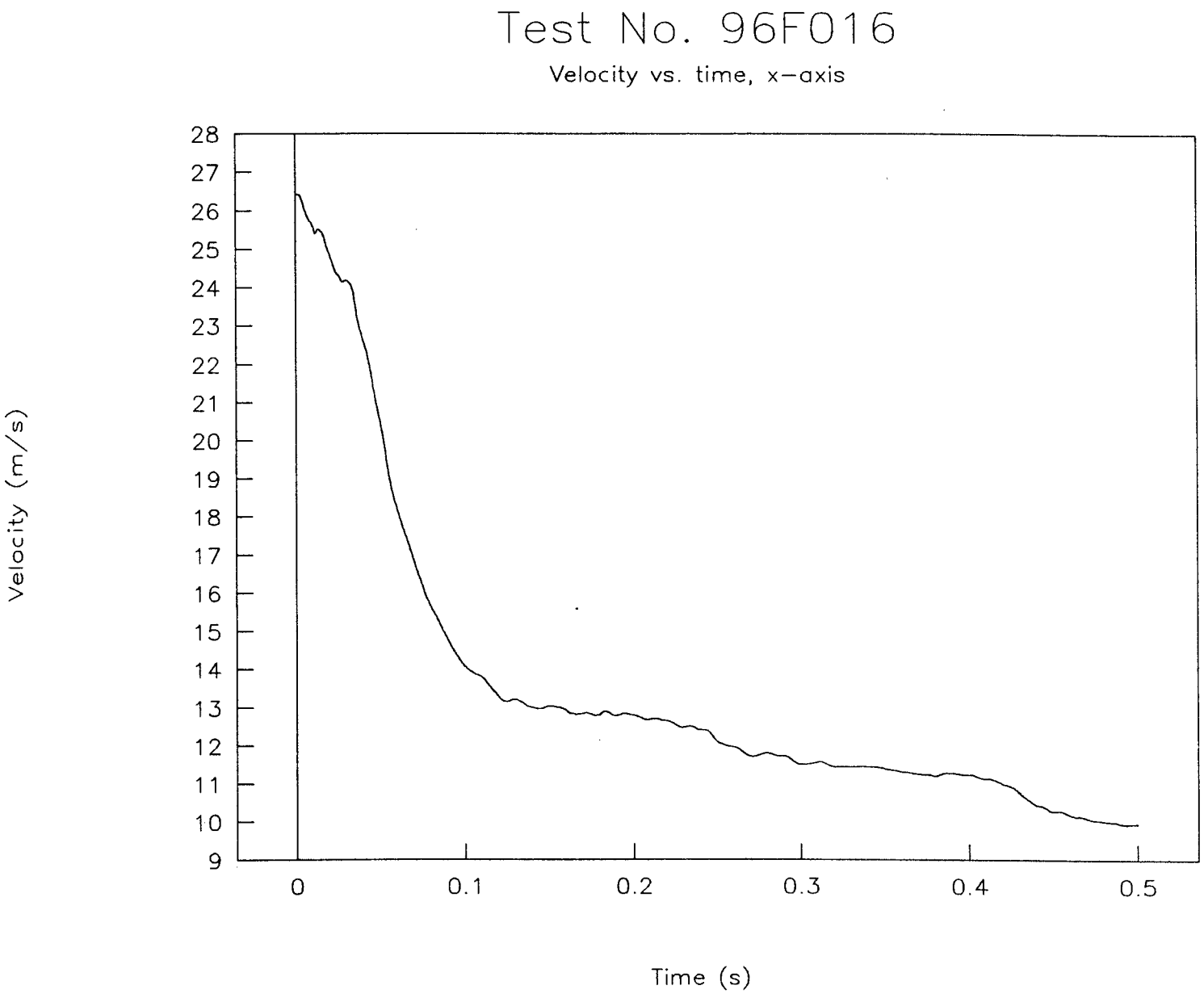

Figure 44. Velocity vs. time, x-axis, test 96F016.

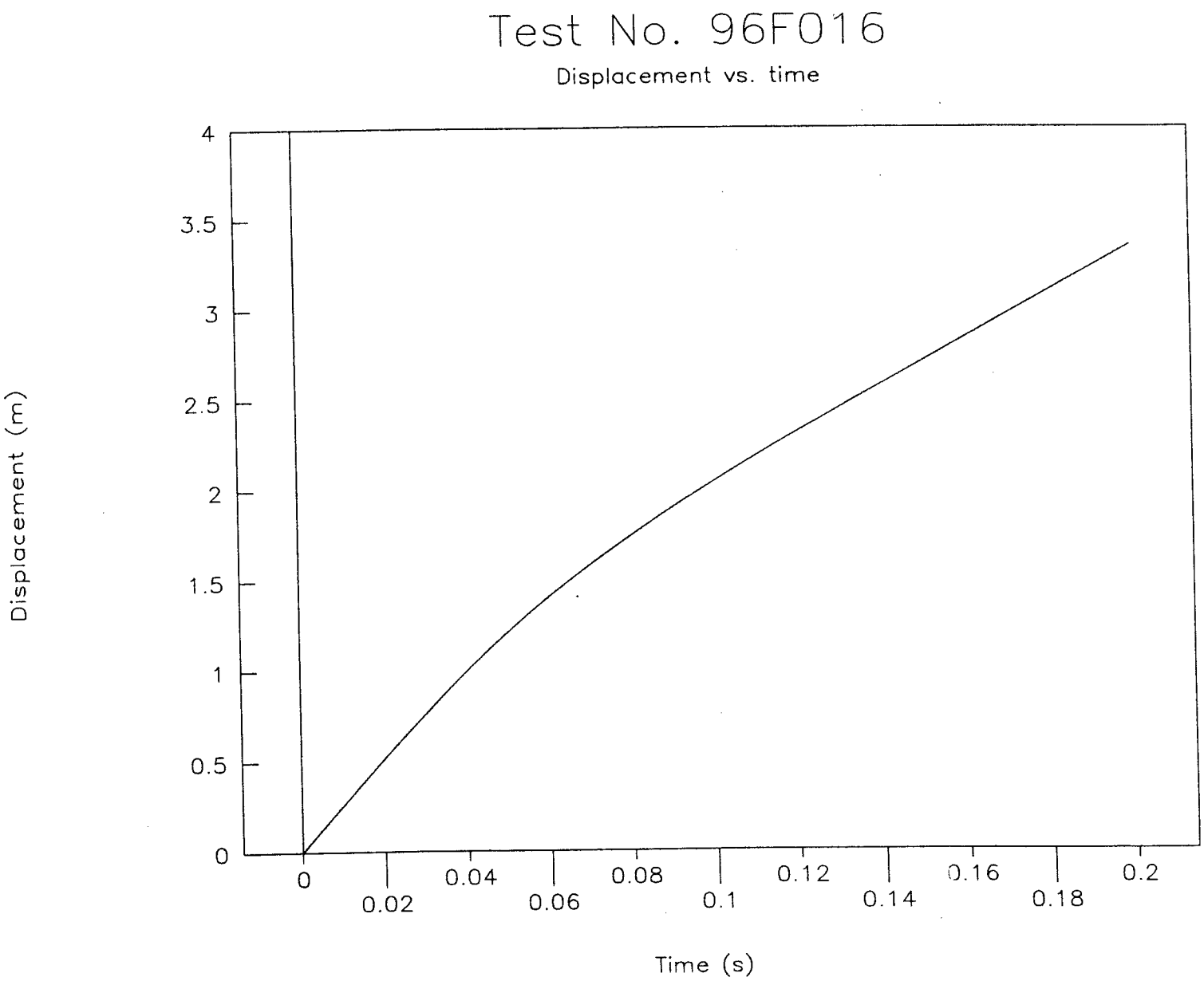

Figure 45. Displacement vs. time, test 96F016.

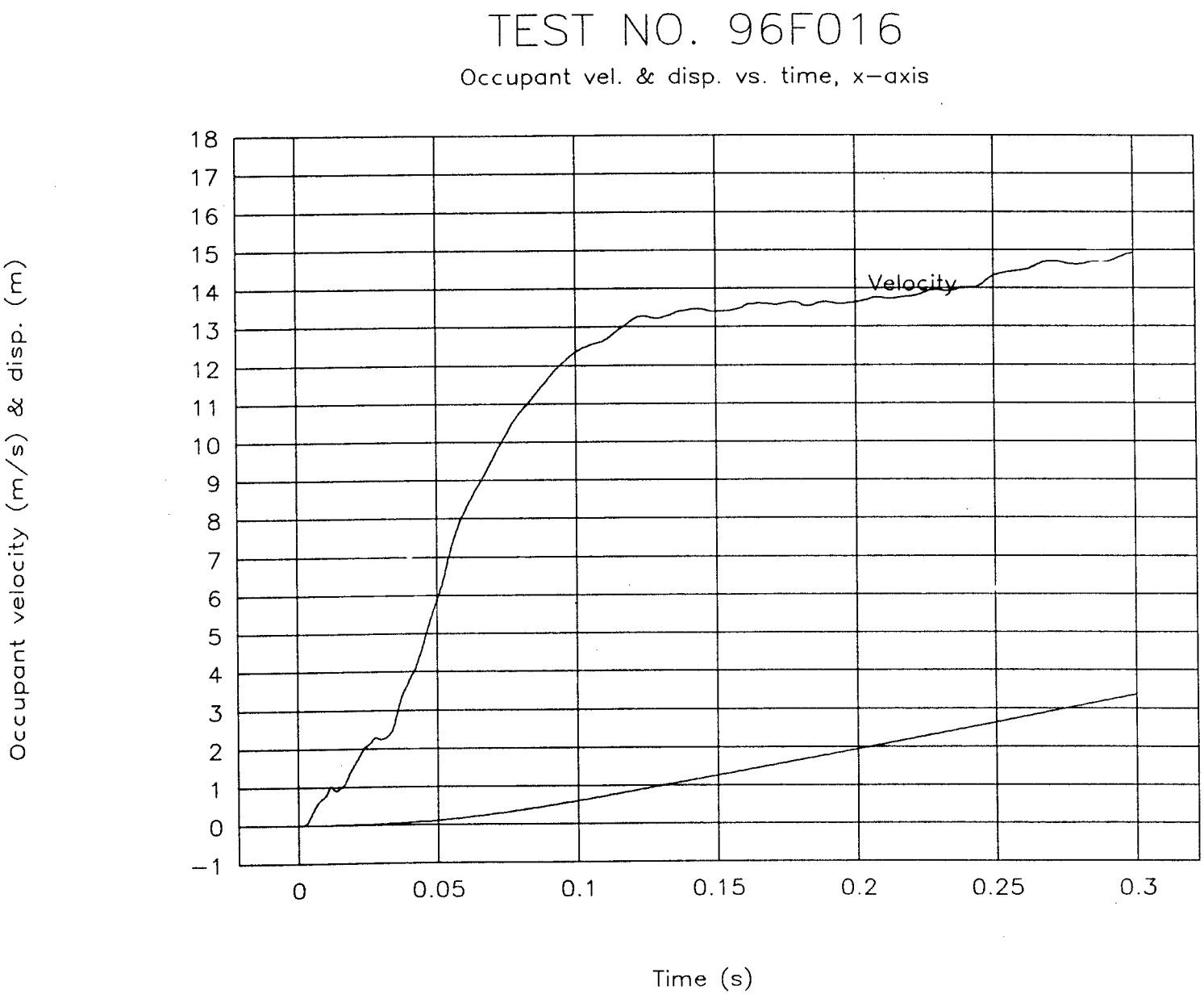

Figure 46. Occupant velocity and displacement vs. time, x-axis, test 96F016.

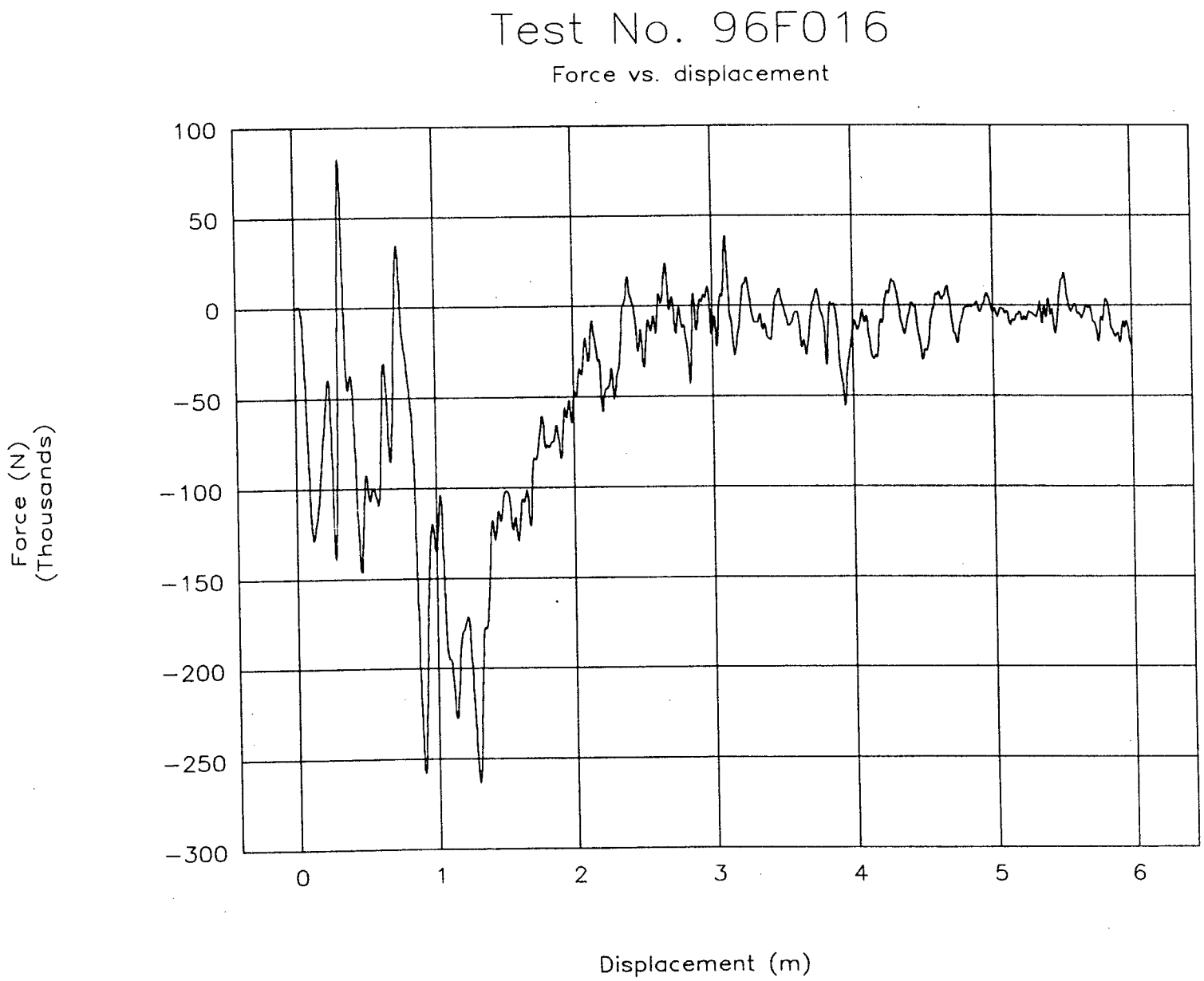

Figure 47. Force vs. displacement, test 96F016.

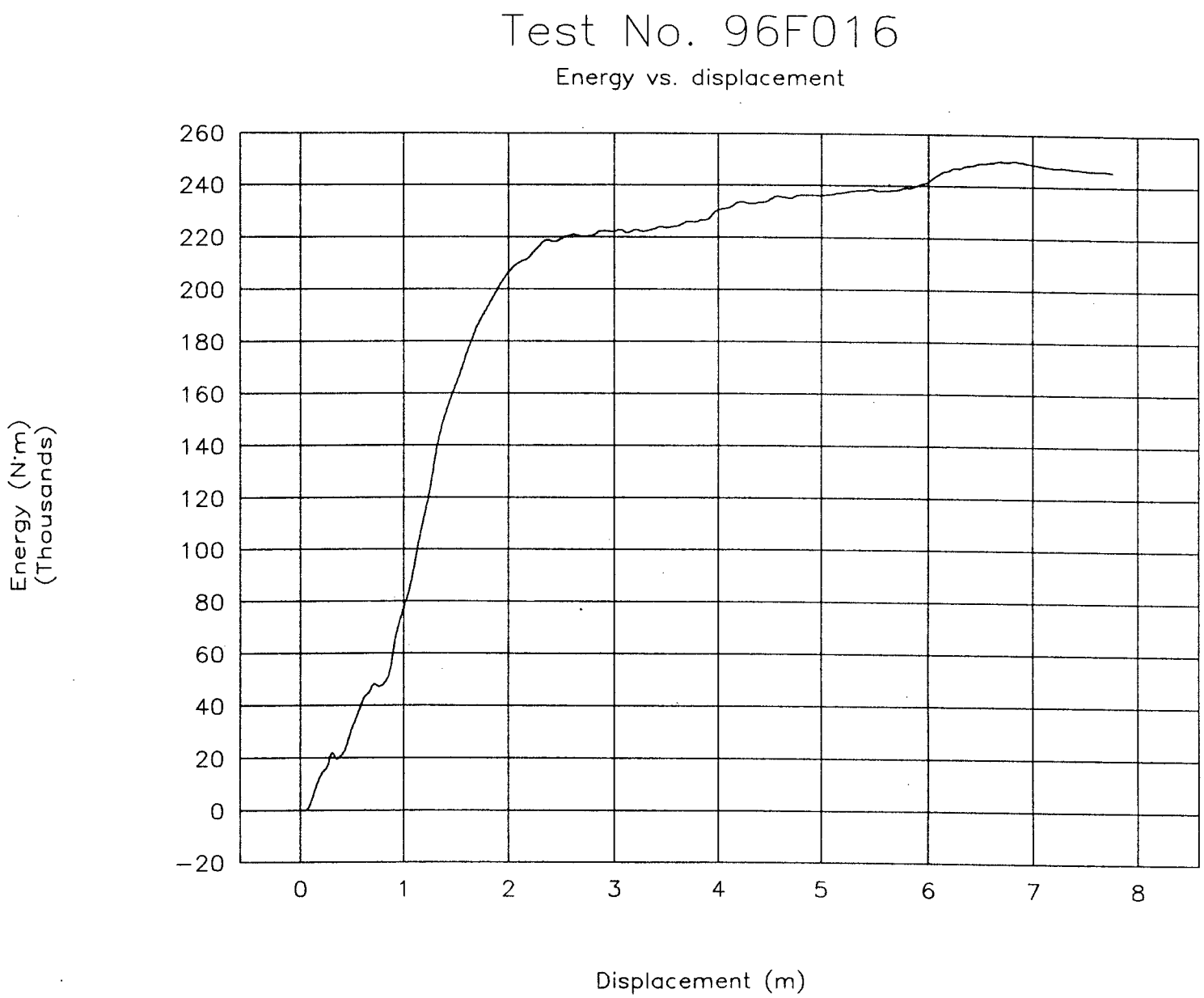

Figure 48. Energy vs. displacement, test 96F016.

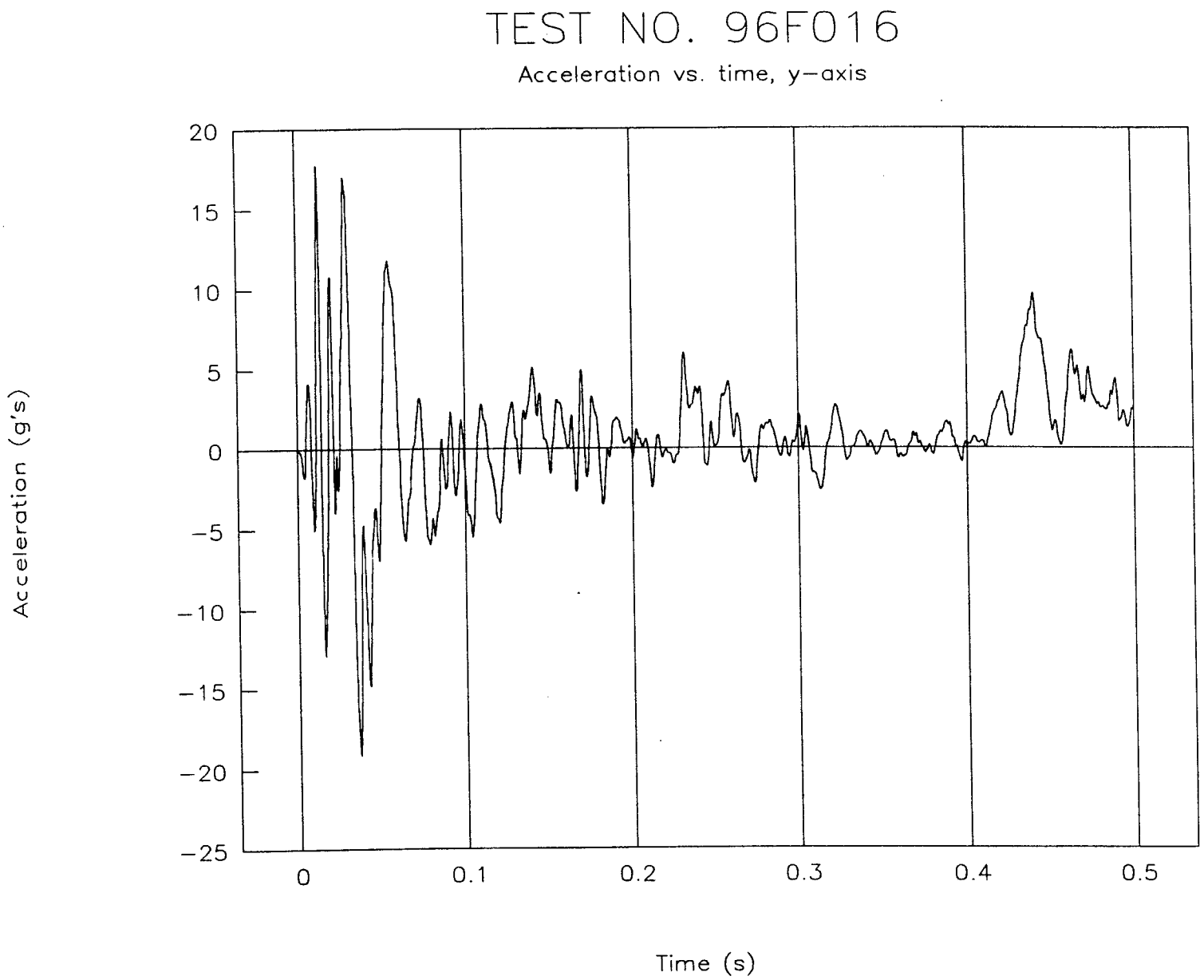

Figure 49. Acceleration vs. time, y-axis, test 96F016.

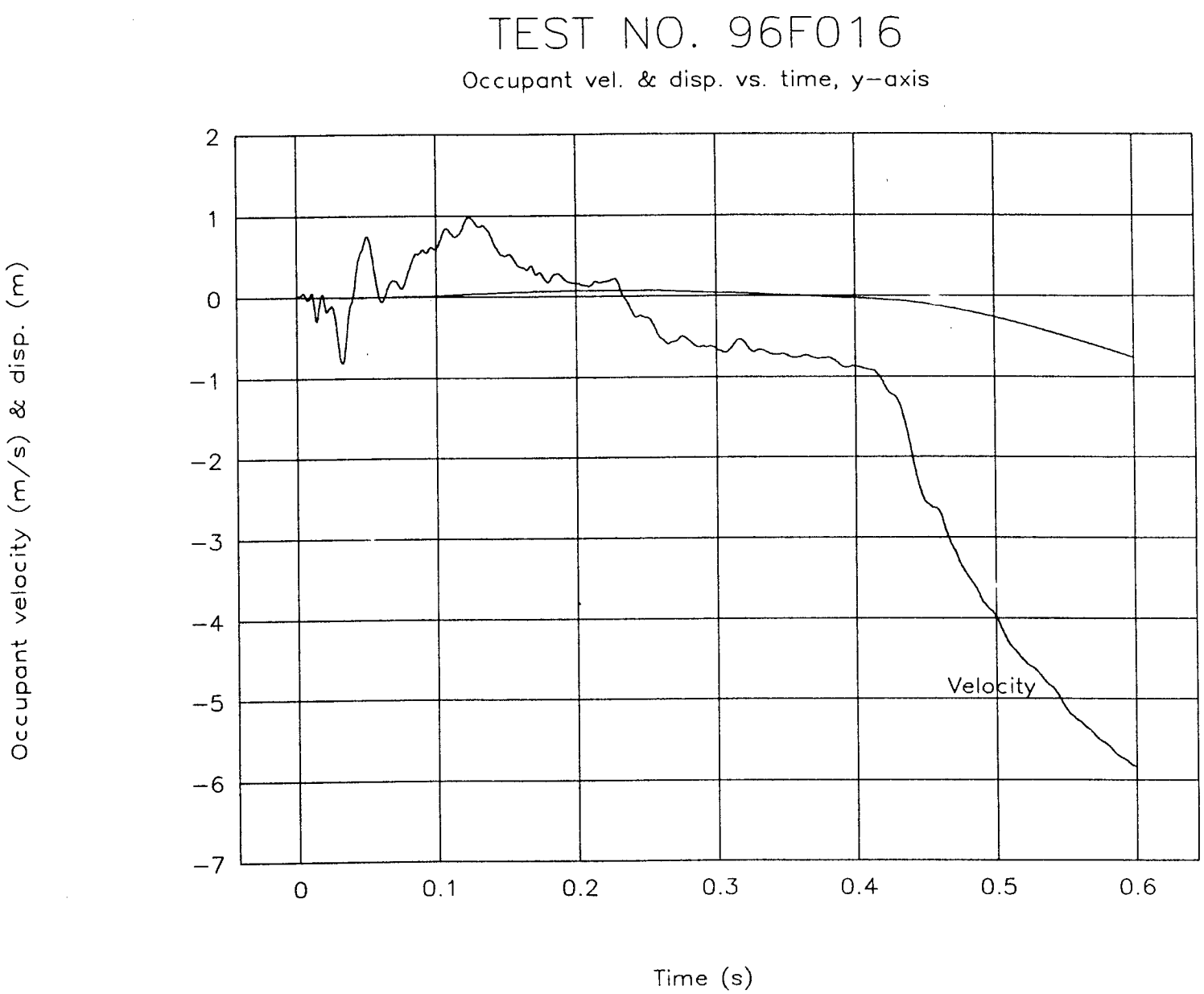

Figure 50. Occupant velocity and displacement vs. time, y-axis, test 96F016.

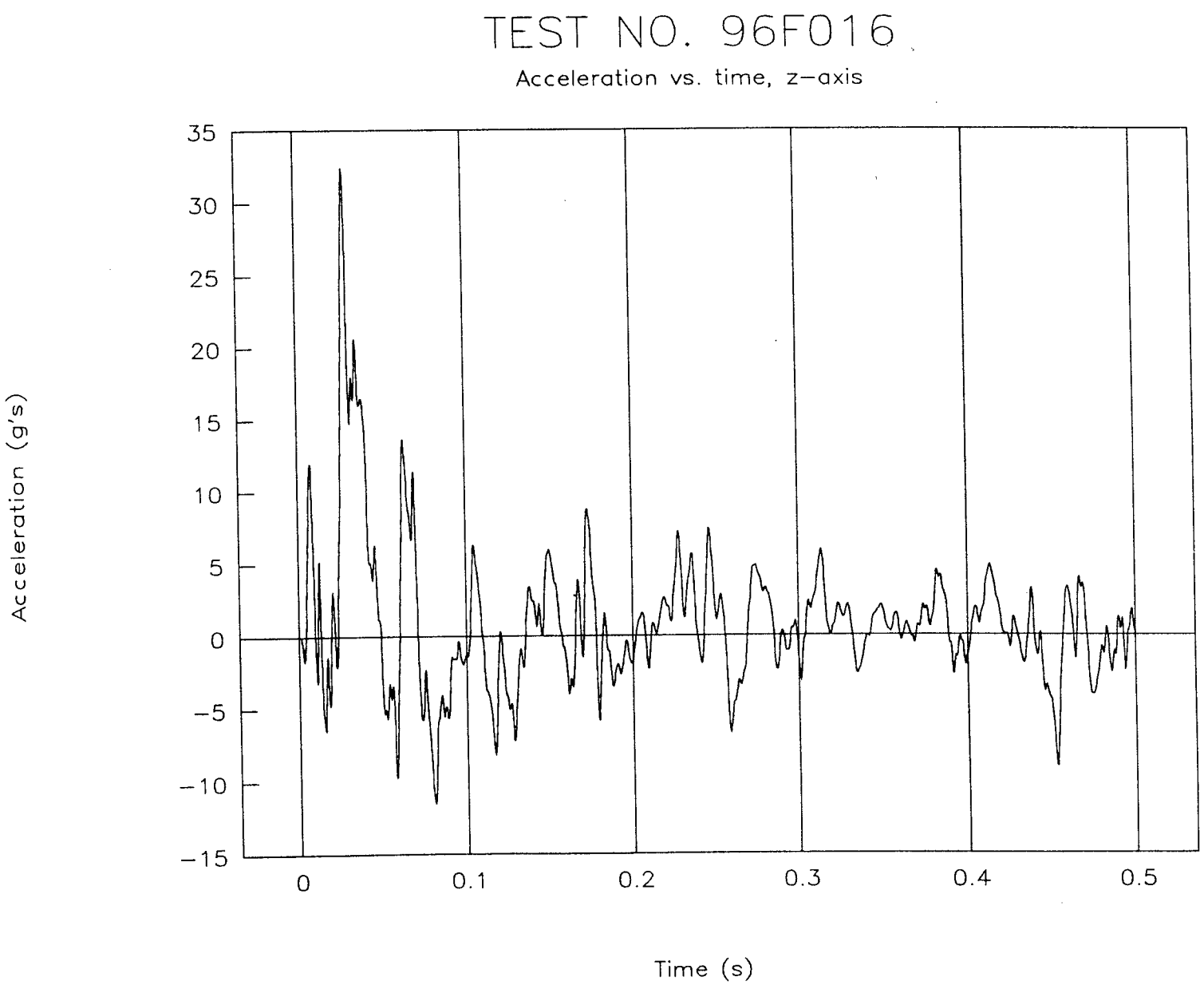

Figure 51. Acceleration vs. time, z-axis, test 96F016.

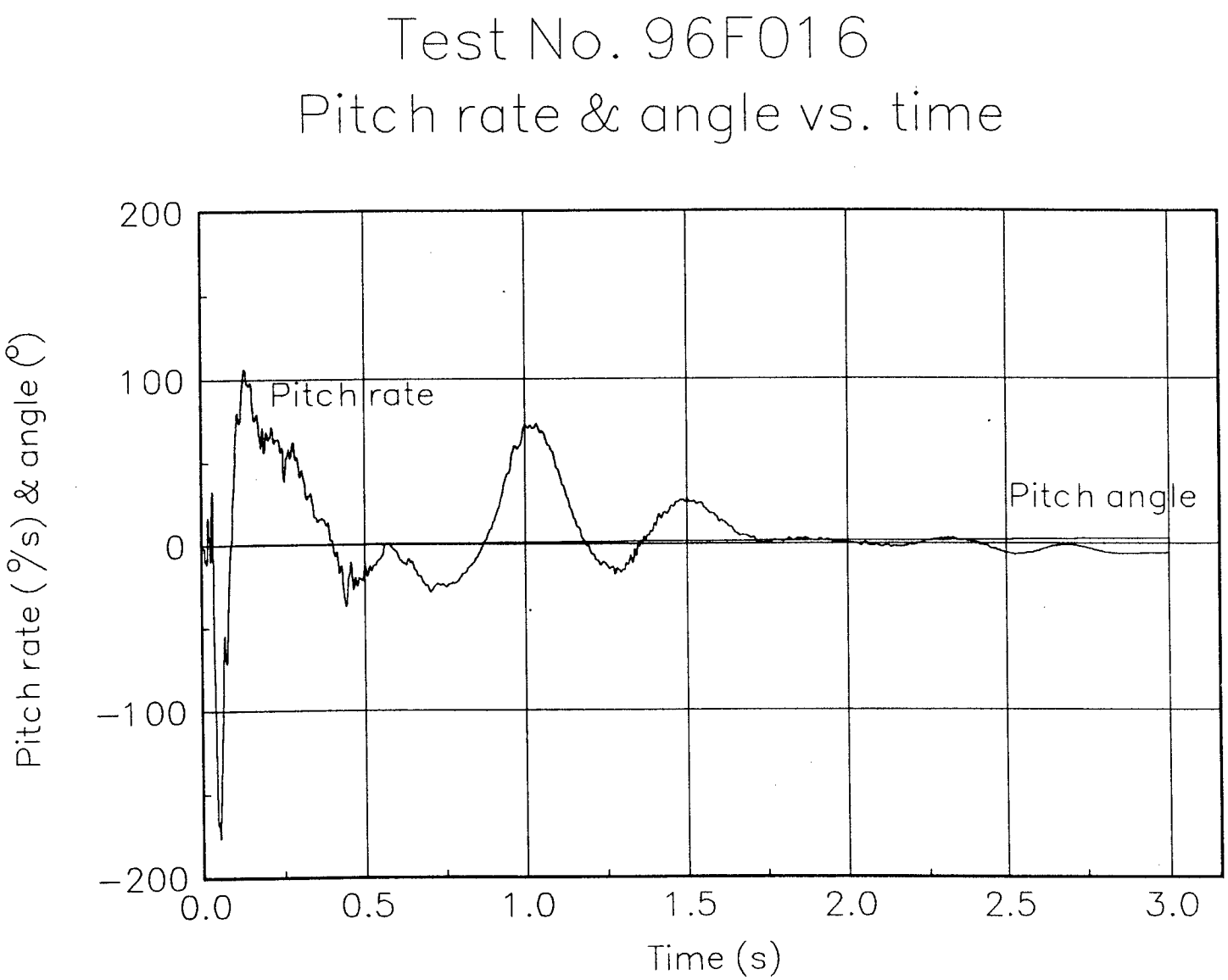

Figure 52. Pitch rate and angle vs. time, test 96F016.

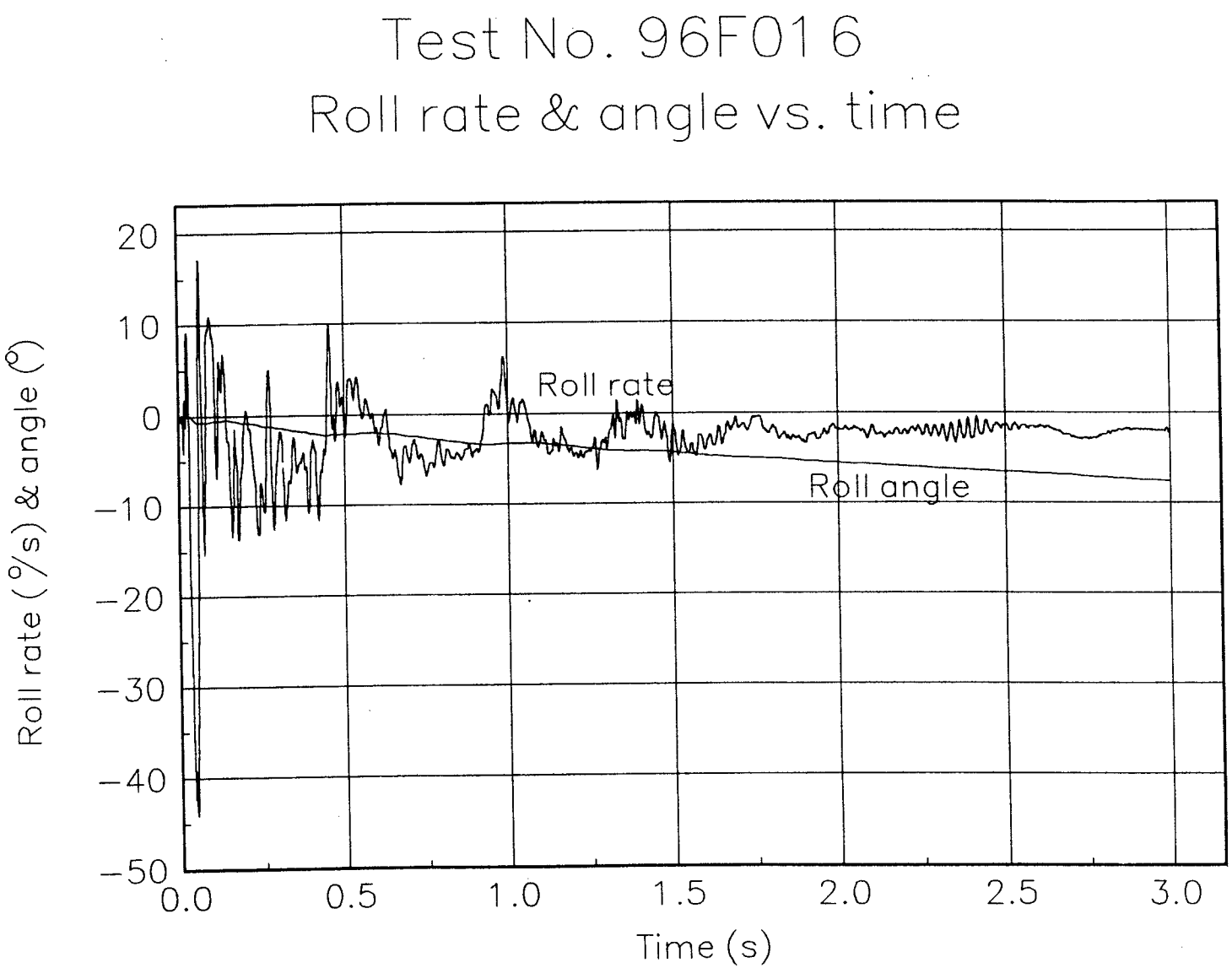

Figure 53. Roll rate and angle vs. time, test 96F016.

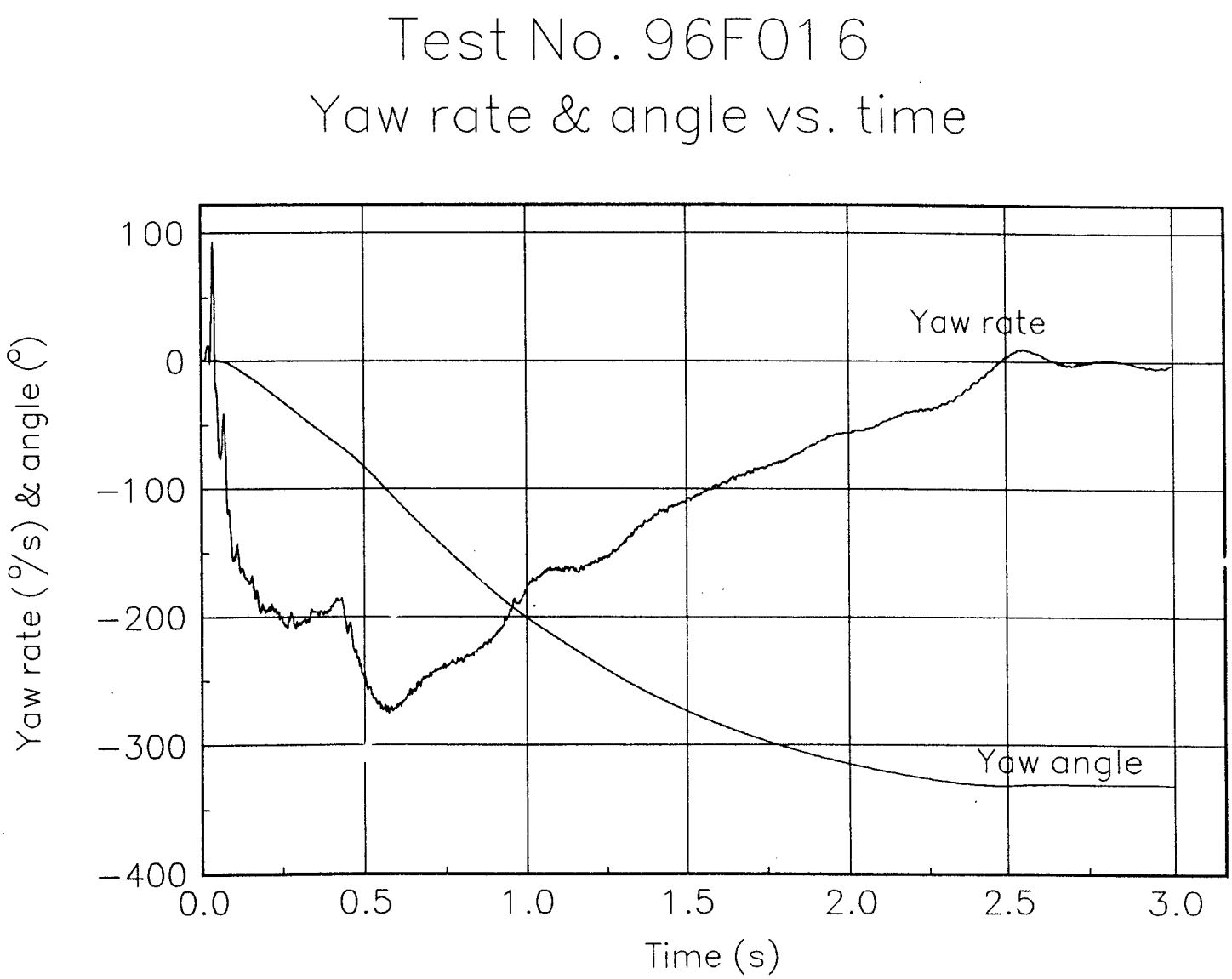

Figure 54. Yaw rate and angle vs. time, test 96F016.

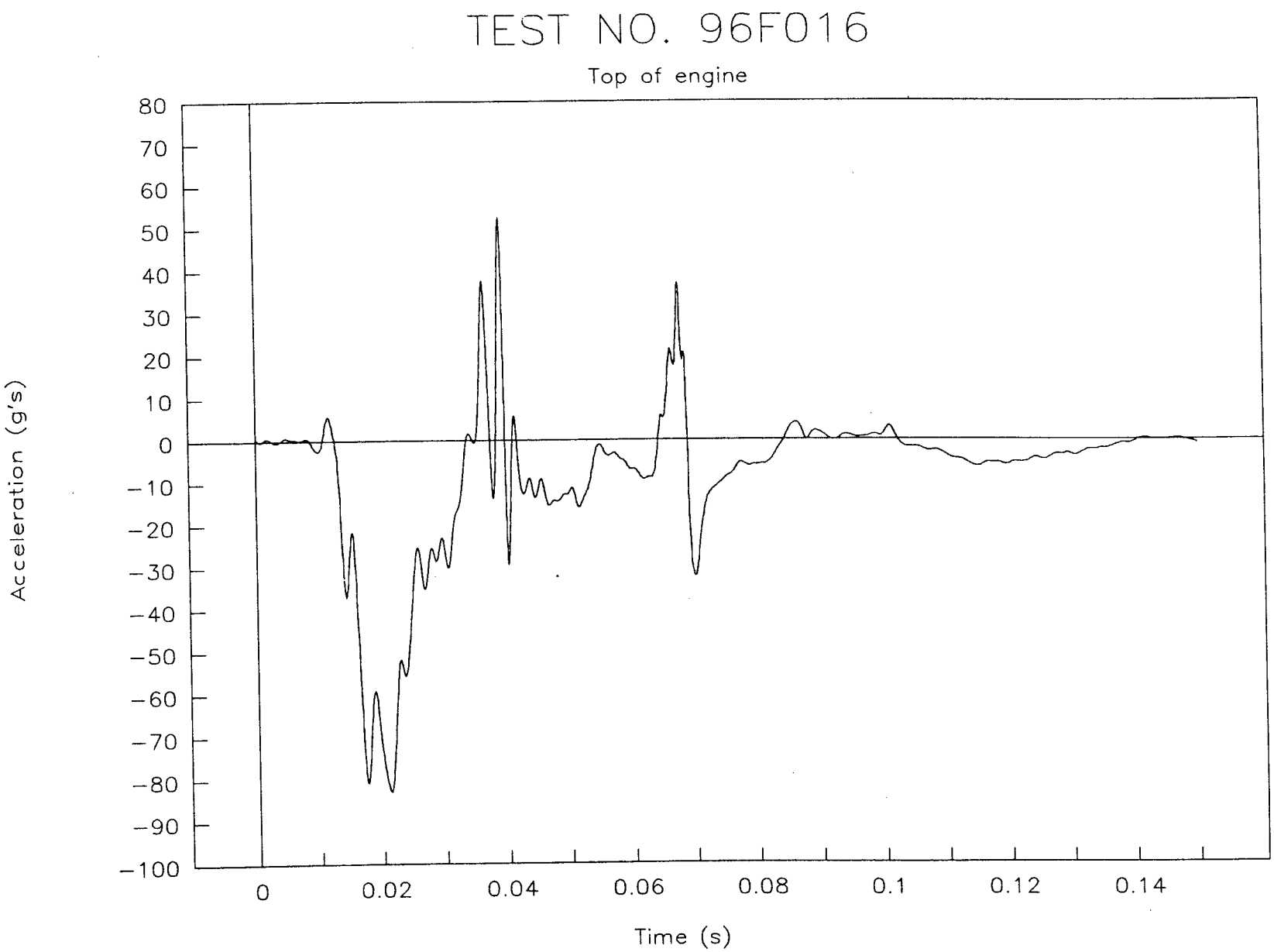

Figure 55. Acceleration vs. time, top of engine, test 96F016.

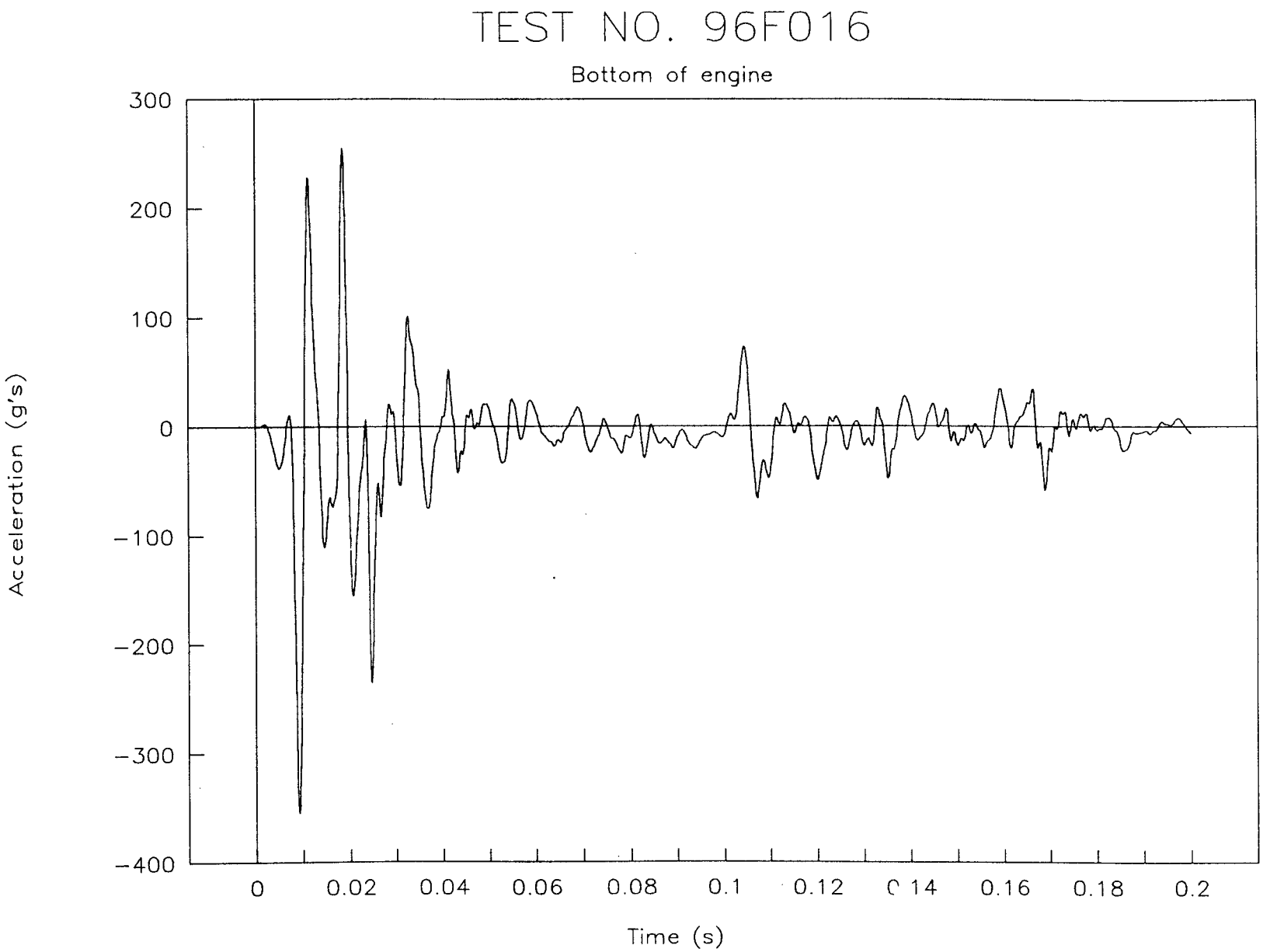

Figure 56. Acceleration vs. time, bottom of engine, test 96F016.

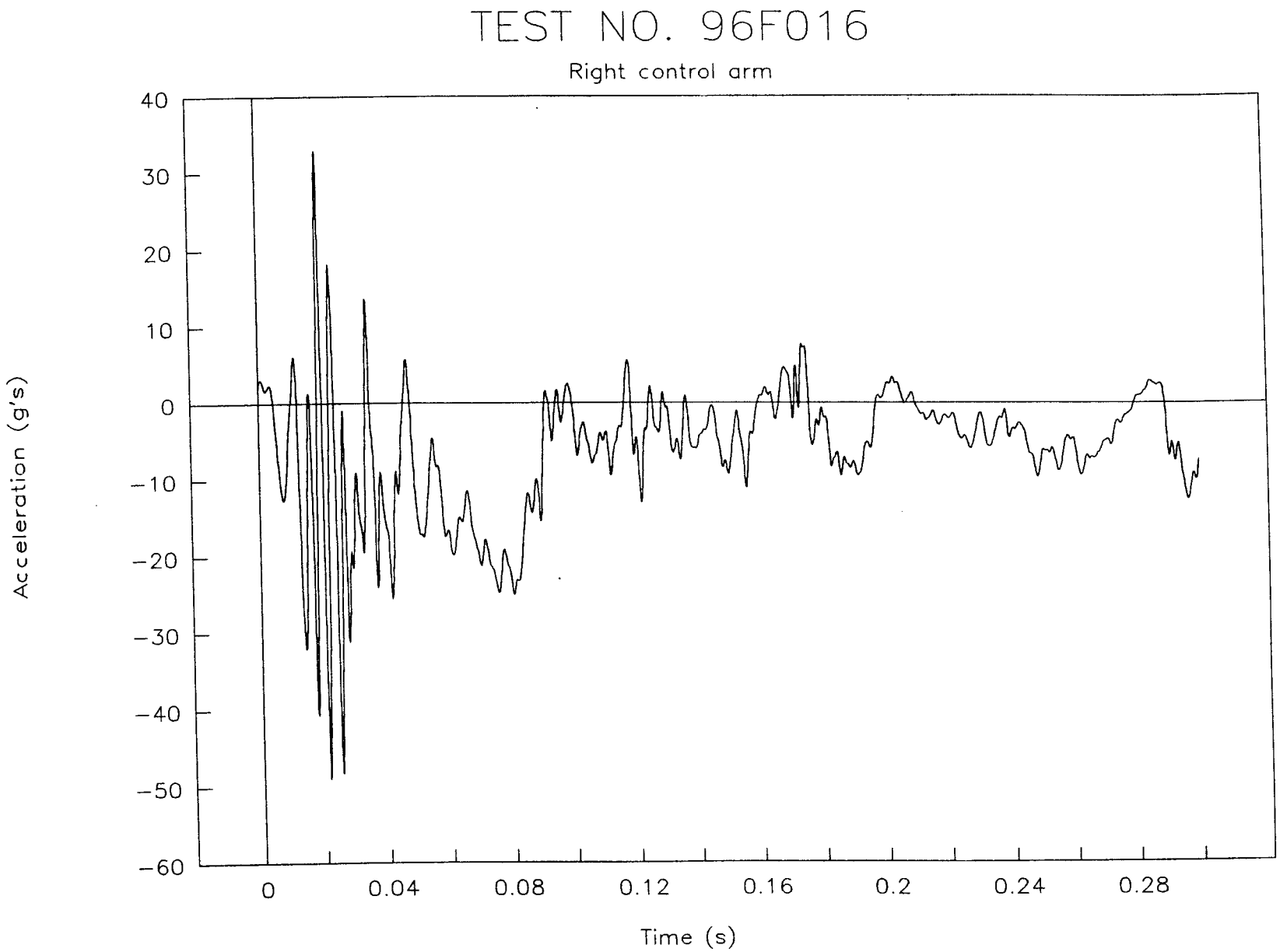

Figure 57. Acceleration vs. time, right control arm, test 96F016.

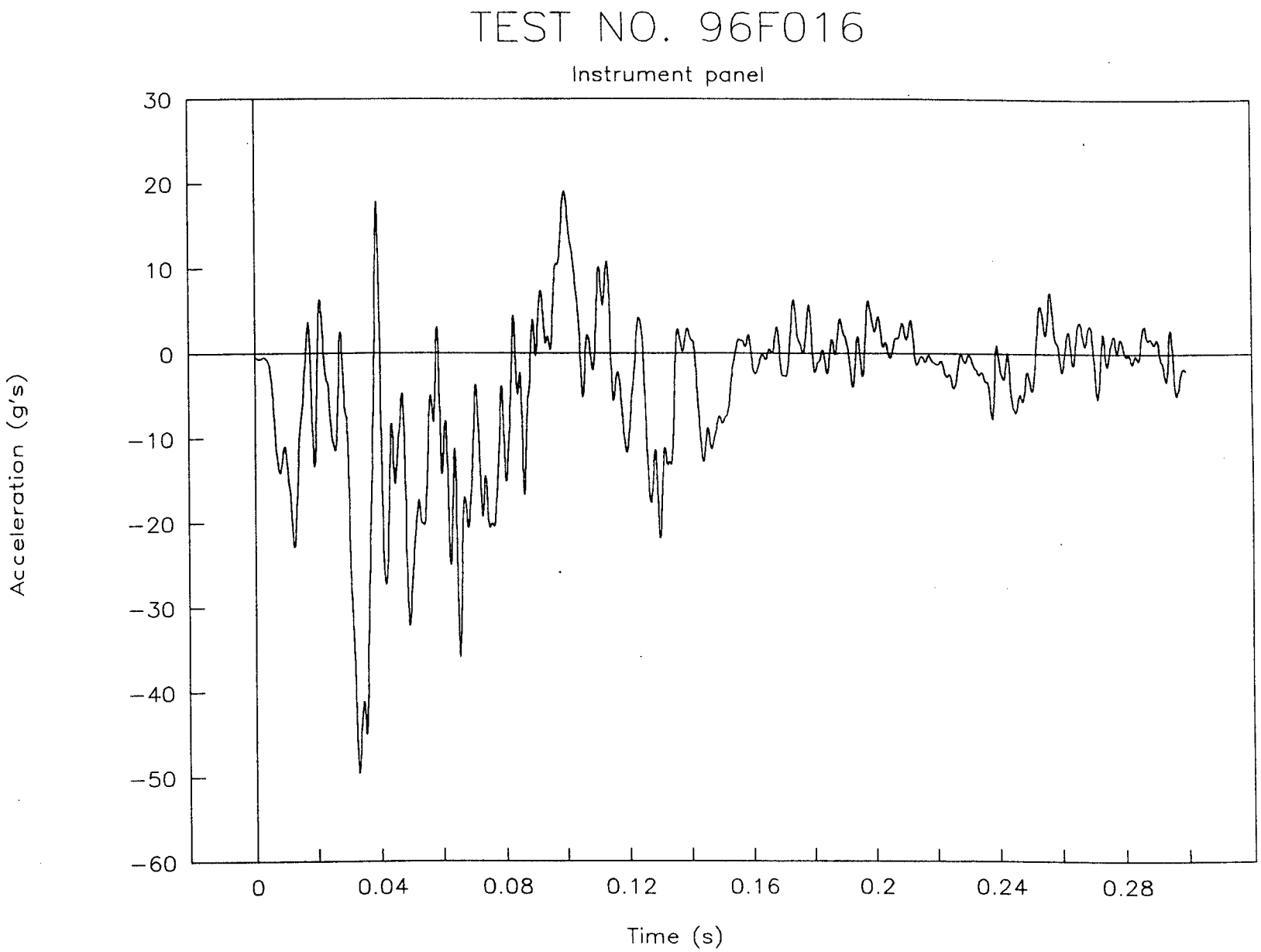

Figure 58. Acceleration vs. time, instrument panel, test 96F016.

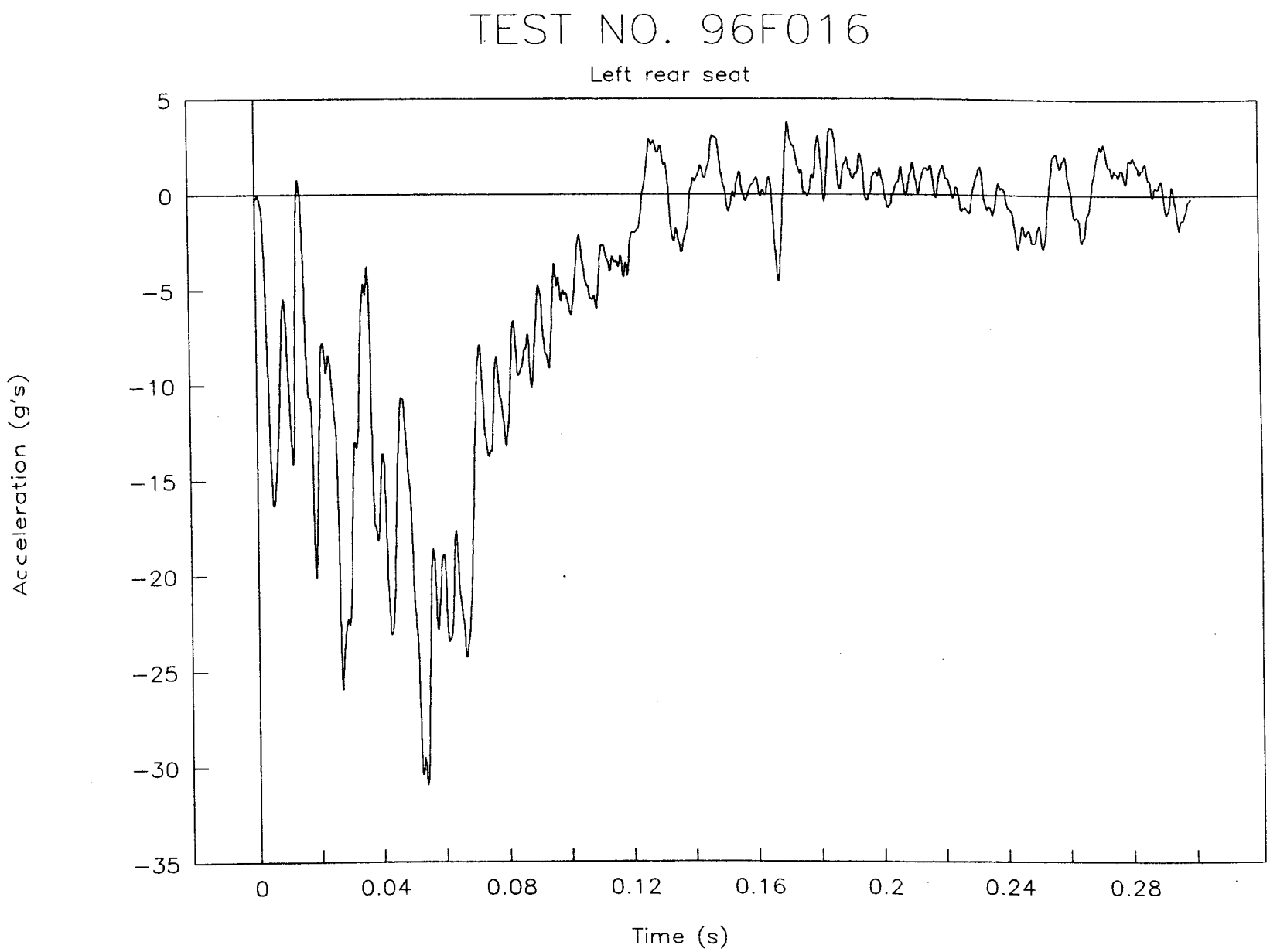

Figure 59. Acceleration vs. time, left rear seat, test 96F016.

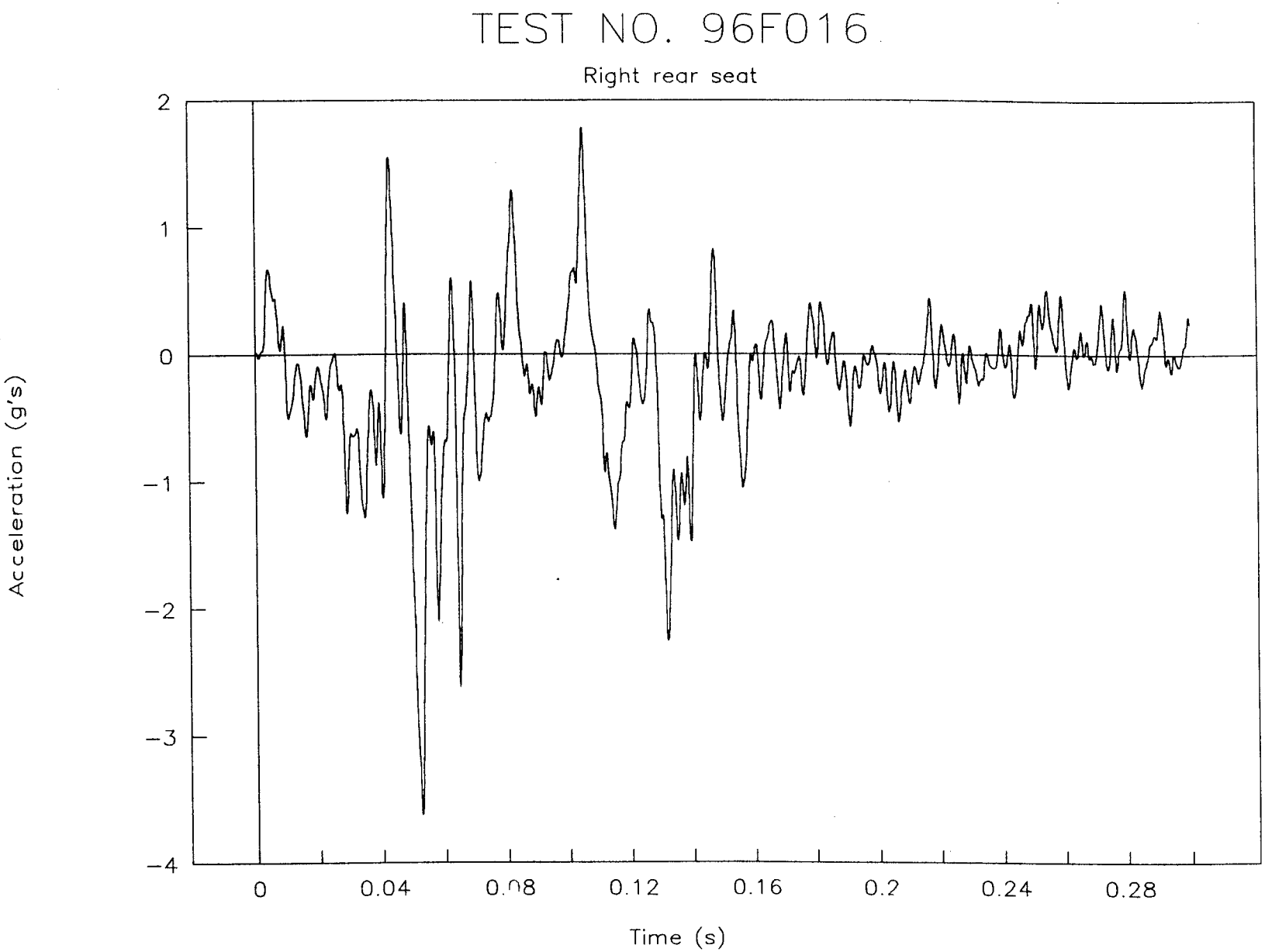

Figure 60. Acceleration vs. time, right rear seat, test 96F016.

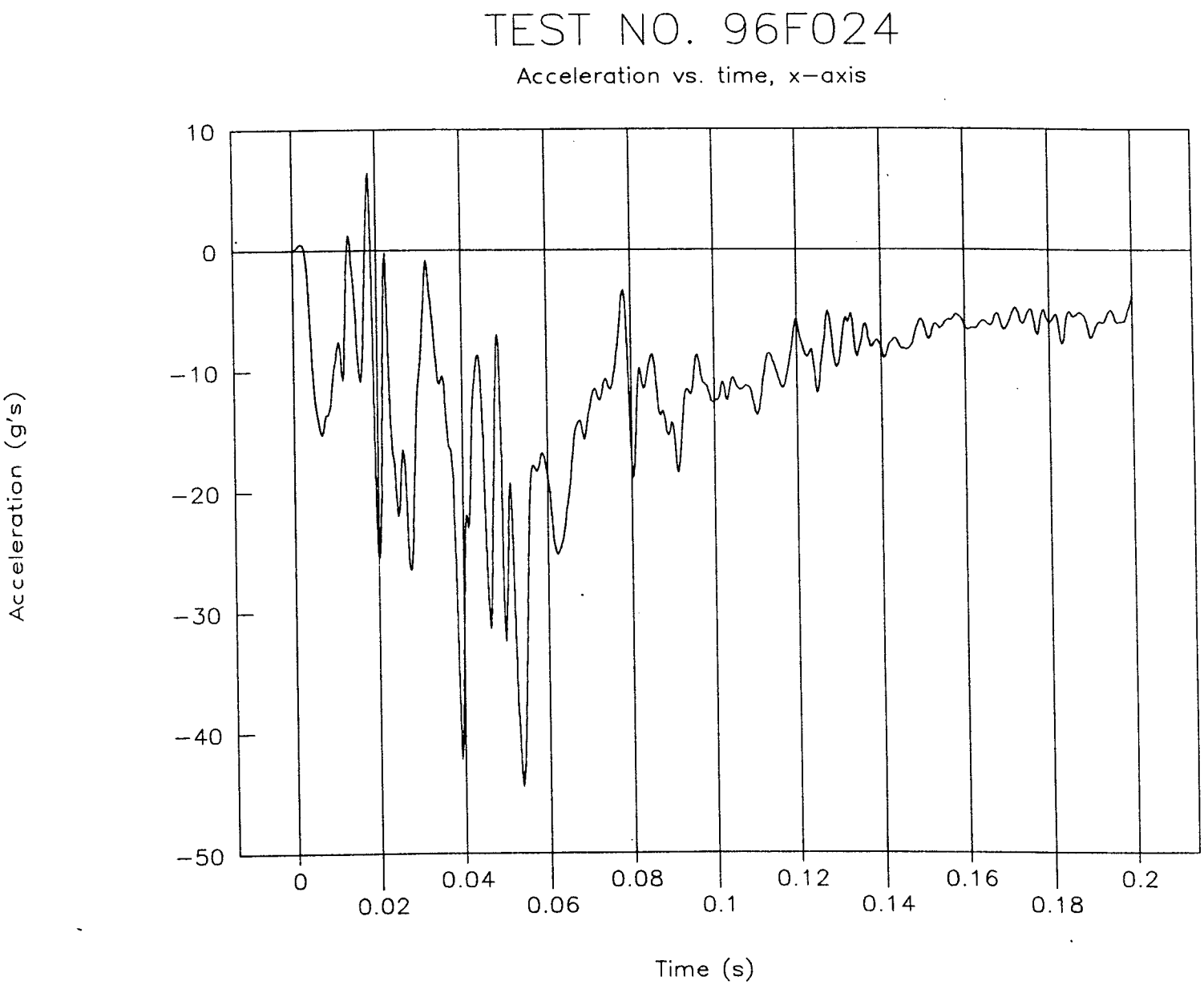

Figure 61. Acceleration vs. time, x-axis, test 96F024.

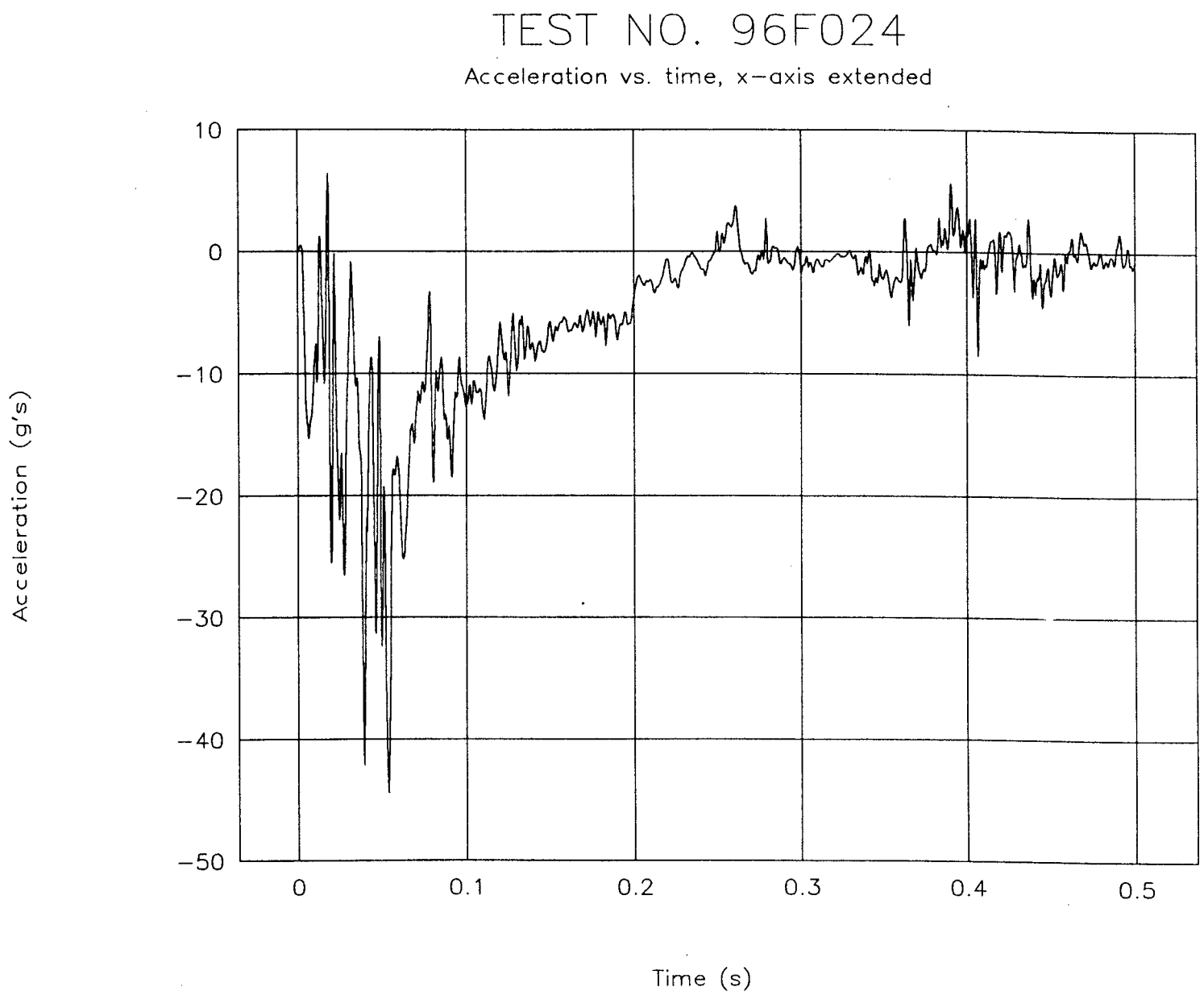

Figure 62. Acceleration vs. time, x-axis extended, test 96F024.

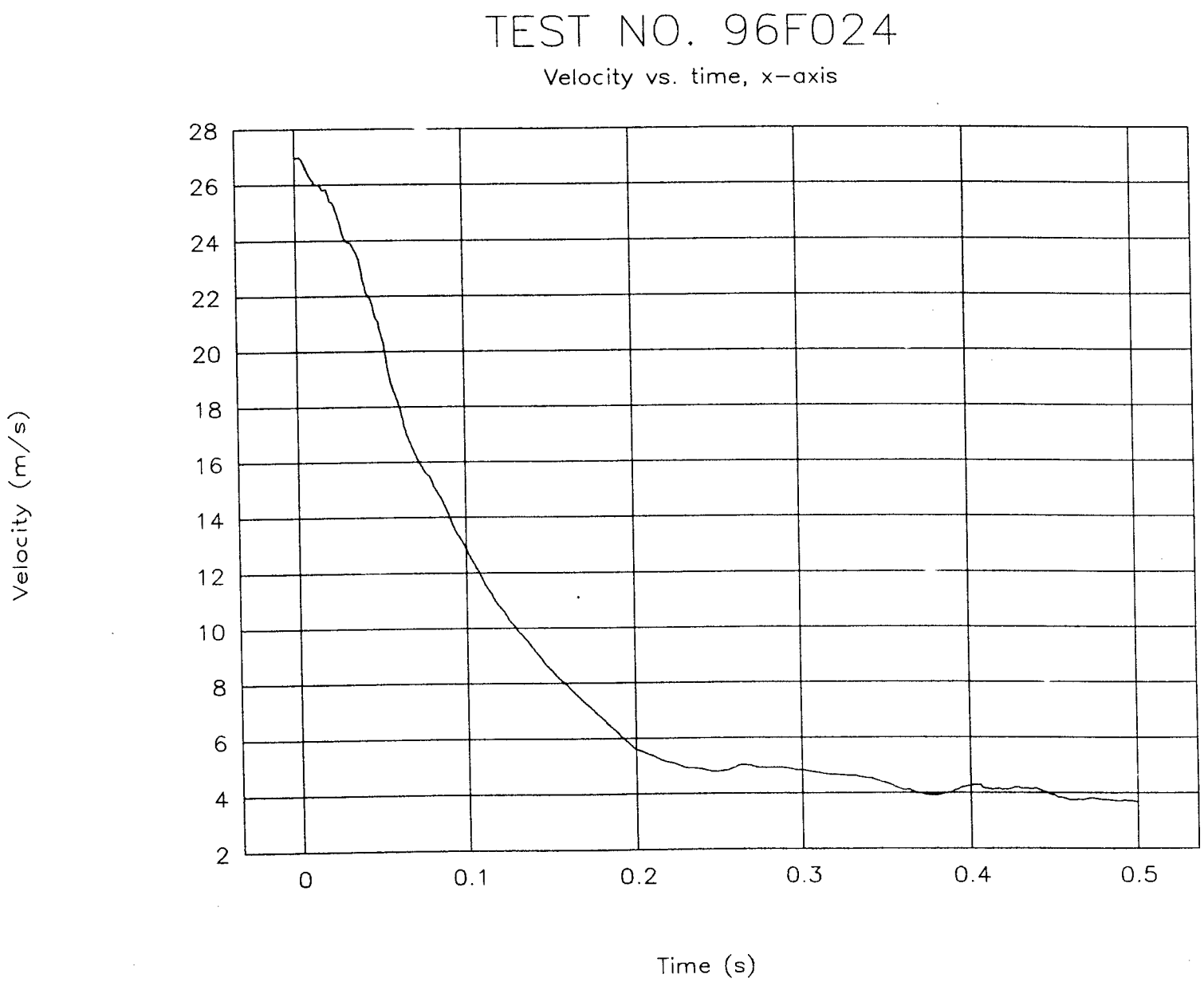

Figure 63. Velocity vs. time, x-axis, test 96F024.

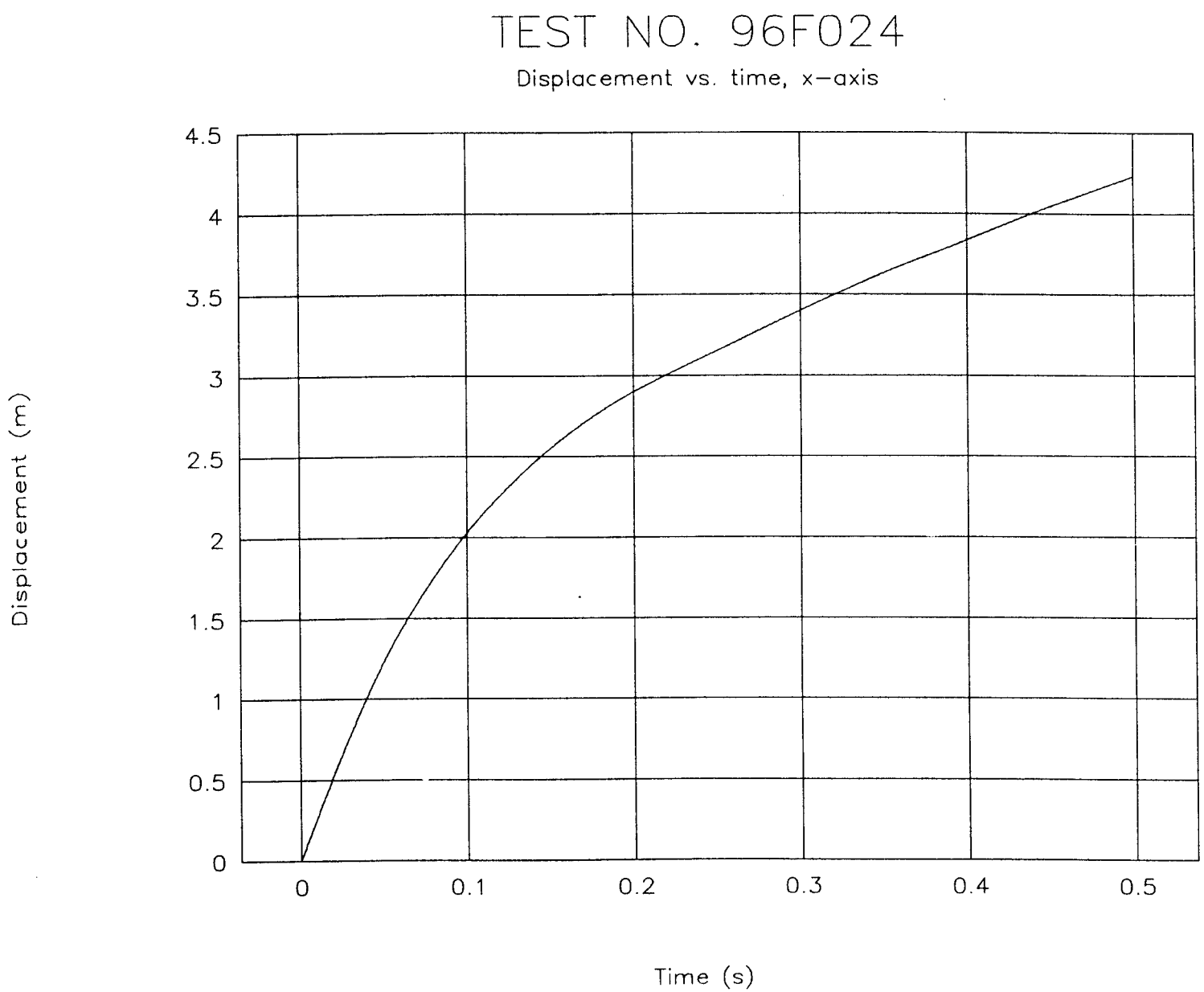

Figure 64. Displacement vs. time, x-axis, test 96F024.

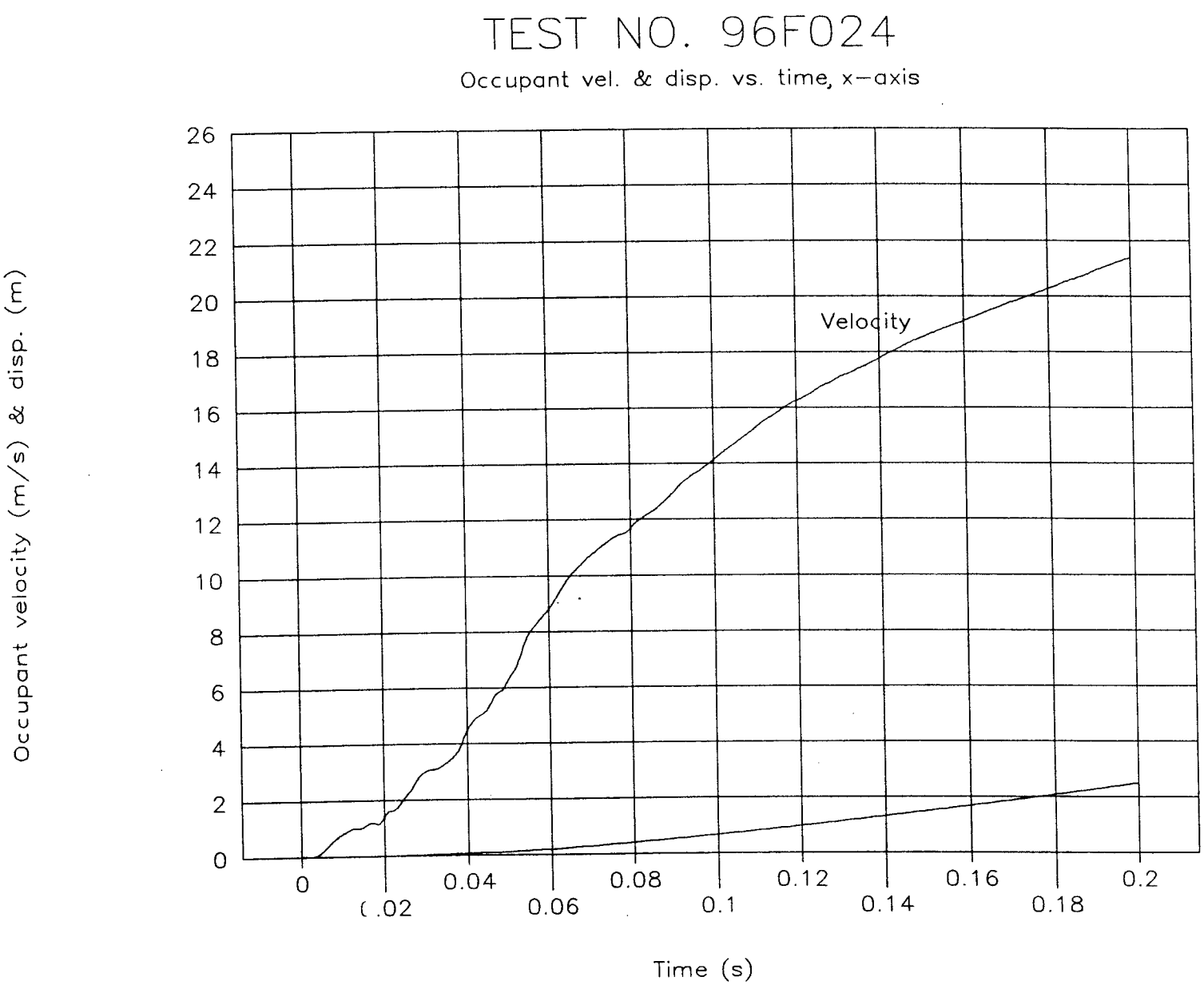

Figure 65. Occupant velocity and displacement vs. time, x-axis, test 96F024.

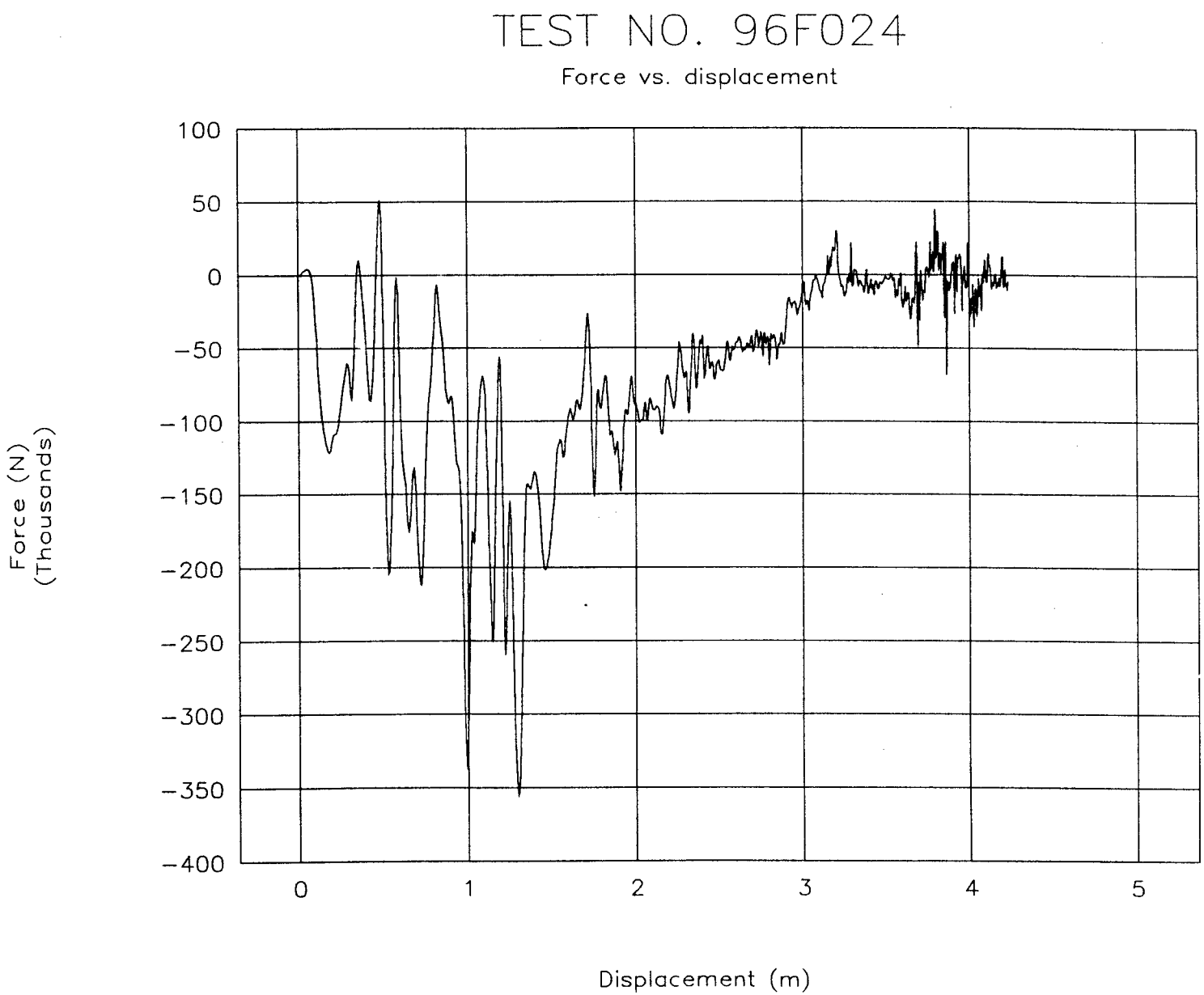

Figure 66. Force vs. displacement, test 96F024.

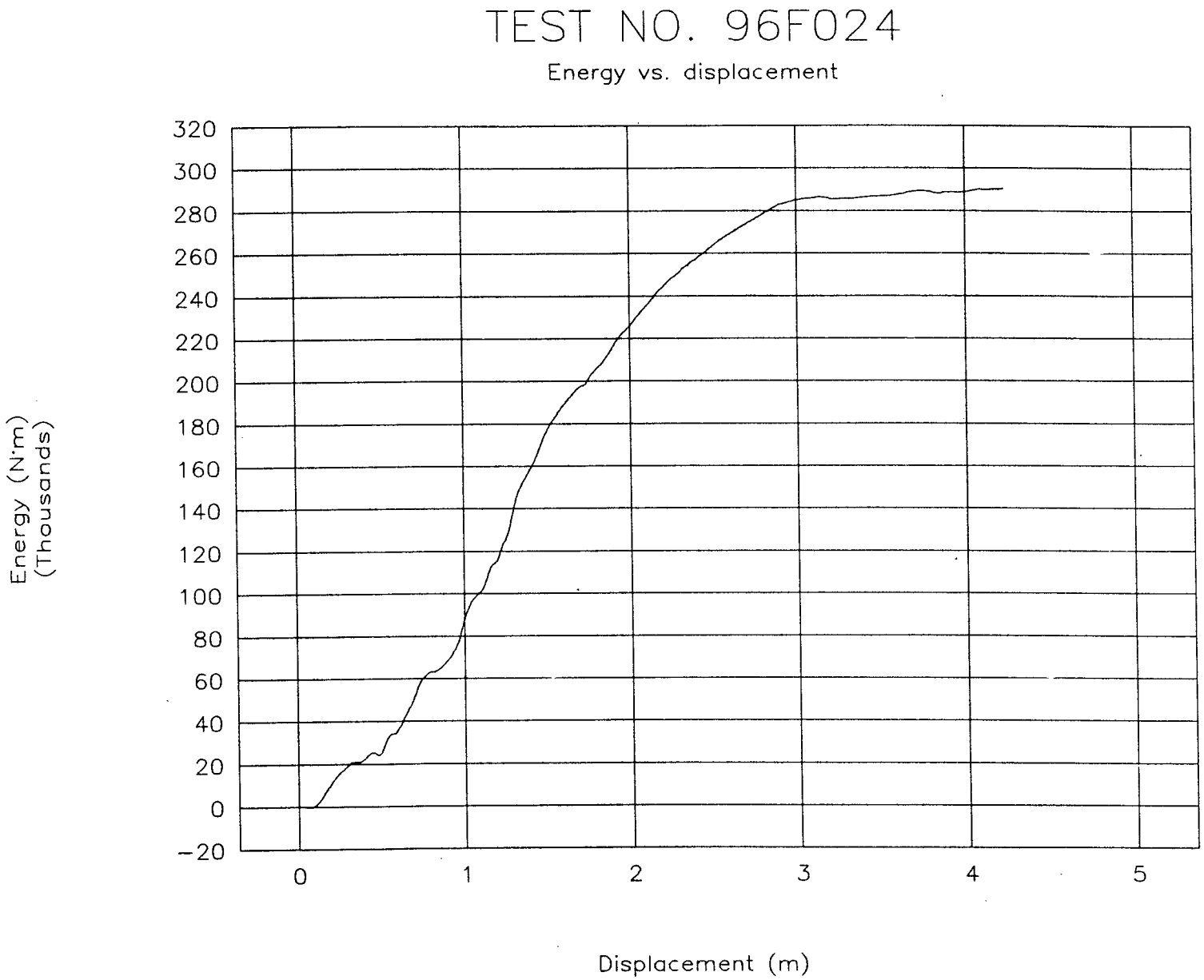

Figure 67. Energy vs. displacement, test 96F024.

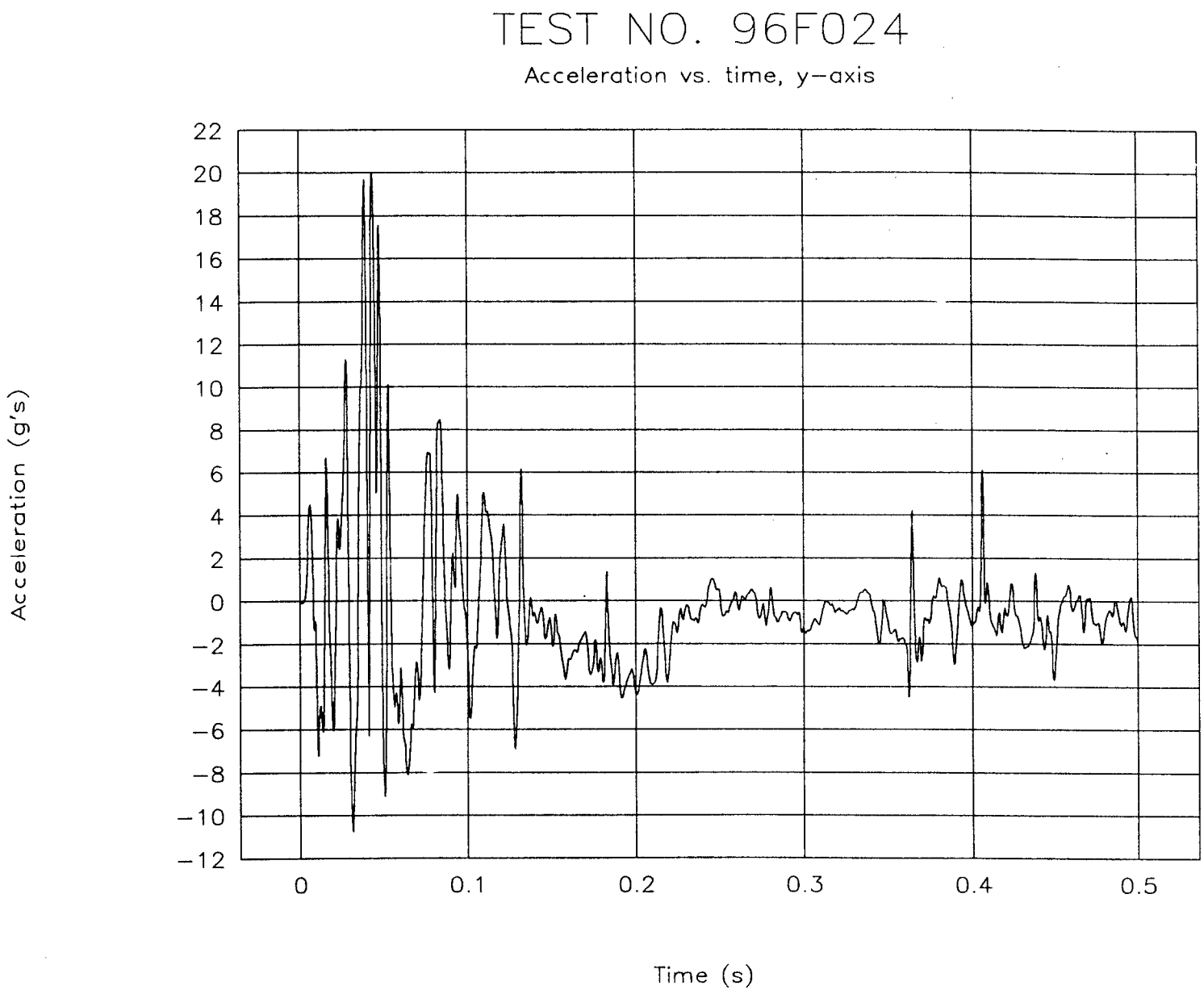

Figure 68. Acceleration vs. time, y-axis, test 96F024.

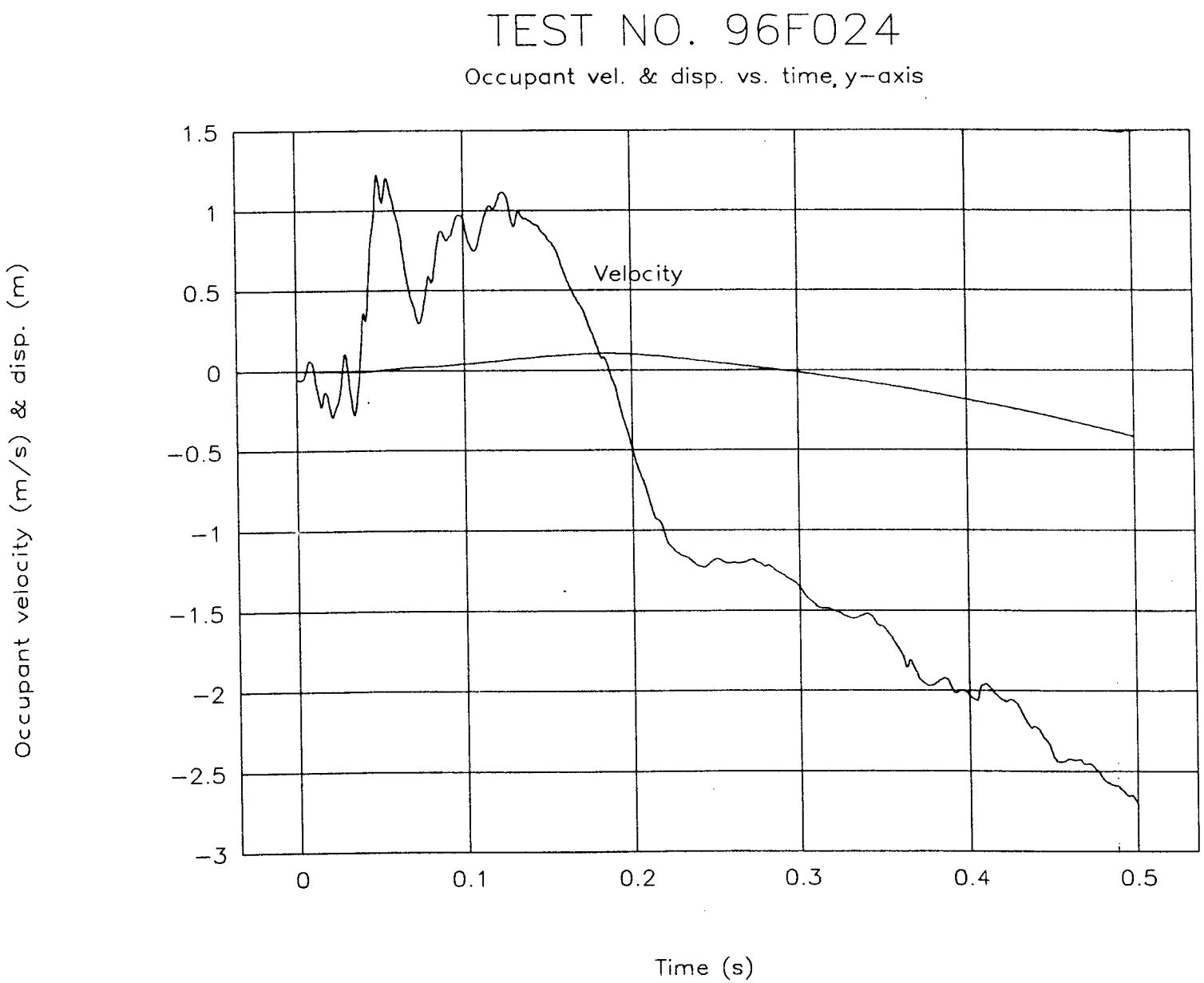

Figure 69. Occupant velocity and displacement vs. time, y-axis, test 96F024.

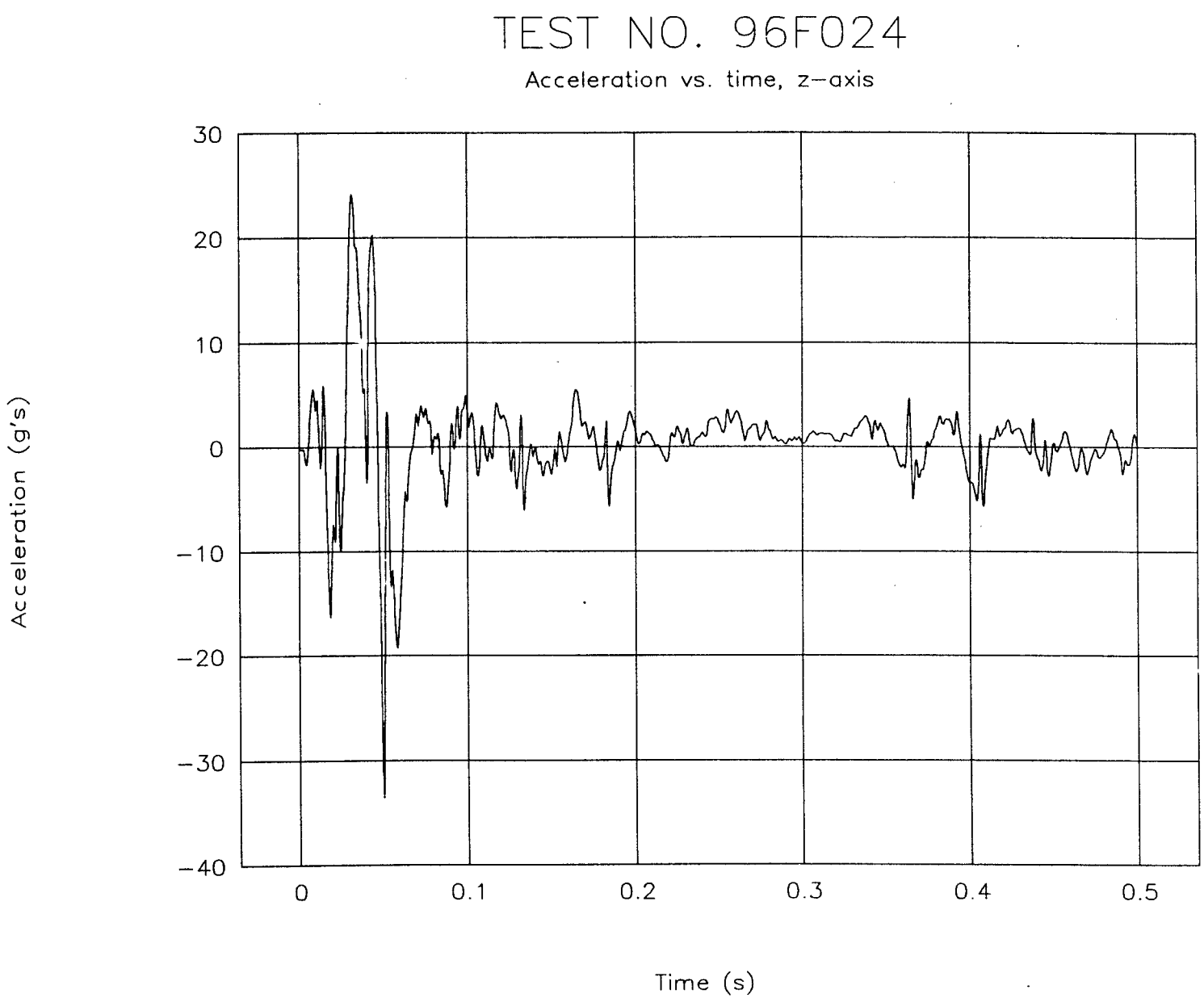

Figure 70. Acceleration vs. time, z-axis, test 96F024.

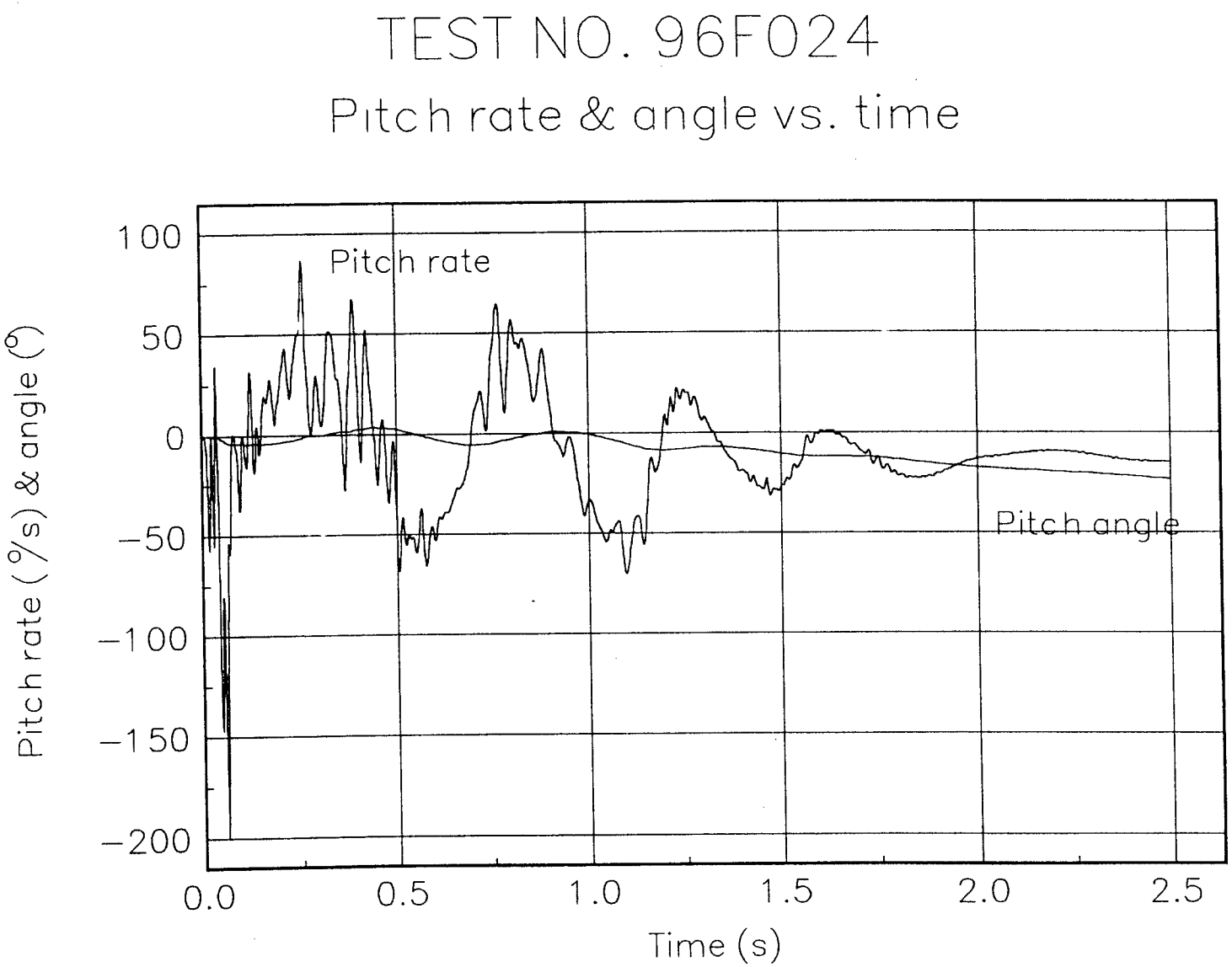

Figure 71. Pitch rate and angle vs. time, test 96F024.

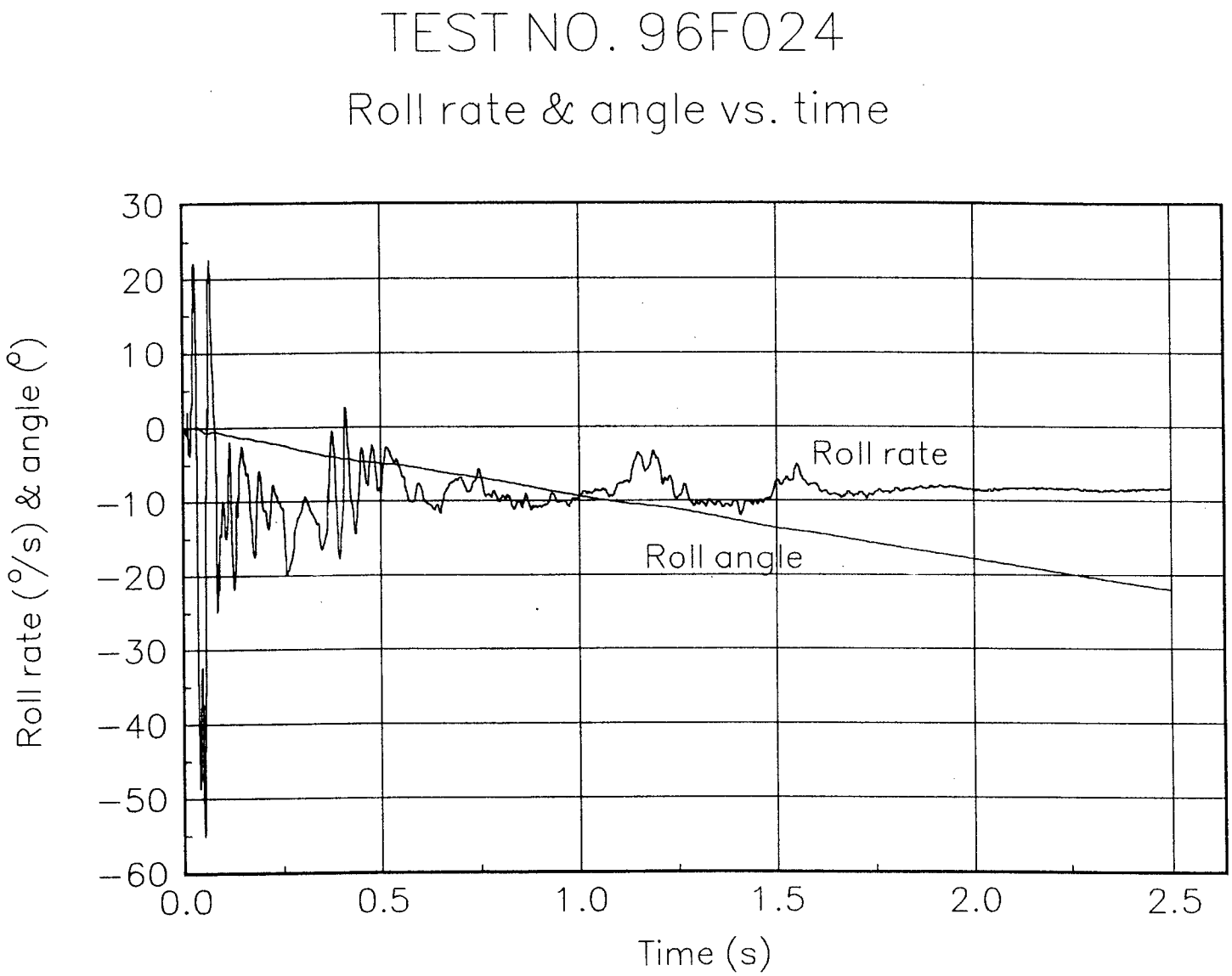

Figure 72. Roll rate and angle vs. time, test 96F024.

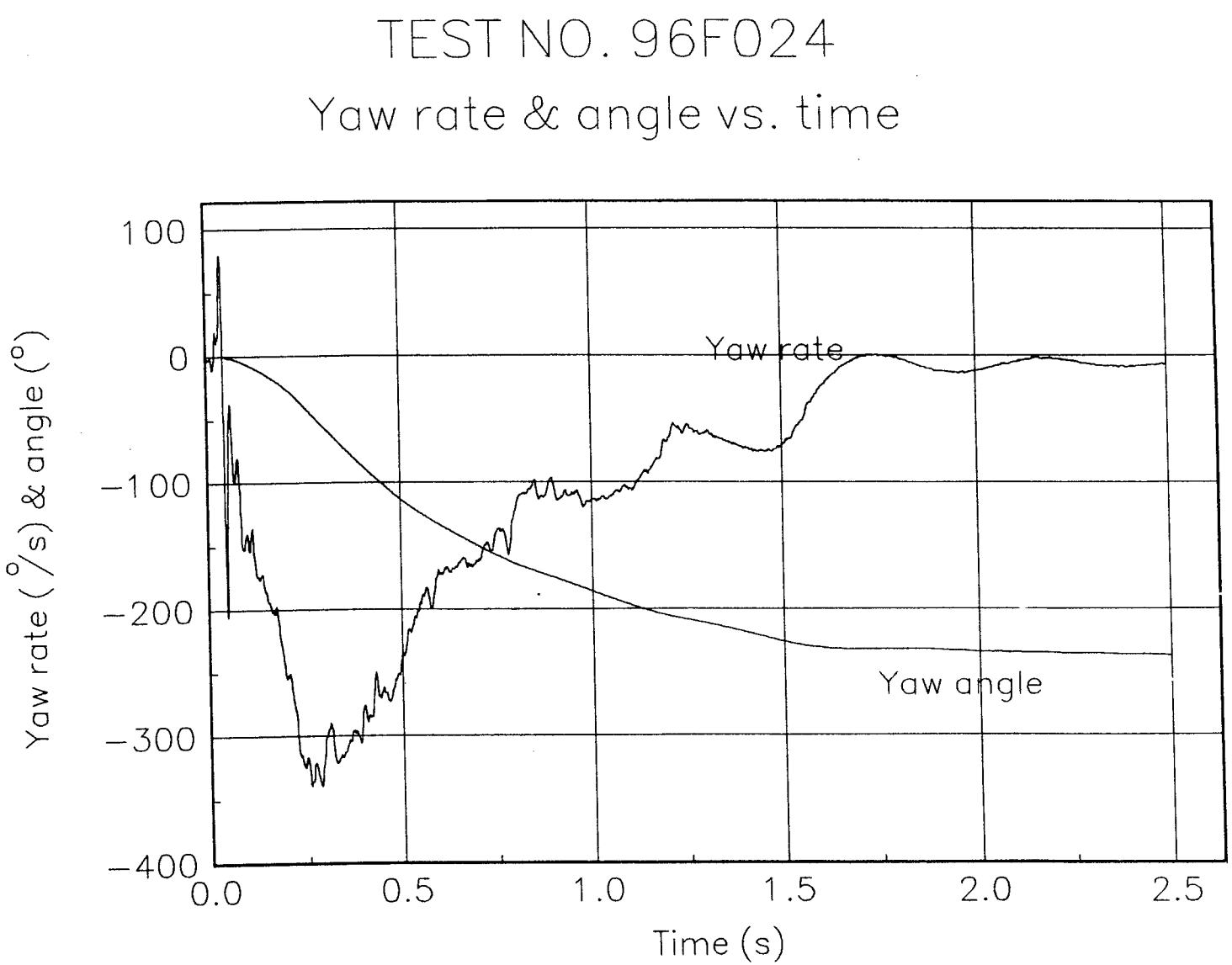

Figure 73. Yaw rate and angle vs. time, test 96F024.

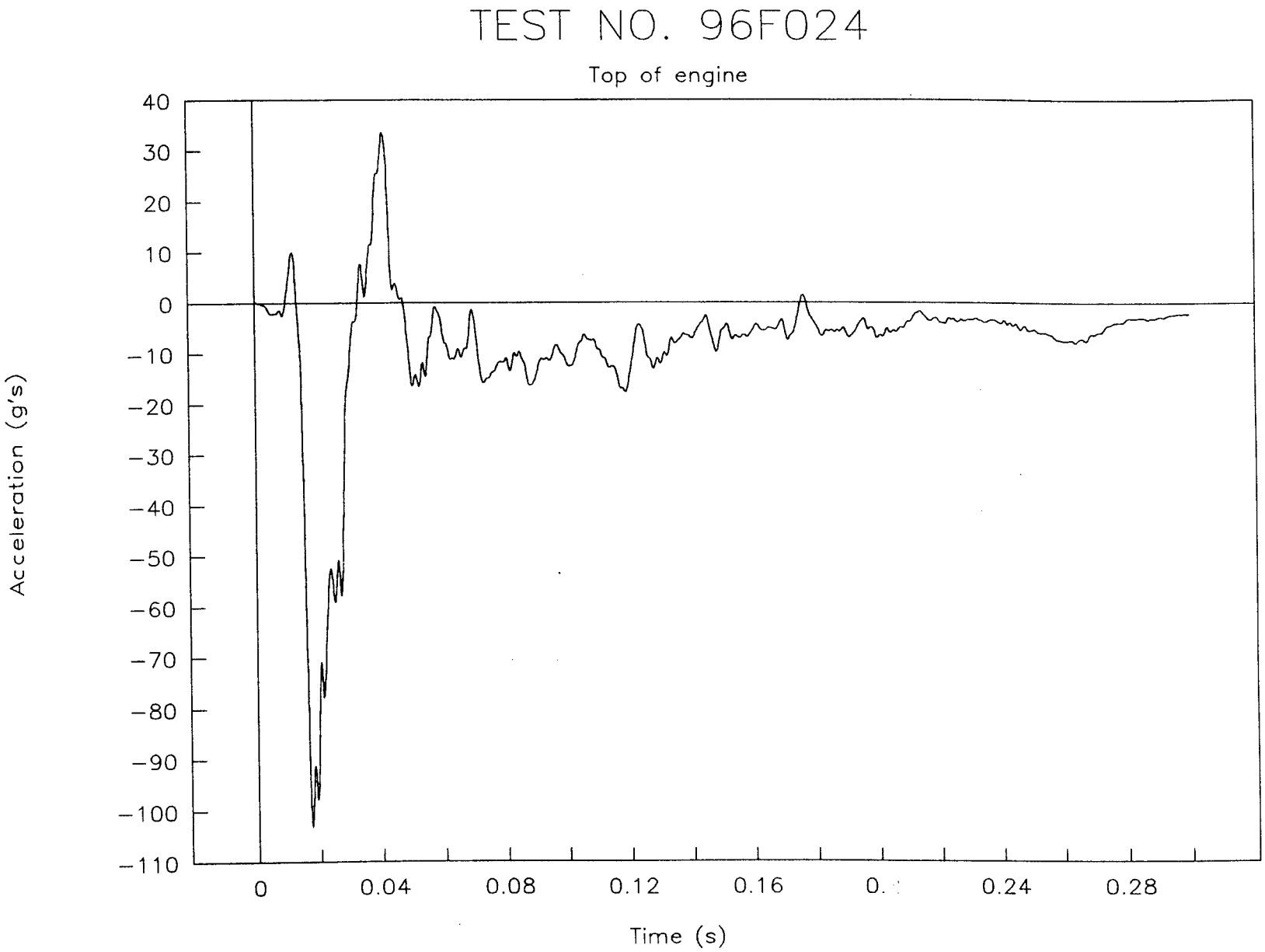

Figure 74. Acceleration vs. time, top of engine, test 96F024.

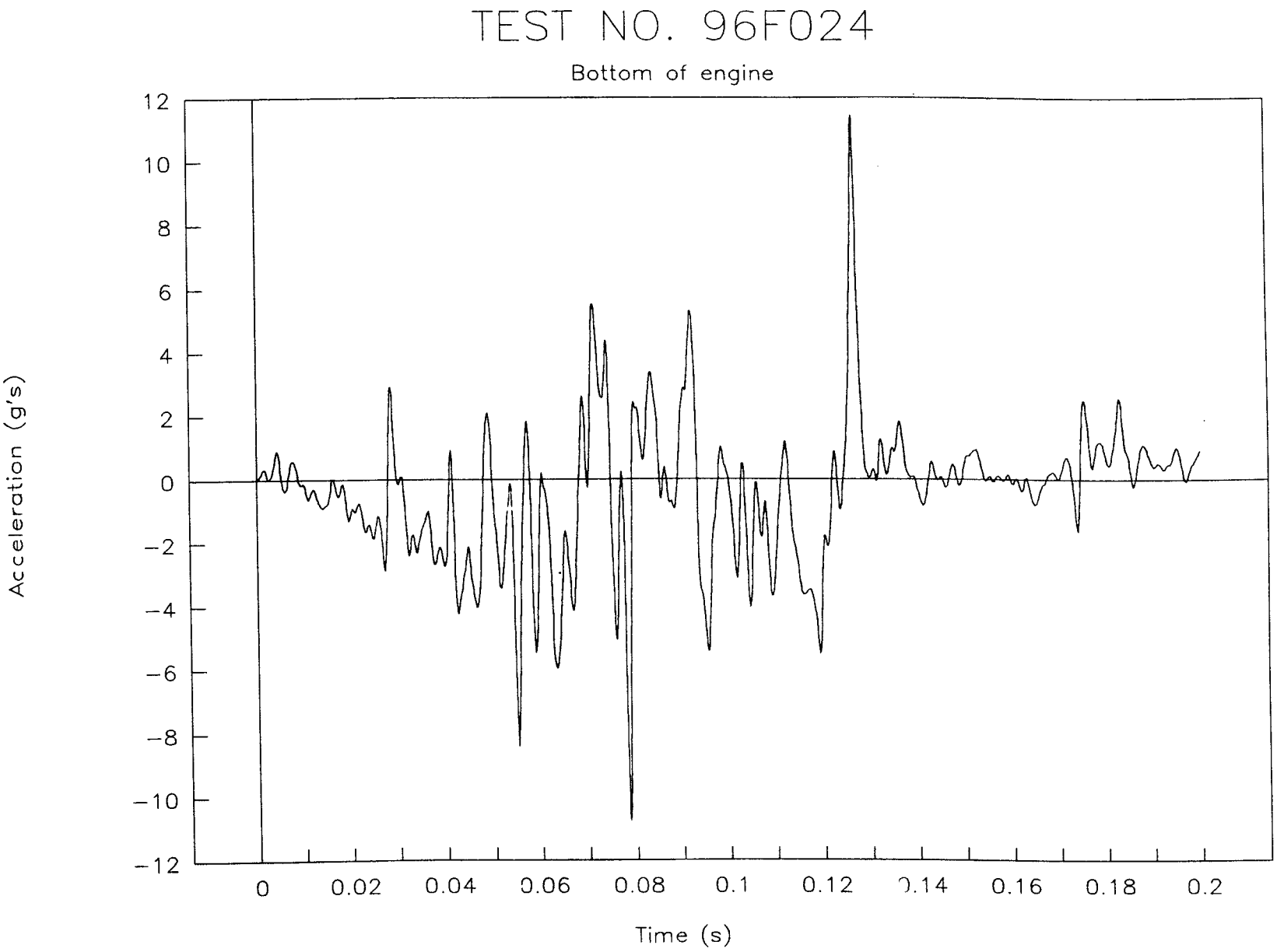

Figure 75. Acceleration vs. time, bottom of engine, test 96F024.

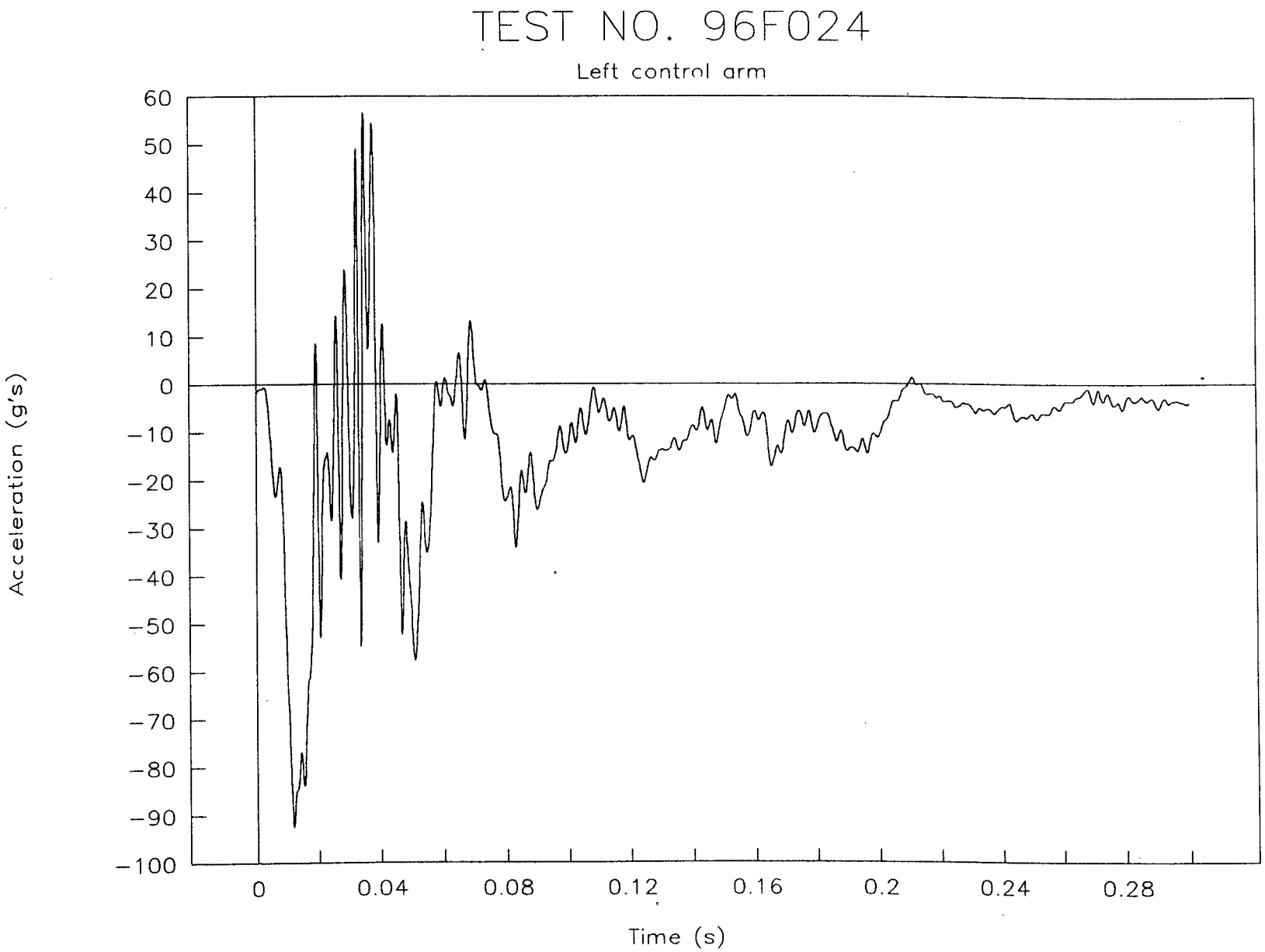

Figure 76. Acceleration vs. time, left control arm, test 96F024.

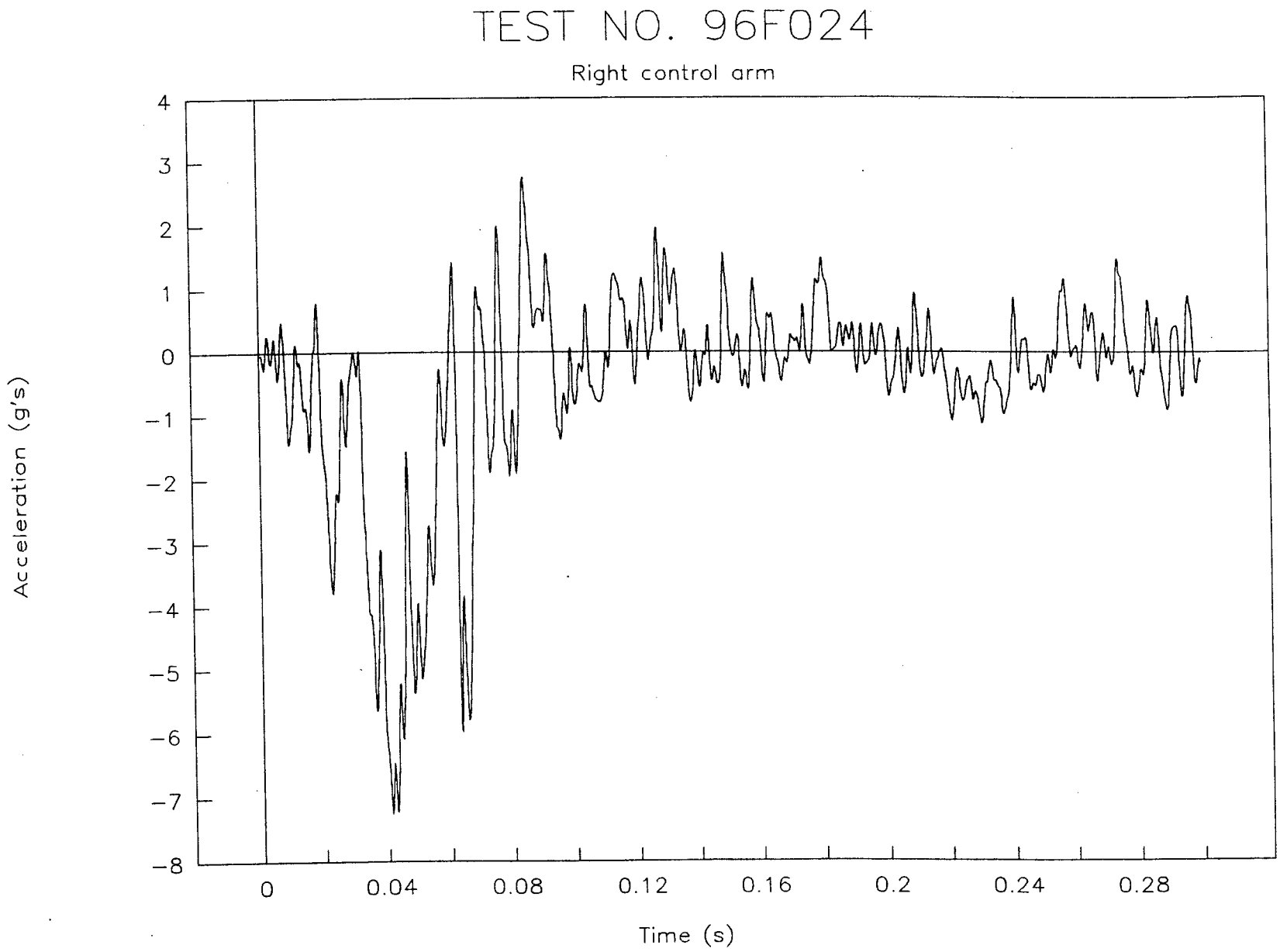

Figure 77. Acceleration vs. time, right control arm, test 96F024.

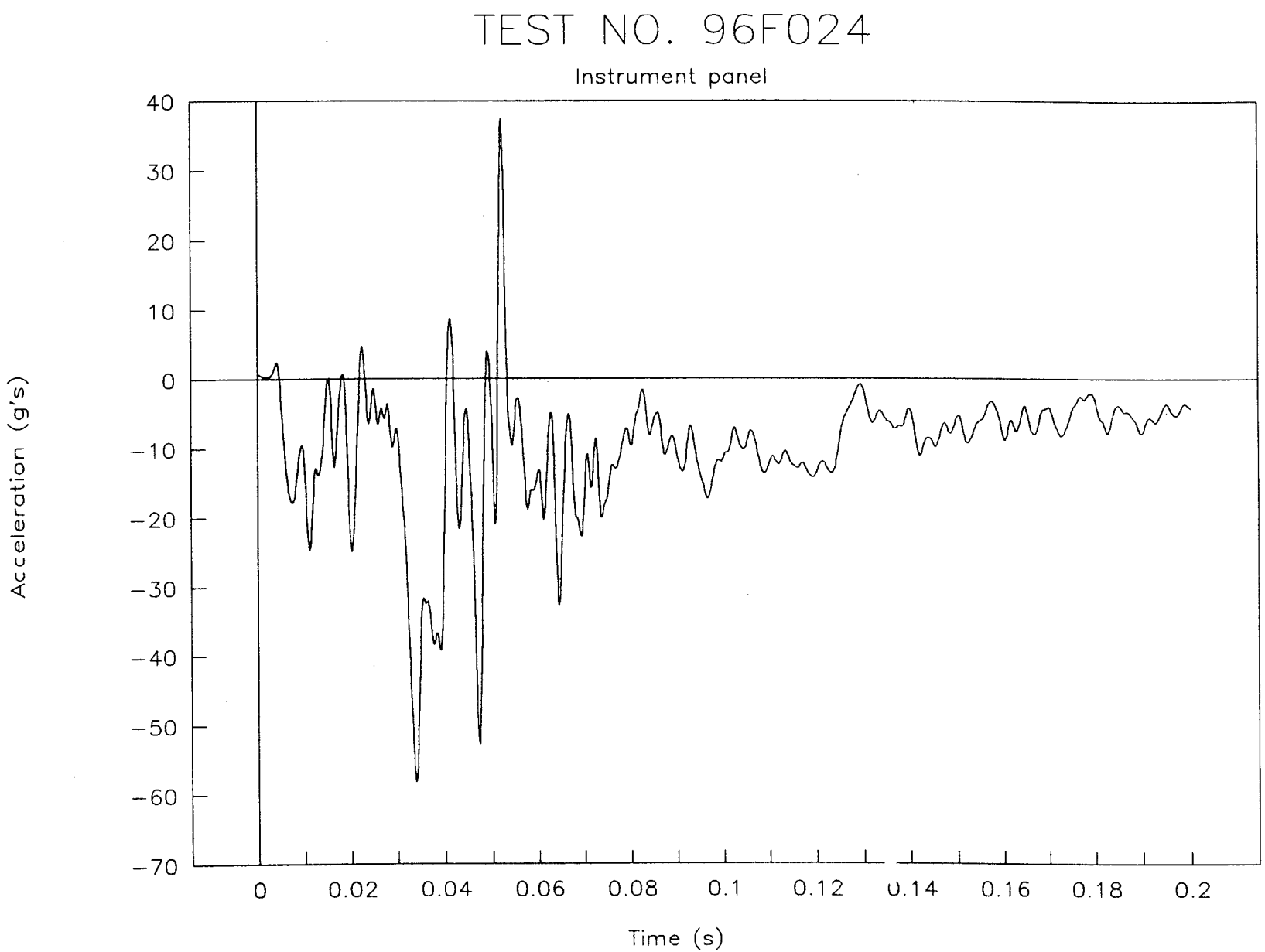

Figure 78. Acceleration vs. time, instrument panel, test 96F024.

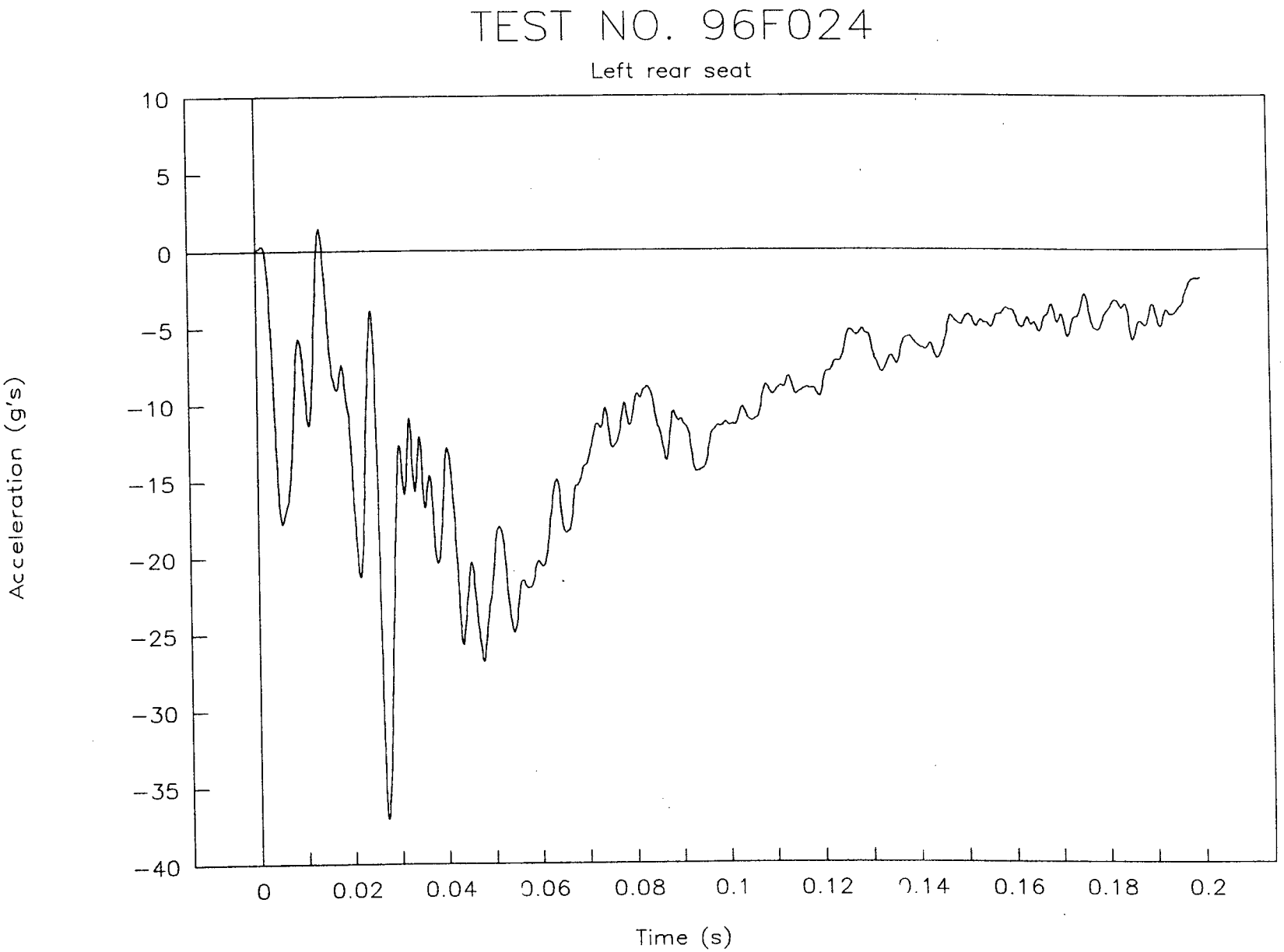

Figure 79. Acceleration vs. time, left rear seat, test 96F024.

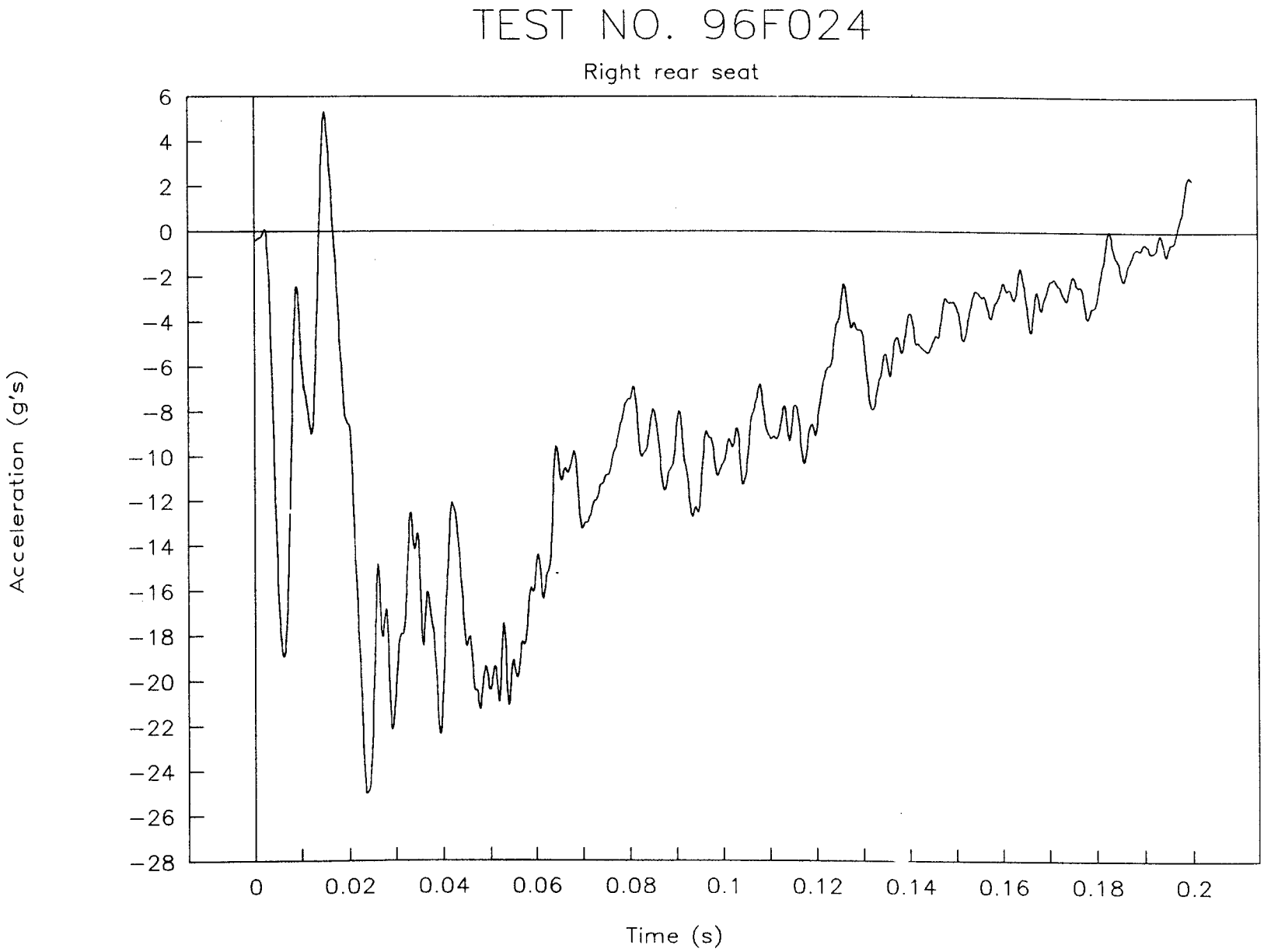

Figure 80. Acceleration vs. time, right rear seat, test 96F024.

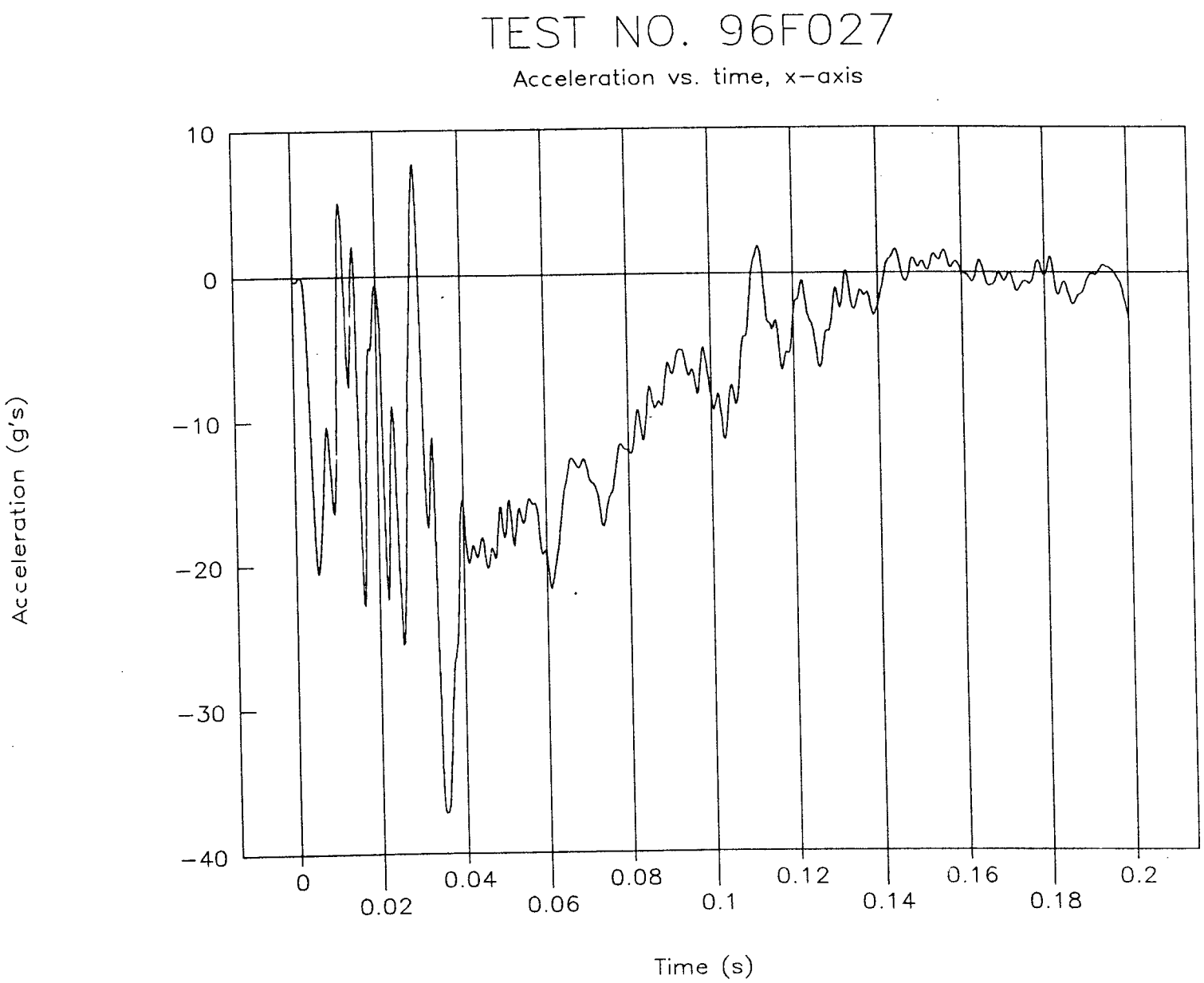

Figure 81. Acceleration vs. time, x-axis, test 96F027.

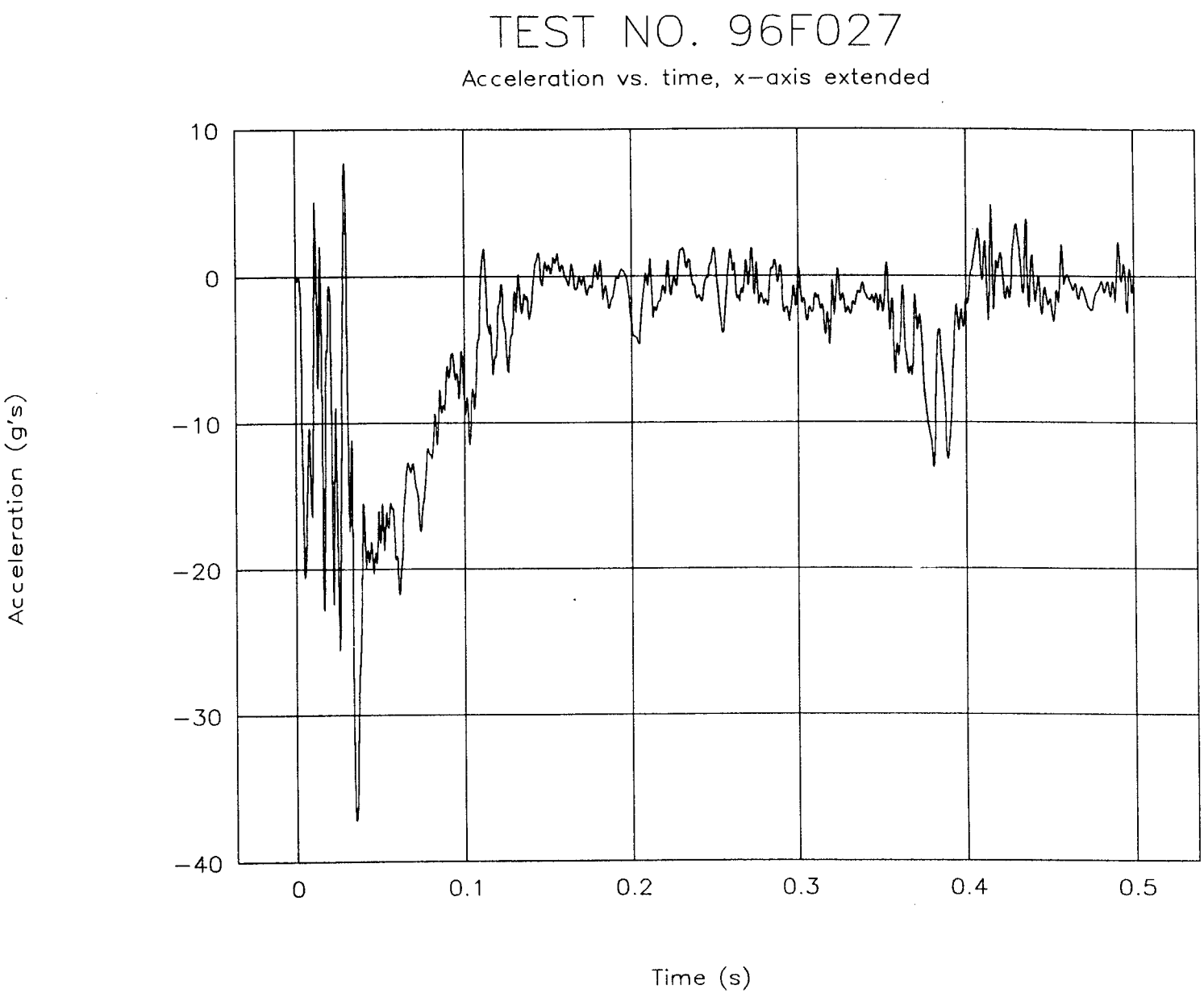

Figure 82. Acceleration vs. time, x-axis extended, test 96F027.

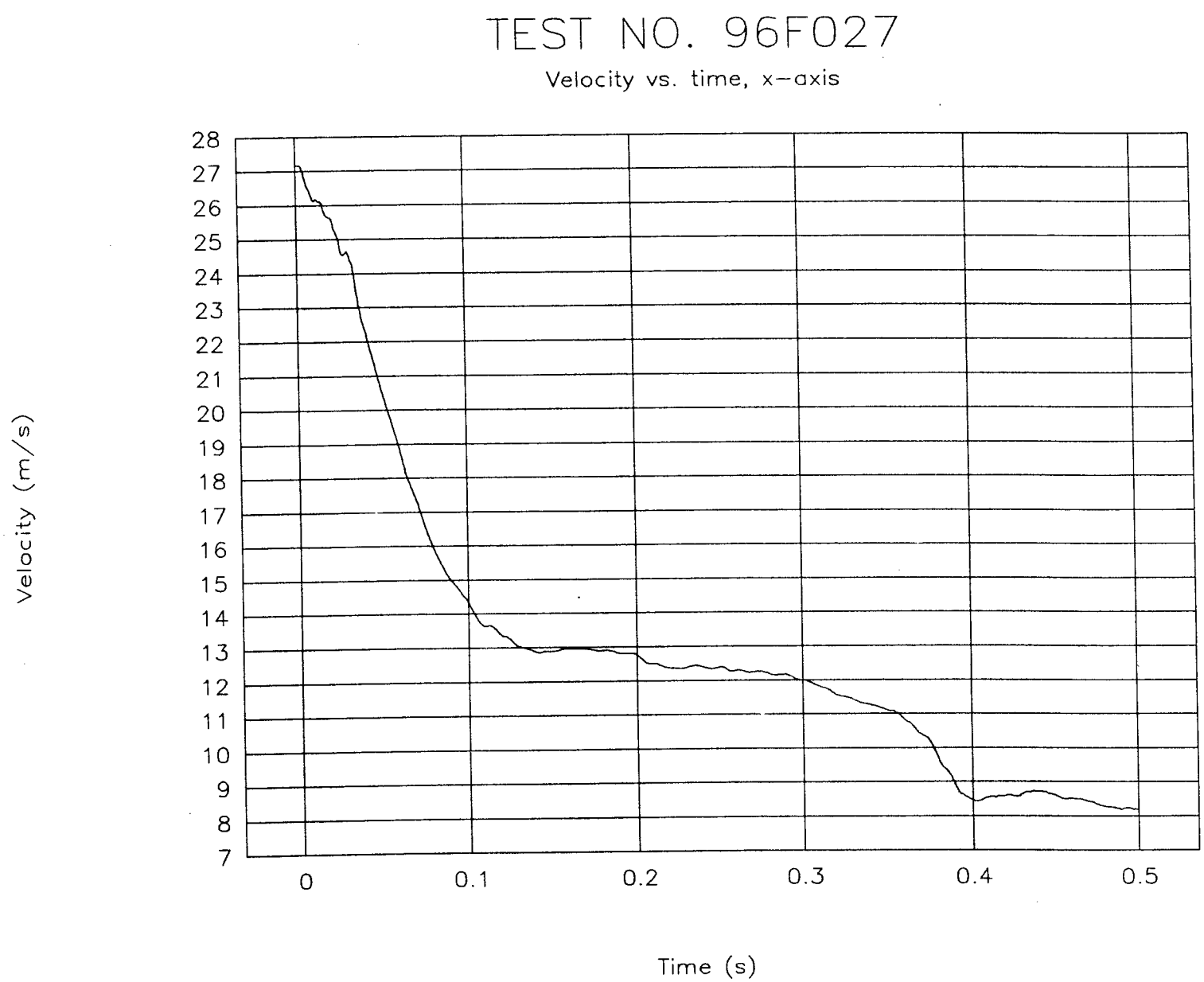

Figure 83. Velocity vs. time, x-axis, test 96F027.

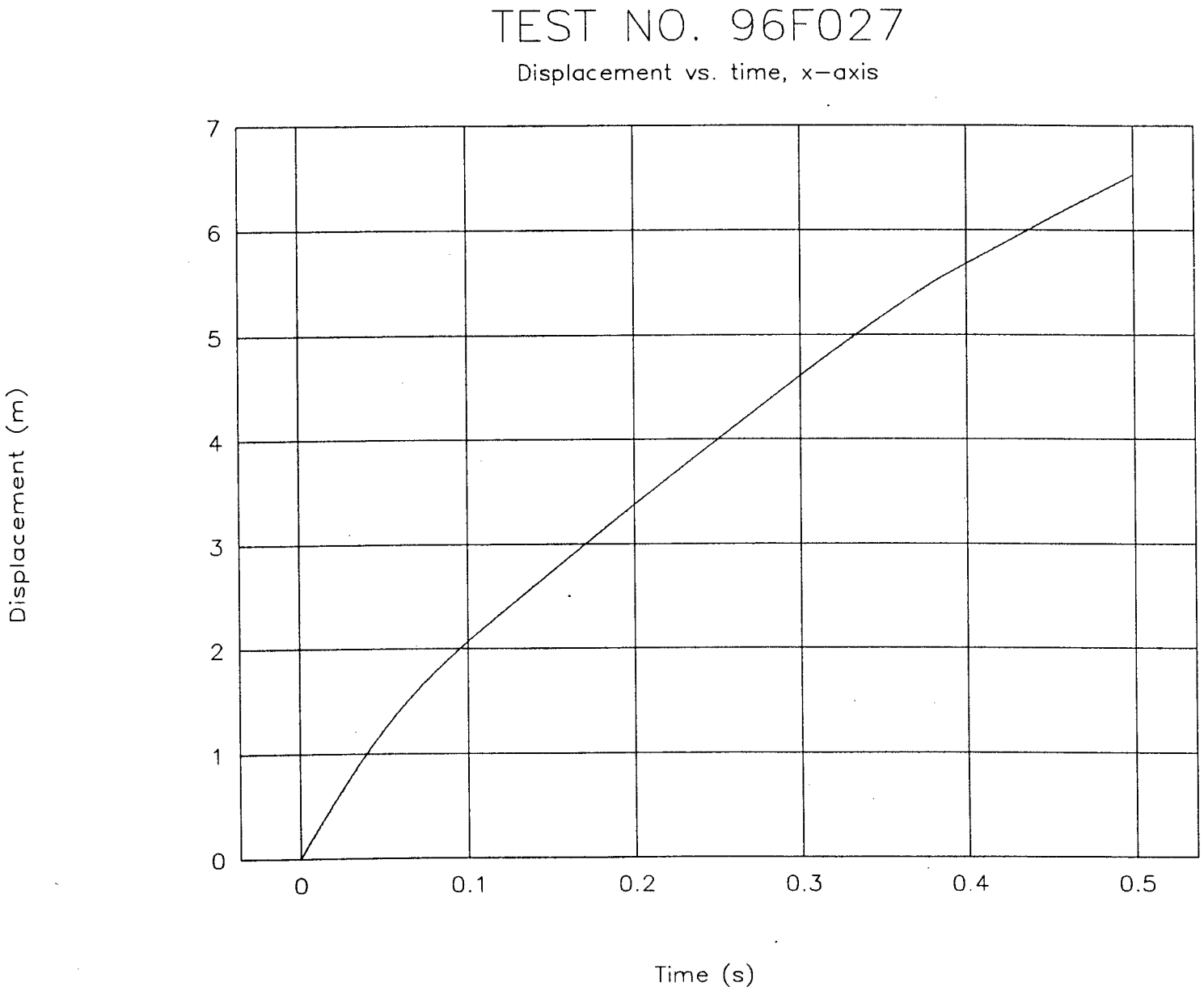

Figure 84. Displacement vs. time, x-axis, test 96F027.

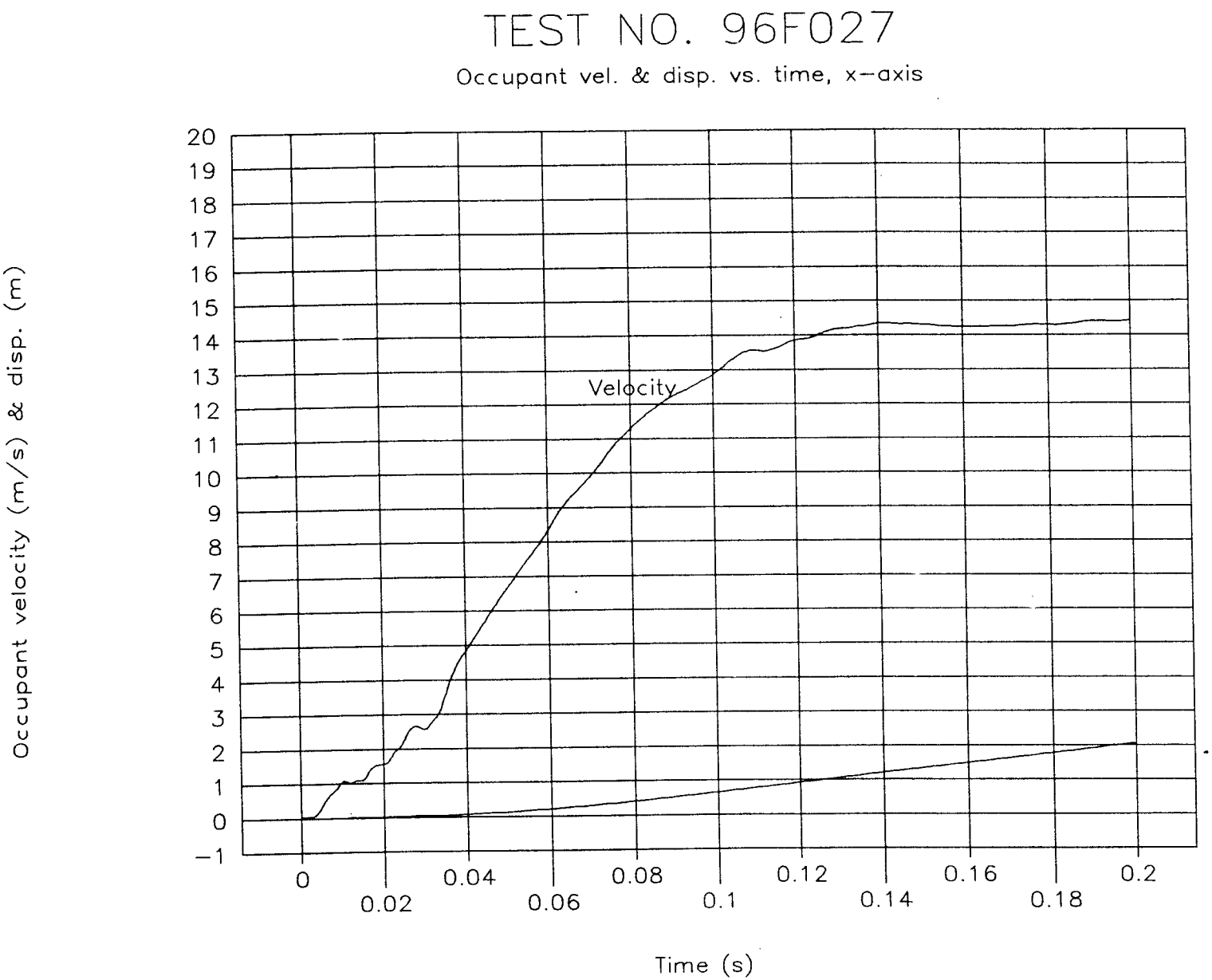

Figure 85. Occupant velocity and displacement vs. time, x-axis, test 96F027.

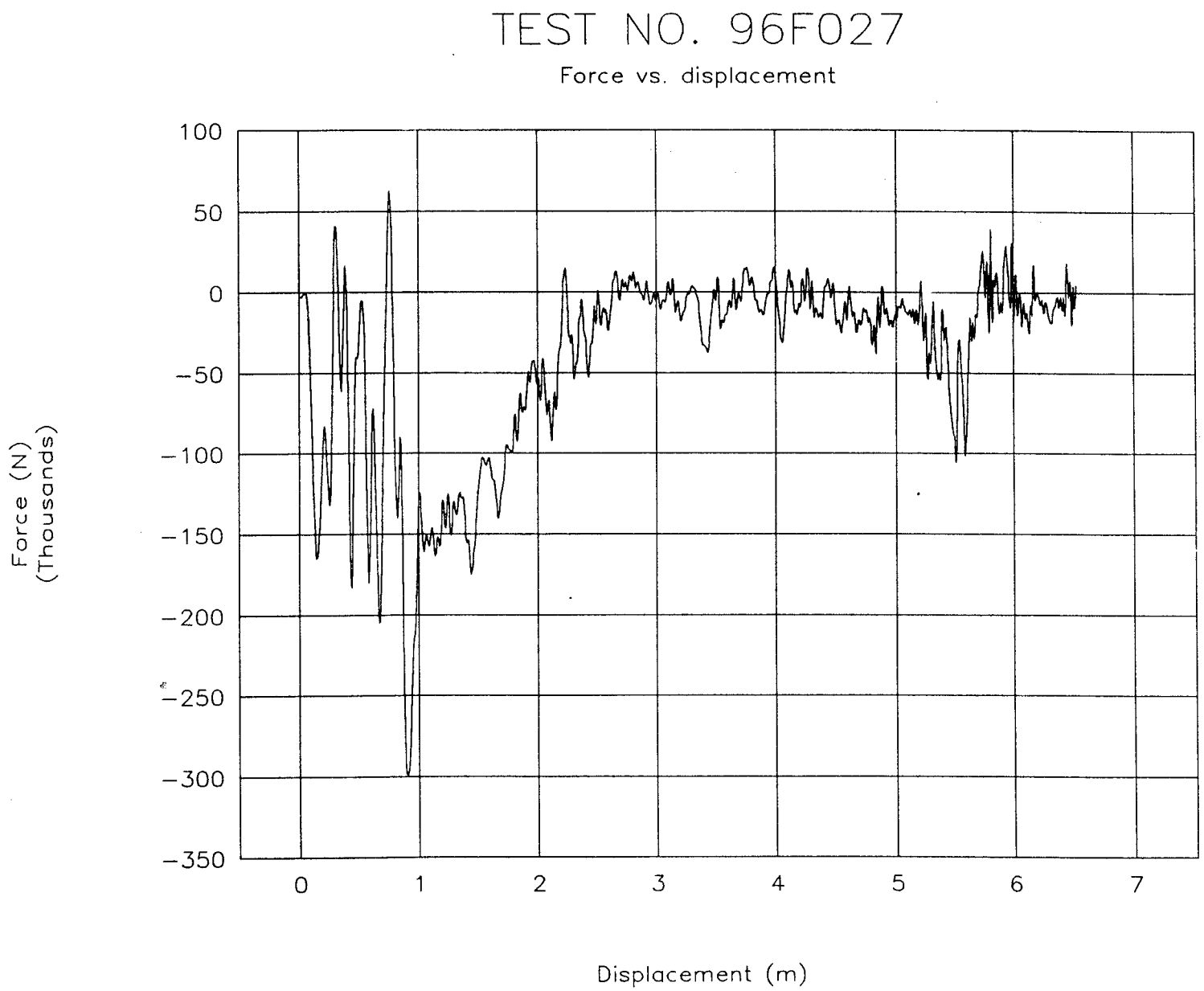

Figure 86. Force vs. displacement, test 96F027.

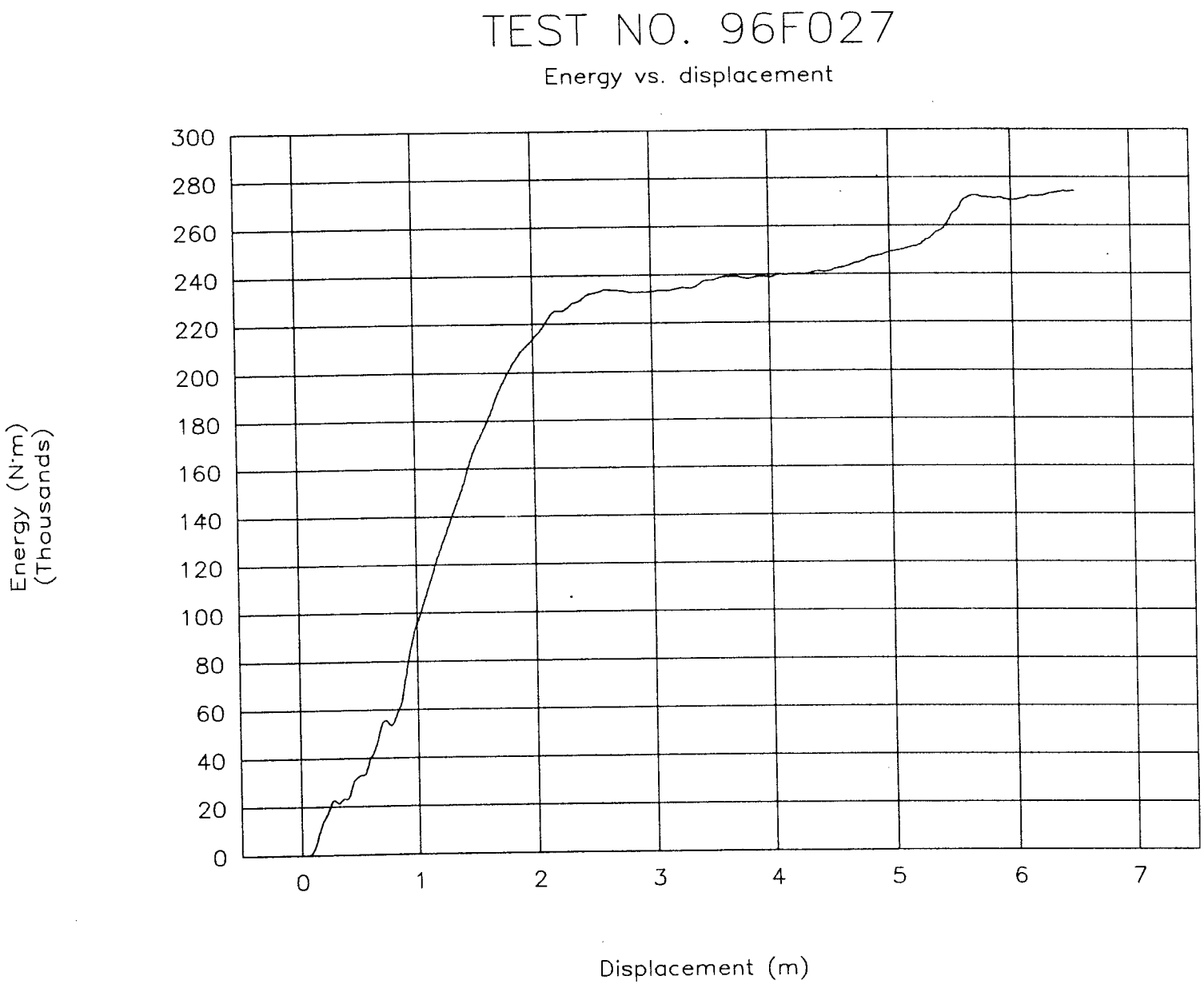

Figure 87. Energy vs. displacement, test 96F027.

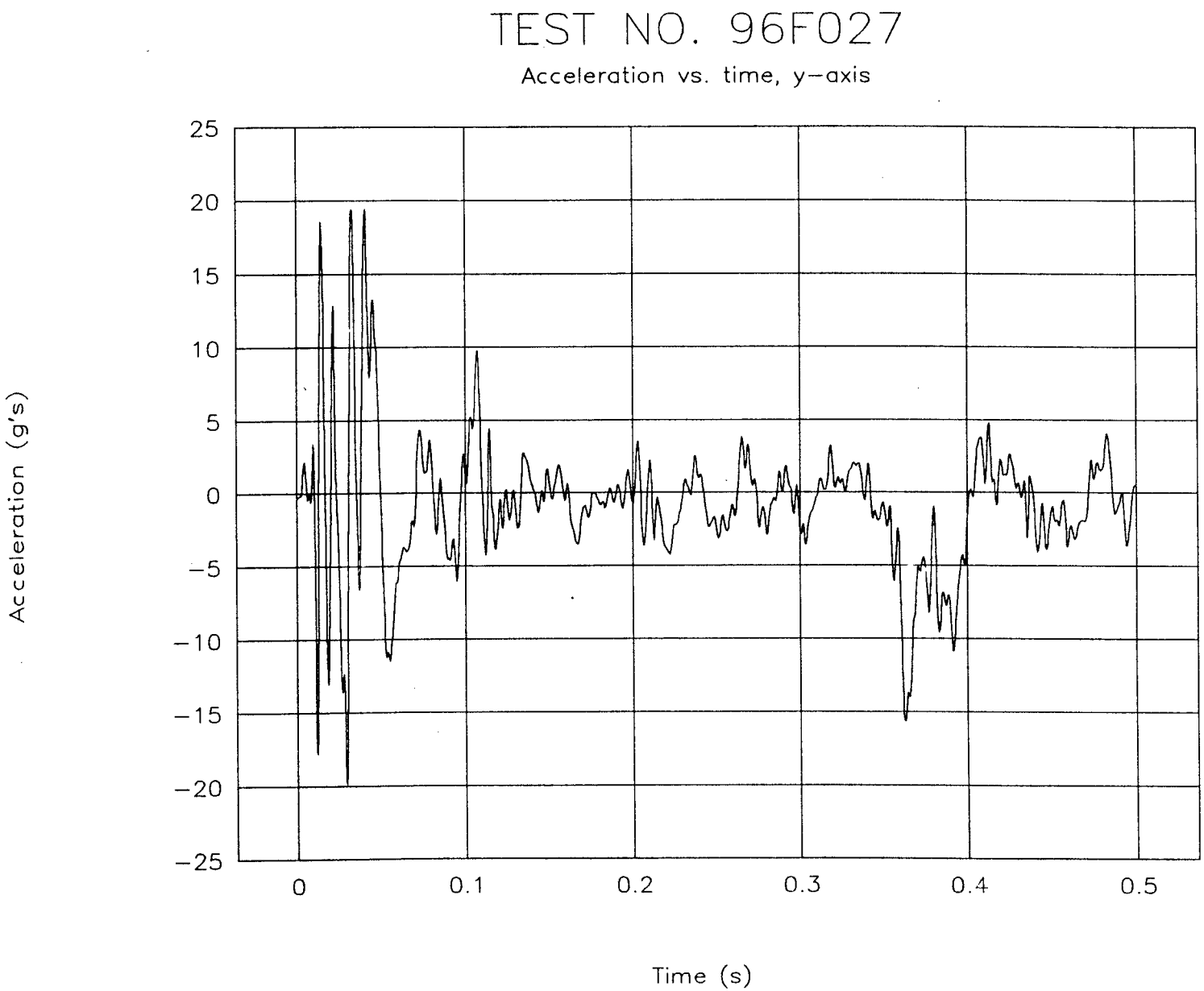

Figure 88. Acceleration vs. time, y-axis, test 96F027.

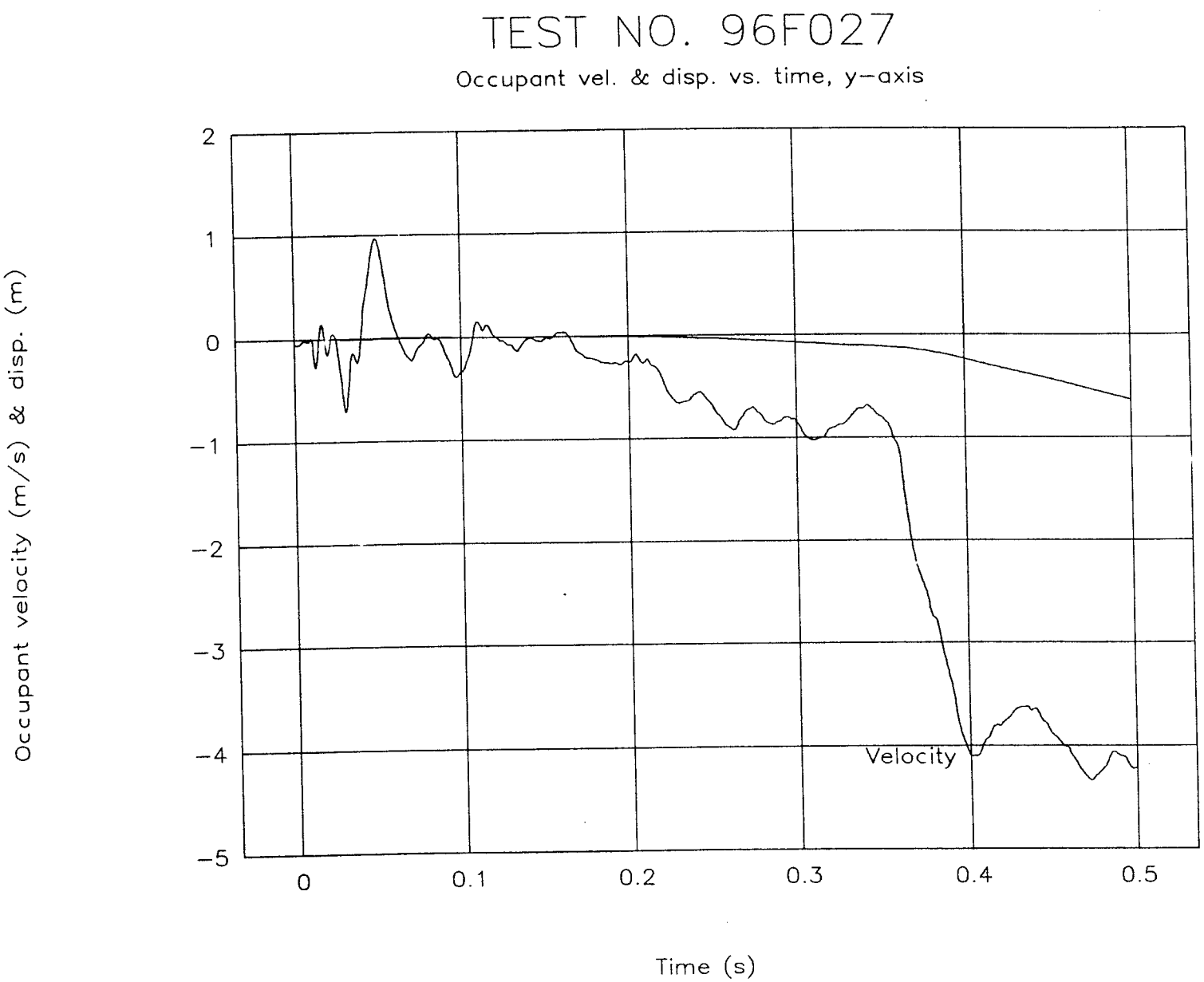

Figure 89. Occupant velocity and displacement vs. time, y-axis, test 96F027.

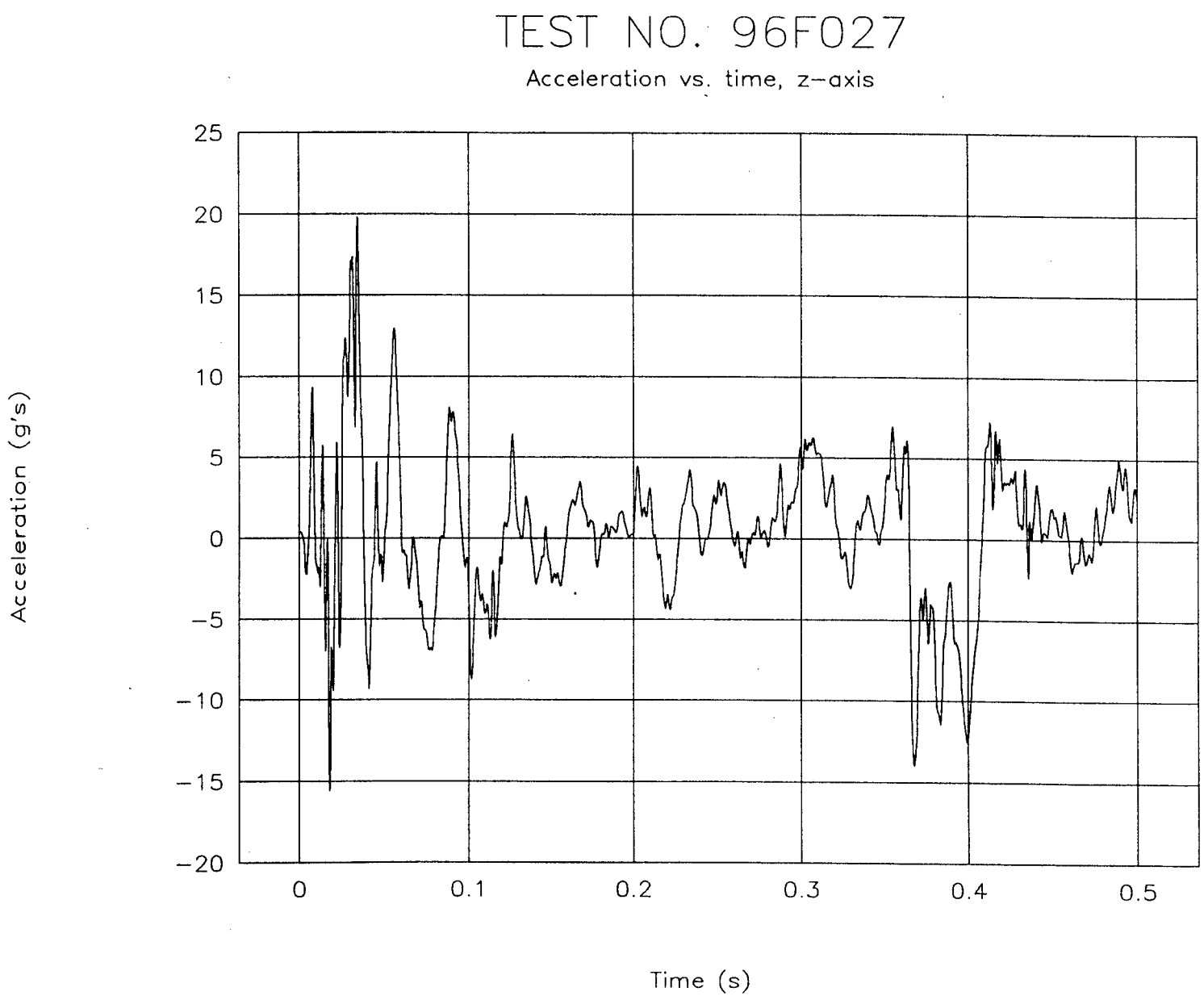

Figure 90. Acceleration vs. time, z-axis, test 96F027.

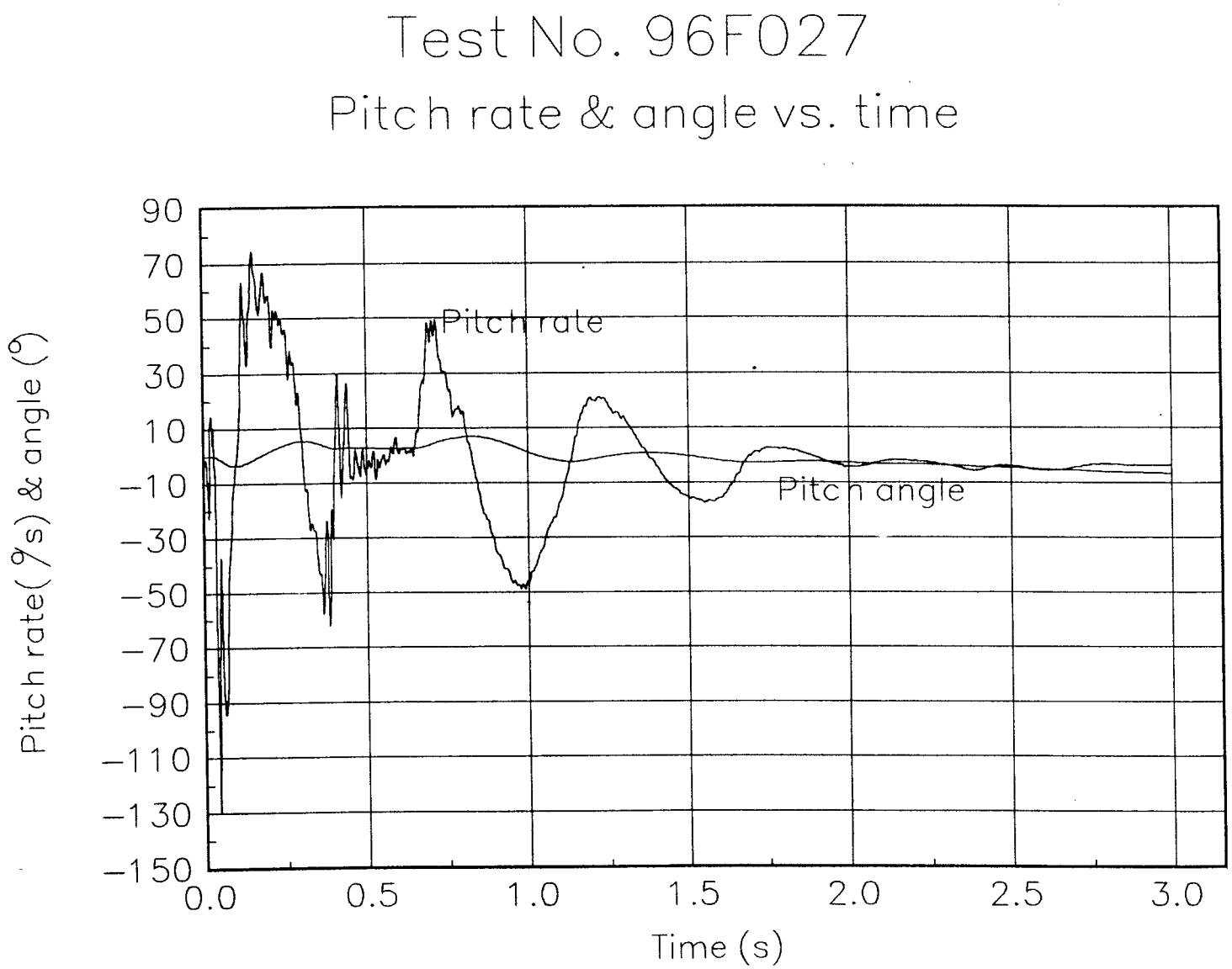

Figure 91. Pitch rate and angle vs. time, test 96F027.

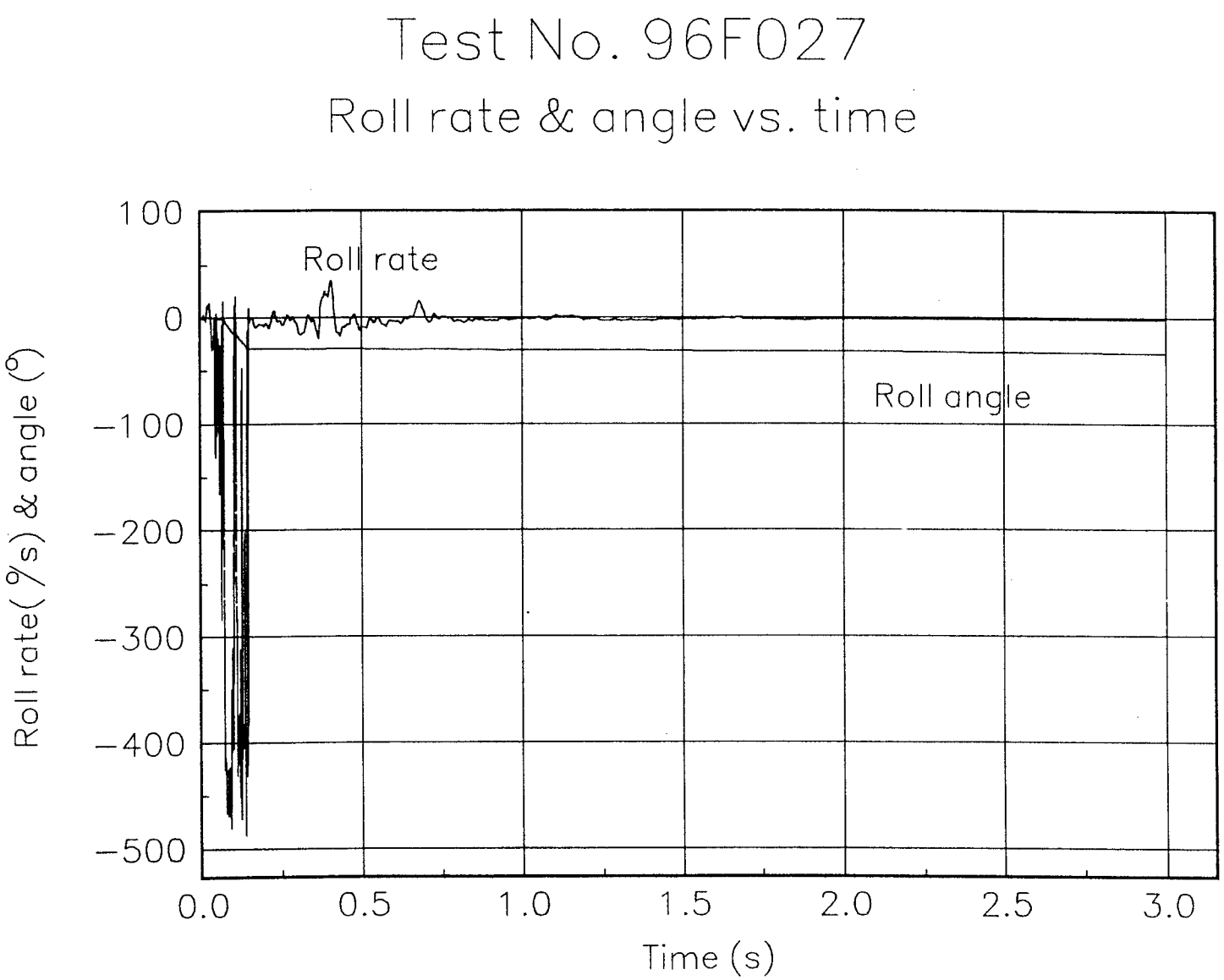

Figure 92. Roll rate and angle vs. time, test 96F027.

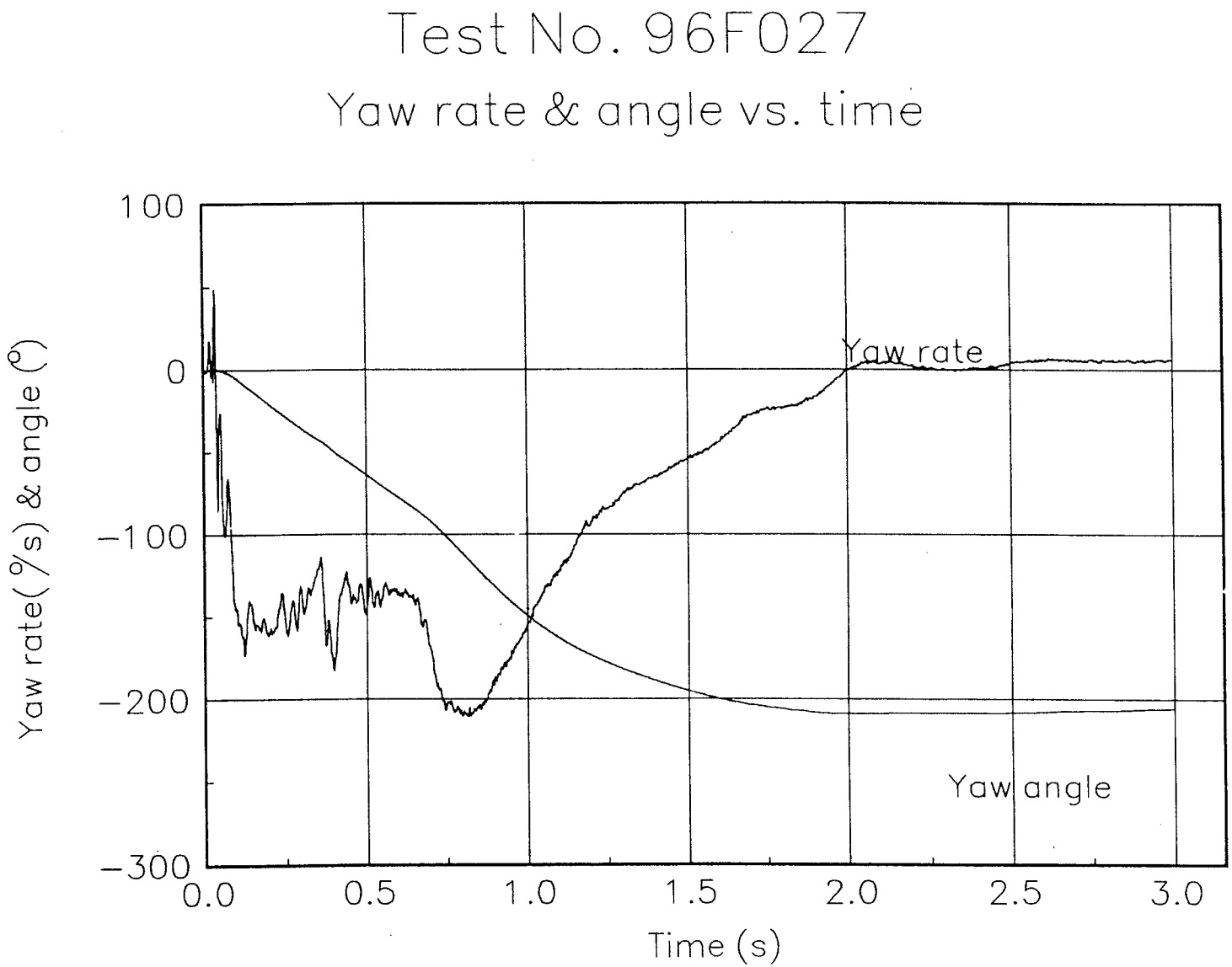

Figure 93. Yaw rate and angle vs. time, test 96F027.

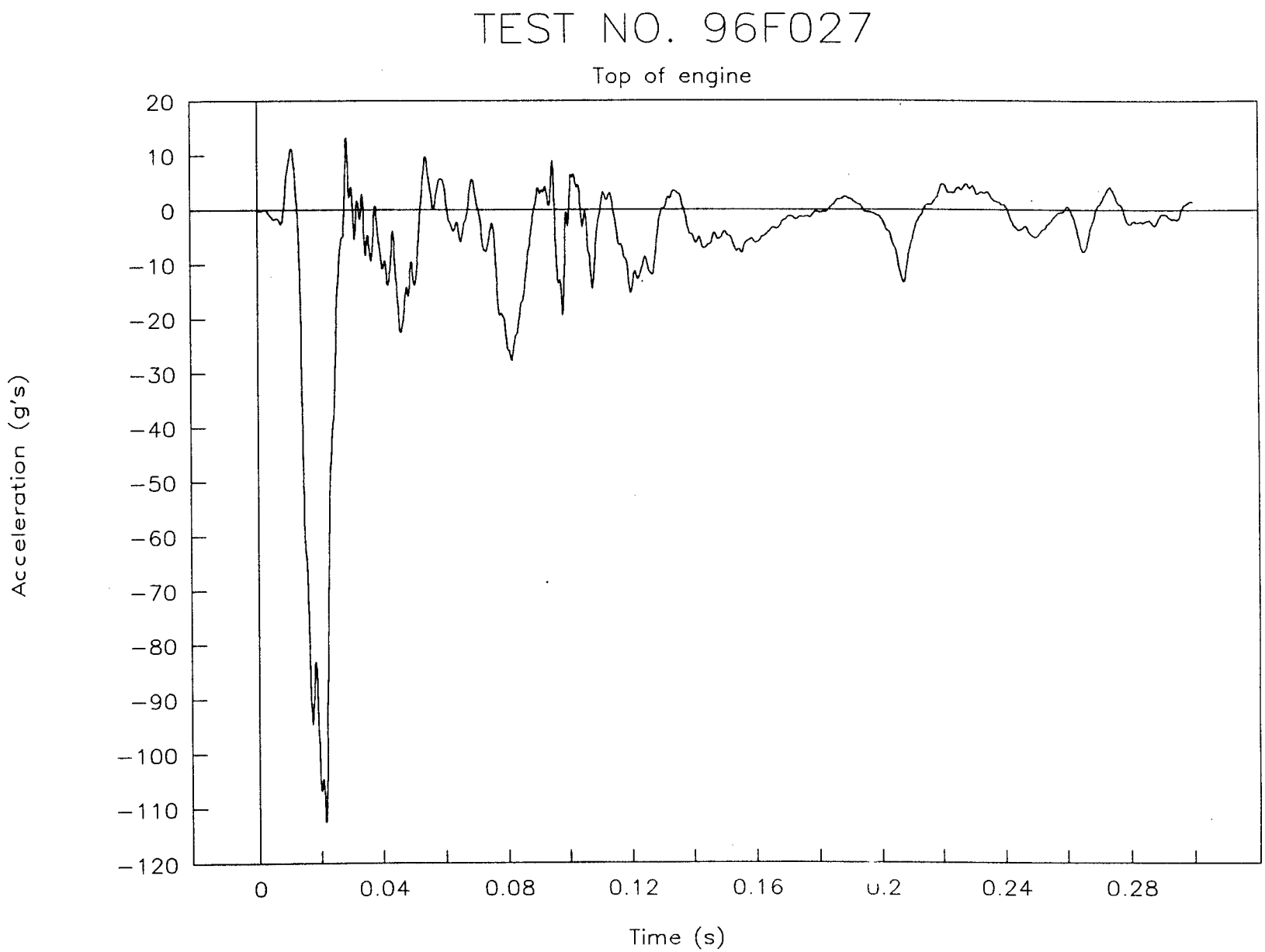

Figure 94. Acceleration vs. time, top of engine, test 96F027.

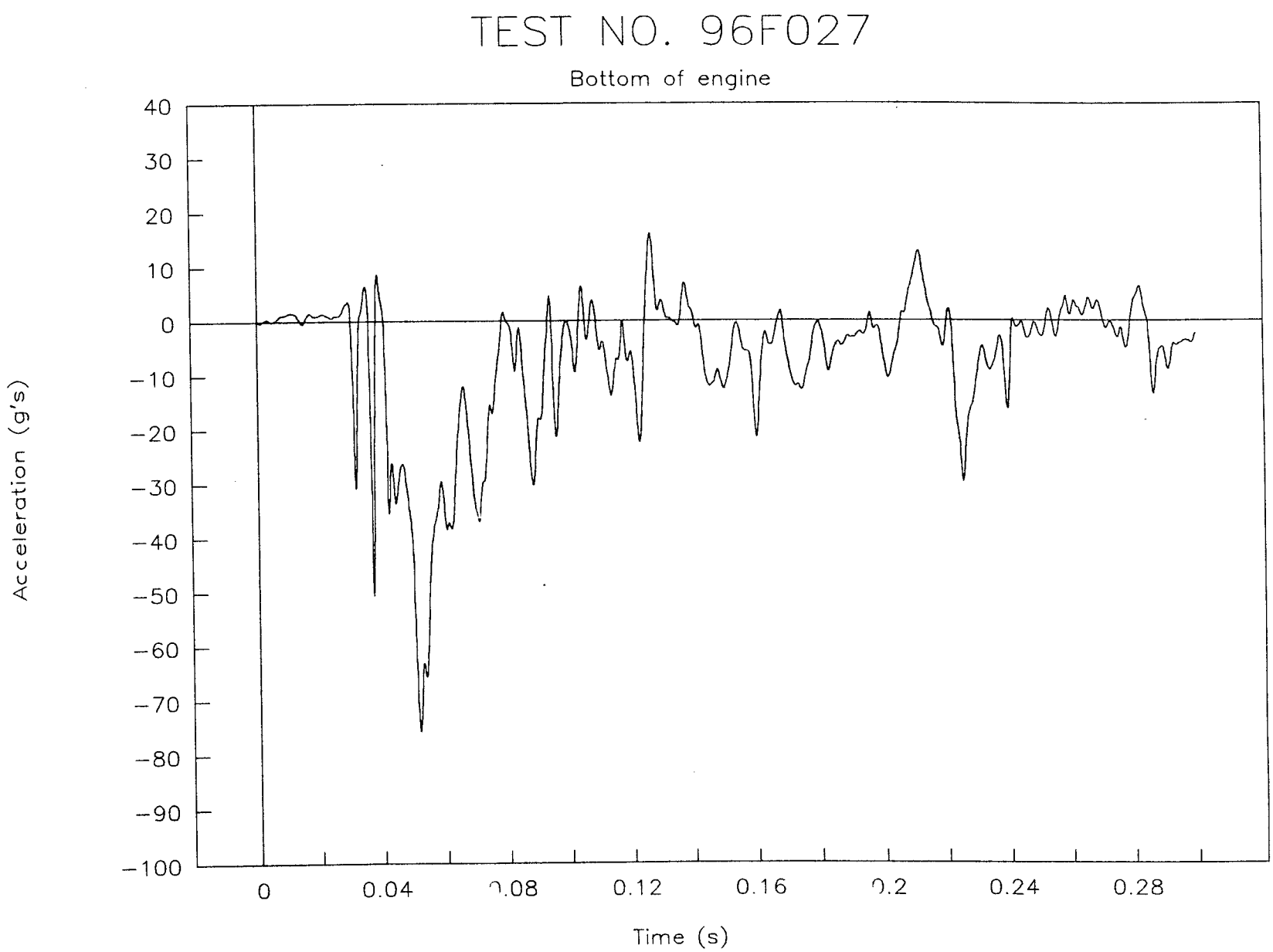

Figure 95. Acceleration vs. time, bottom of engine, test 96F027.

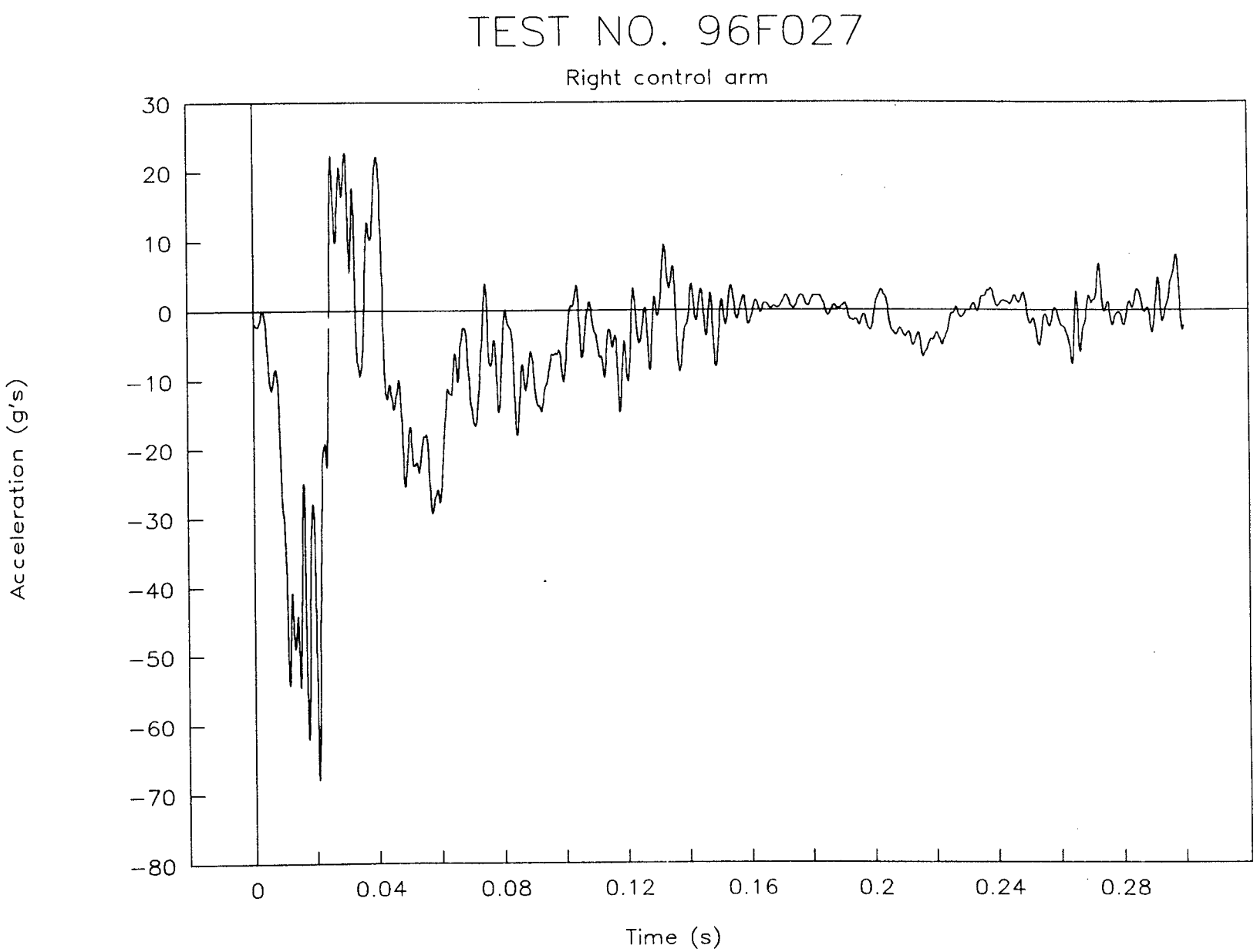

Figure 96. Acceleration vs. time, right control arm, test 96F027.

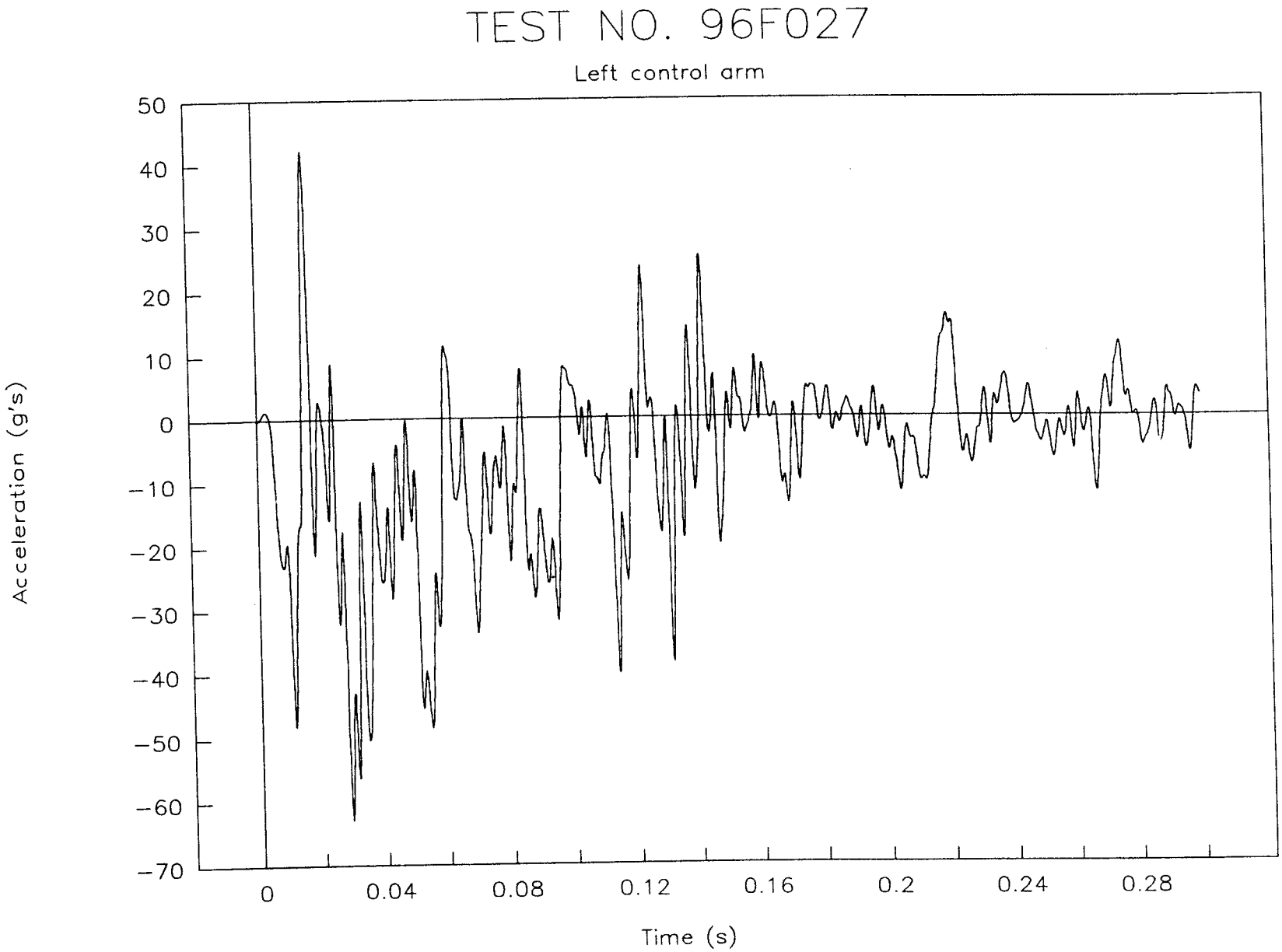

Figure 97. Acceleration vs. time, left control arm, test 96F027.

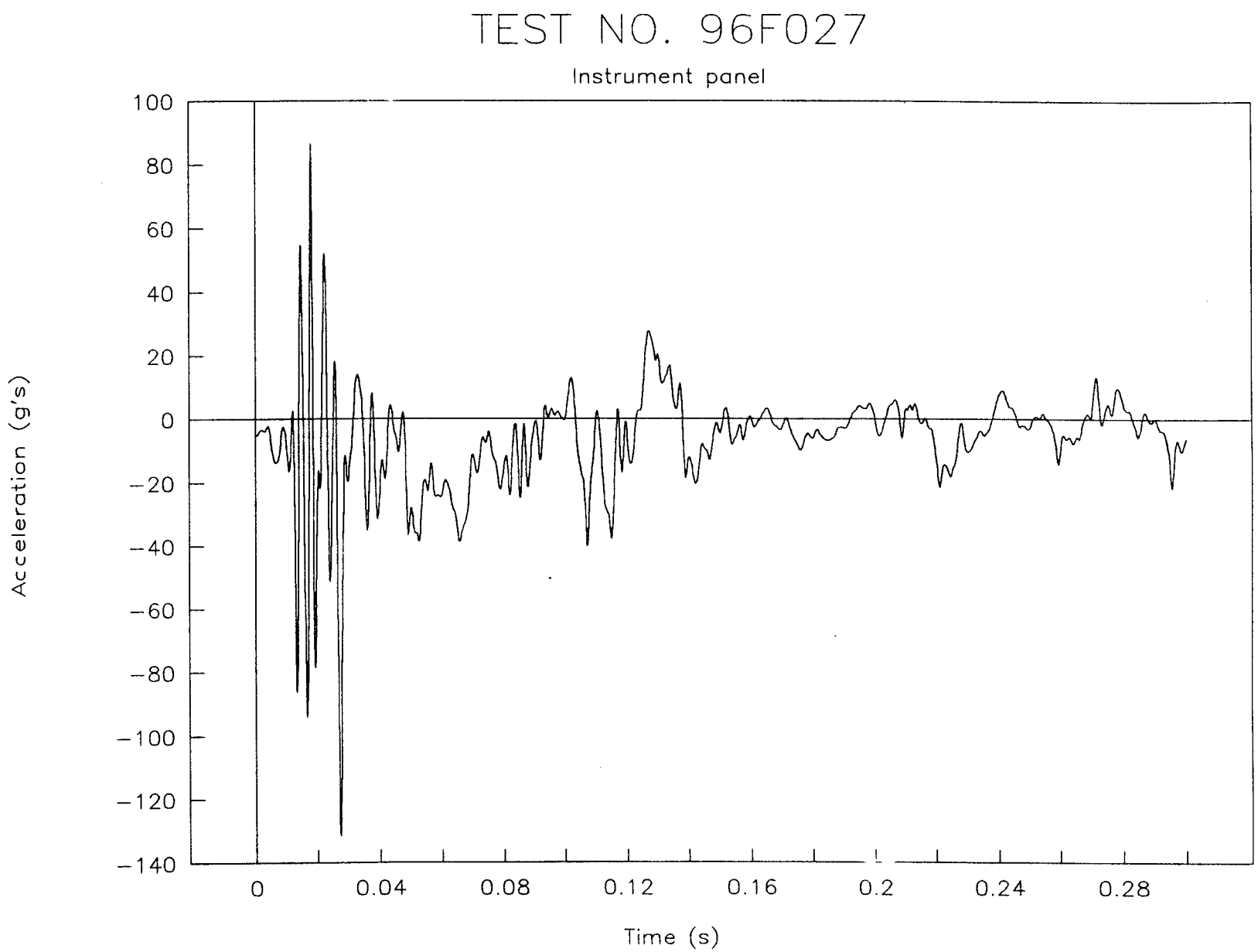

Figure 98. Acceleration vs. time, instrument panel, test 96F027.

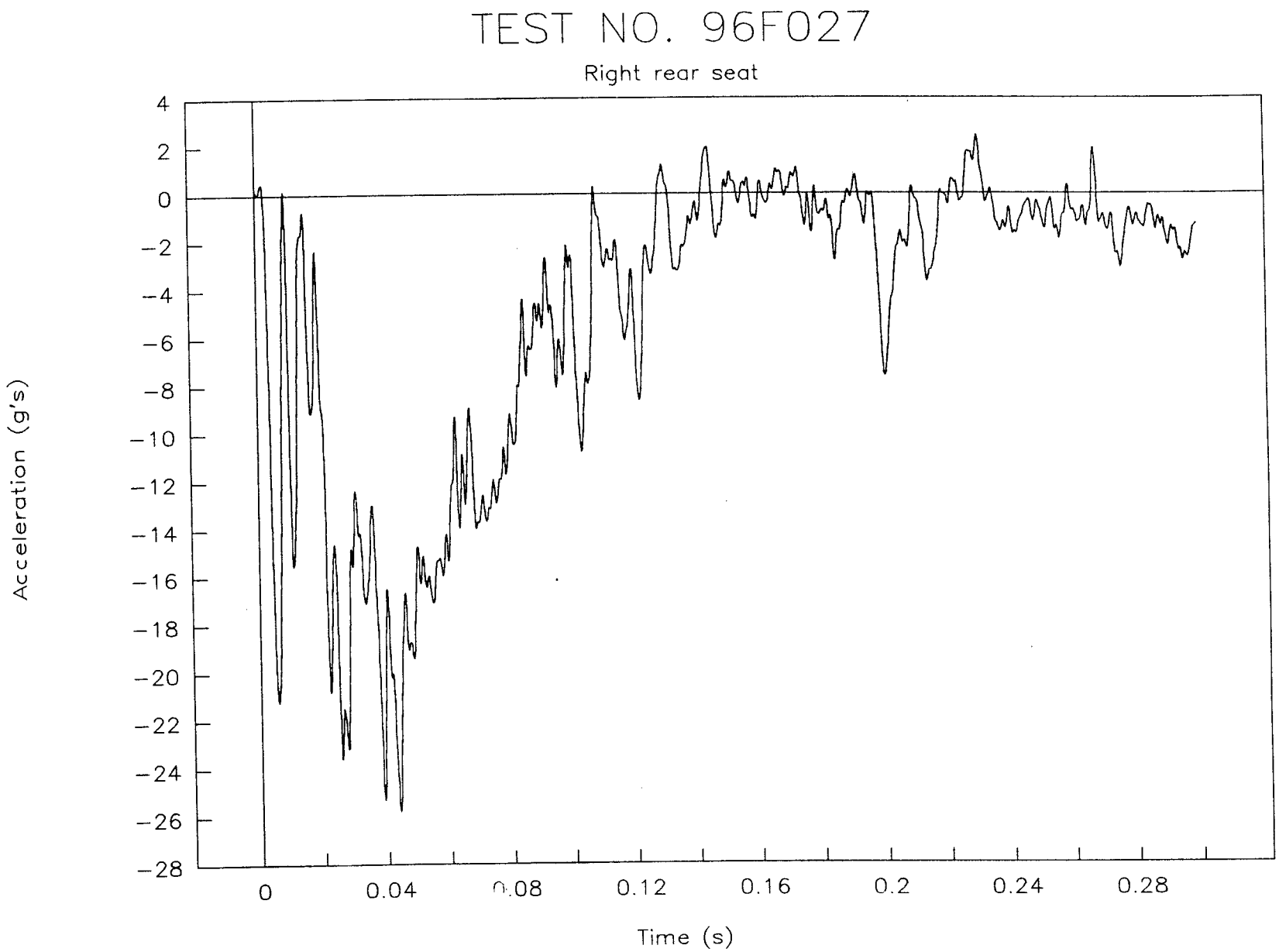

Figure 99. Acceleration vs. time, right rear seat, test 96F027.

REFERENCES

(1) H.E. Ross, Jr., D. L. Sicking, R. A. Zimmer, and J.D. Michie, *Recommended Procedures for the Safety Performance Evaluation of Highway Features, NCHRP Report 350*, National Highway Research Program, Transportation Research Board, Washington, DC, 1993.

(2) NHTSA. *Laboratory Procedures for Federal Motor Vehicle Safety Standard 208*, National Highway Traffic Safety Administration, Washington, DC, May 1992.

NTIS does not permit return of items for credit or refund. A replacement will be provided if an error is made in filling your order, if the item was received in damaged condition, or if the item is defective.

Reproduced by NTIS

National Technical Information Service
Springfield, VA 22161

This report was printed specifically for your order from nearly 3 million titles available in our collection.

For economy and efficiency, NTIS does not maintain stock of its vast collection of technical reports. Rather, most documents are printed for each order. Documents that are not in electronic format are reproduced from master archival copies and are the best possible reproductions available. If you have any questions concerning this document or any order you have placed with NTIS, please call our Customer Service Department at (703) 487-4660.

About NTIS

NTIS collects scientific, technical, engineering, and business related information — then organizes, maintains, and disseminates that information in a variety of formats — from microfiche to online services. The NTIS collection of nearly 3 million titles includes reports describing research conducted or sponsored by federal agencies and their contractors; statistical and business information; U.S. military publications; audiovisual products; computer software and electronic databases developed by federal agencies; training tools; and technical reports prepared by research organizations worldwide. Approximately 100,000 *new* titles are added and indexed into the NTIS collection annually.

For more information about NTIS products and services, call NTIS at (703) 487-4650 and request the free *NTIS Catalog of Products and Services*, PR-827LPG, or visit the NTIS Web site **http://www.ntis.gov**.

NTIS
Your indispensable resource for government-sponsored information—U.S. and worldwide

U.S. DEPARTMENT OF COMMERCE
Technology Administration
National Technical Information Service
Springfield, VA 22161 (703) 487-4650